Zeitschrift: IABSE reports = Rapports AIPC = IVBH Berichte
Band: 62 (1991)

Rubrik: D-regions and nodes

Experimental Studies of Nodes in Strut-and-Tie Models

Etude des régions nodales dans le cas de l'analogie du treillis

Verhalten von Knotenbereichen und Stabwerkmodellen

James O. JIRSA
Prof. of Civil Eng.
University of Texas
Austin, TX, USA

John E. BREEN
Prof. of Civil Eng.
University of Texas
Austin, TX, USA

Konrad BERGMEISTER
Dr.
University of Stuttgart
Stuttgart, Germany

David BARTON
Staff Engineer
Omega Marine Eng. Systems
Houston, TX, USA

Robert ANDERSON
Bridge Eng.
Greiner, Inc.
Tampa, FL, USA

Hakim BOUADI
Ph.D. Candidate
University of Texas
Austin, TX, USA

SUMMARY

This paper presents the results of a series of tests in which the behaviour of the nodal regions used in strut-and-tie models (STM) was studied. The research program included the construction and loading to failure, of a series of dapped beams and two series of isolated node specimens which simulated CTT and CCT node portions of the dapped beams. The test results supported the use of the STM in detailing. They indicated that the commonly used approach for determining the required development for hooked and straight bars may be overly conservative for node design and showed the beneficial effect of confinement of the concrete in the node and around the tie bars.

RÉSUMÉ

Cet article présente les résultats d'une série de tests étudiant le comportement des régions nodales dans le cas de l'analogie du treillis. Le programme de la recherche incluait la construction et le chargement jusqu'à la rupture d'une série de poutres à décrochement d'extrémité, ainsi que l'étude de deux séries de nœuds isolés simulant les nœuds CTT et TTC de la poutre (T = traction, C = compression). Les résultats confirment la validité de l'application de l'analogie du treillis dans la conception. Ils indiquent que les méthodes communément utilisées pour calculer les longueurs d'ancrage des barres droites ou à crochet peuvent être trop conservatives dans le dimensionnement des nœuds et que l'effet de confinement du béton a un effet favorable sur le nœud et autour des barres formant tirant.

ZUSAMMENFASSUNG

In dieser Veröffentlichung werden die Ergebnisse einer Reihe von Versuchen präsentiert, in denen das Verhalten von Knotenbereichen, wie sie in Stabwerkmodellen auftreten, untersucht wurde. Die Versuche umfassten eine Reihe von Trägern mit ausgeklinkten Auflagern und zwei Testserien, in denen die Druck-Zug-Zug und Druck-Druck-Zug Knoten in den ausgeklinkten Trägerenden isoliert betrachtet wurden. Die Ergebnisse bestätigen die Anwendbarkeit von Stabwerkmodellen für Bemessungs- und Konstruktionsaufgaben. Es wurde beobachtet, dass die üblichen Vorgehensweisen für die Bestimmung der Verankerungslänge von geraden Bewehrungsstäben oder solchen mit Endhaken für die Bemessung von Knotenbereichen sehr konservative Ergebnisse liefern, und dass eine Umschnürung des Betons festigkeitssteigernd wirkt.

1. INTRODUCTION

1.1 Background

Mies van der Rohe restated a traditional German proverb in a positive fashion when he said, "The hand of God is in the details". Clearly, the success of any integrated conceptual approach to the proper design of structural concrete must finally succeed or fail according to the degree of assistance it gives the designer in developing adequate and economic details. Marti [1] states "Dimensioning and detailing of D-regions has often been regarded as an inferior task, while in fact, it is of paramount importance for the quality of any reinforced concrete structure." Schlaich [2] urges that dimensioning be carried out initially on the basis of relatively simple models, such as the strut-and-tie model (STM), with a following step of review at "a suitable level of sophistication" to ensure that the details in fact carry out the intent of the dimensioning model. He quite properly points out that even the most sophisticated non-linear finite element analysis (FEA) has important limits when applied to the capacity of details and expecially to describing the behavior of nodes. The authors have felt that the re-emphasis on STM for D regions provides a golden opportunity for introducing rationality of structural concrete detailing. However, in examining the literature, they came to the identical conclusions voiced by MacGregor [3] and Marti [2] who both call for further experimental investigation of nodal zone strength. The authors have been conducting such experimental studies for several years [4,5].

1.2 Objectives

The basic object of this study was to critically examine the application of STM in the detailing of D-regions. Research cannot be carried out to develop empirical design procedures to cover *every* detailing situation. The STM uses a few basic principles to cover a large range of design problems. While the literature contains considerable general information, there is a lack of test data to corroborate assumptions of the strut-and tie model. Working with a specific application to help verify strut-and-tie procedures, a dapped-end beam detail (See Fig. 1) was selected for testing. The STM principles outlined by Schlaich et al. [6] were used to develop details for the discontinuity regions. It became immediately apparent that the existing state of knowledge was particularly troublesome which applied to the nodes. Major attention was then devoted to tests on isolated nodes (Fig. 1b and Fig. 1c).

1.3 Test Series

1.3.1 Dapped Beam Tests

Three different procedures for the design of dapped beam ends were used. Two different STM and two empirically based methods (PCI and Menon/Furlong) were used. A different dapped end detail was tested for each method [4].

1.3.2 Compression-Tension-Tension (CTT Nodes)

To develop an understanding of an isolated CTT-node, a laboratory investigation identified significant behavioral patterns of the CTT-node, and was used to develop design guidelines. The dapped beams served as the prototype for the node tests. Nine node specimens were designed and loaded to duplicate, as closely as possible, boundary conditions that exist at a critical CTT-

node in the dapped beams. Variables included concrete strength, lateral confinement provided by transverse reinforcement, anchorage details, and node geometry [4].

1.3.3 Compression-Compression-Tension (CCT Nodes)

The CCT node was also isolated from the end reaction region of the dapped beam. Ten specimens were tested in which concrete strength, size of bearing area, amount of transverse reinforcement, and longitudinal reinforcement configuration were varied [4].

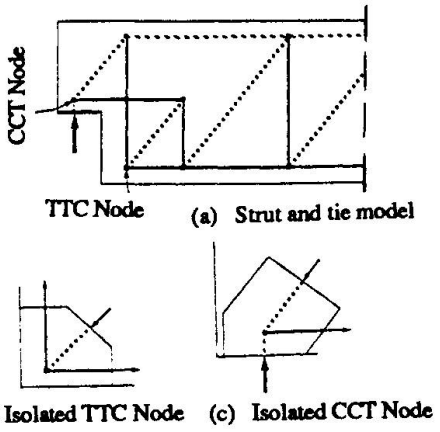

Figure 1 Strut and tie model of the prototype dapped beams.

2. DAPPED END BEAM TESTS

All dapped end details were designed for the same design load levels; a factored ultimate load of 100 kips [4]. The resulting reinforcement layout for the two different STM used, the PCI, and the M/F method designs are shown in Fig. 2. In the actual tests, the dapped end details were provided at the ends of a simply supported beam which was loaded monotonically to failure.

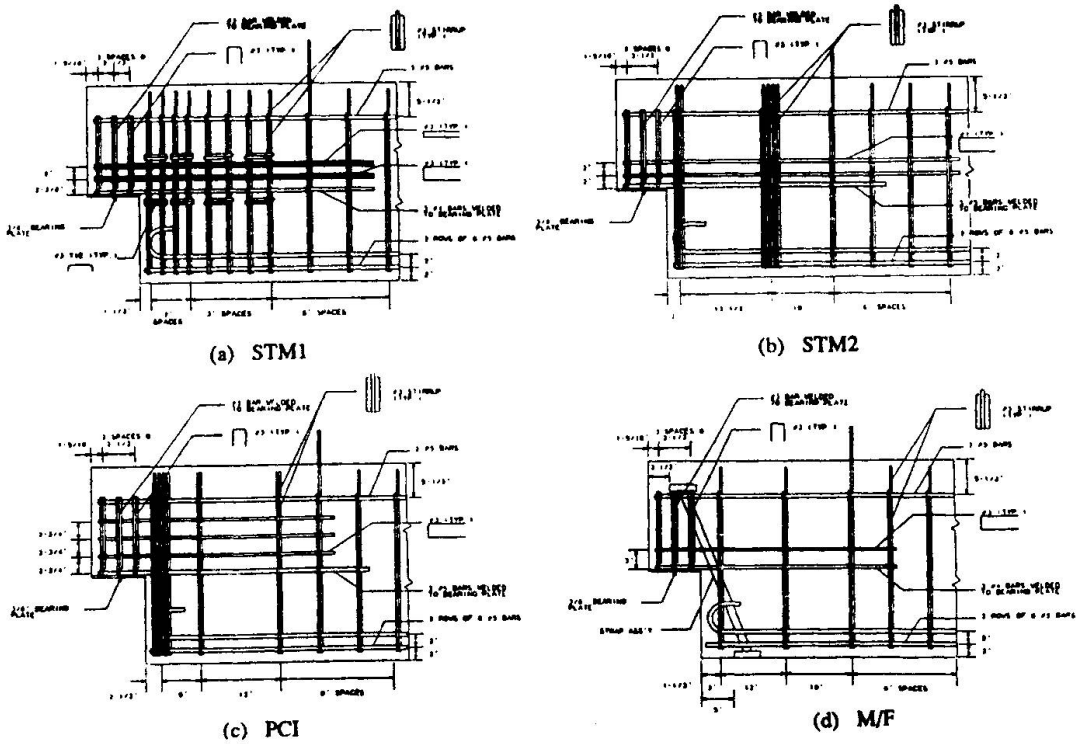

Figure 2. Specimen reinforcement layouts.

The overall behavior of specimens designed using STM was found to be comparable with details designed using current design standards. As shown in Fig. 3 the ultimate capacity of all four specimens substantially exceeded the computed capacity. A ductile failure mode in which the steel yielded before the concrete failed was exhibited by each of the specimens. The STM procedure required slightly more shear reinforcement. The initial cracking load for all specimens ranged from 20 to 30 percent of design ultimate as shown in Fig. 4. In ST-1, cracking was well controlled at service loads. Slightly more cracking was exhibited by ST-2 due to placement of vertical reinforcement farther away from the dap. Initial yielding of reinforcement in both STM specimens was at about 75 percent of design ultimate, substantially earlier than the two empirically designed specimens.

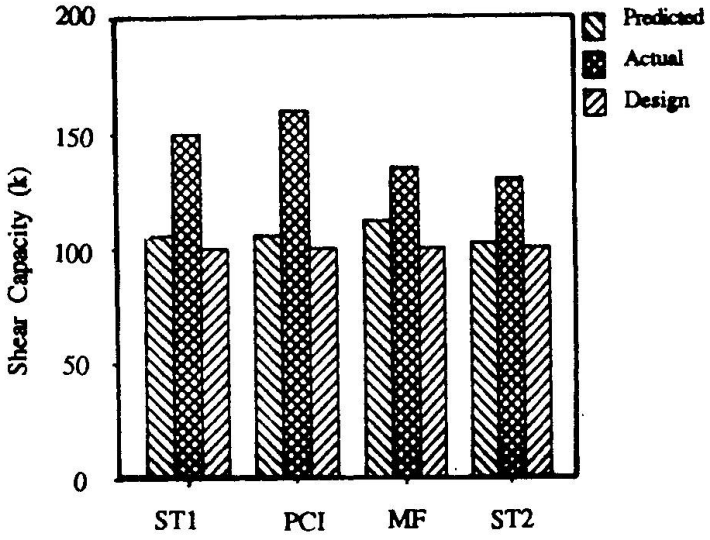

Figure 3 Comparison of specimen shear capacities.

Internal force measurements at the design ultimate load compared well to forces predicted by the design STM. As load was increased beyond the design ultimate load, the distribution of internal forces changed. STM representations of the upper portion of the daps based on measured forces at ultimate were not completely accurate due to the presence of force transfer mechanisms not considered by the STM.

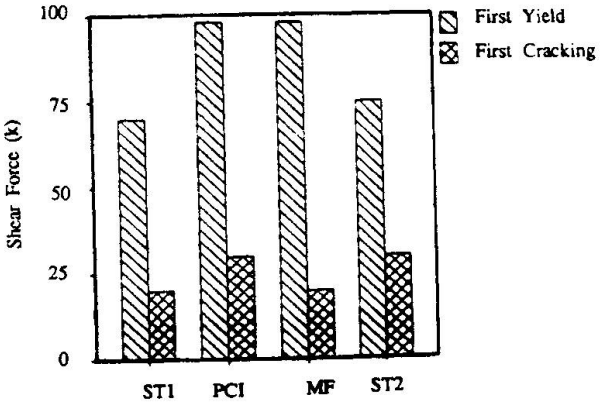

Figure 4 Comparison of cracking and yield loads

Comparison of the behavior of the dapped ends indicates placing the main vertical reinforcement close to the change in section is most efficient. In addition, grouping the reinforcement with as small a spacing as possible appears to offer the best performance. Anchorage requirements based on the STM were found to be conservative and resulted in applied loads well beyond design values. Proper anchorage of the dap horizontal reinforcement and the beam flexural reinforcement was found to be particularly important.

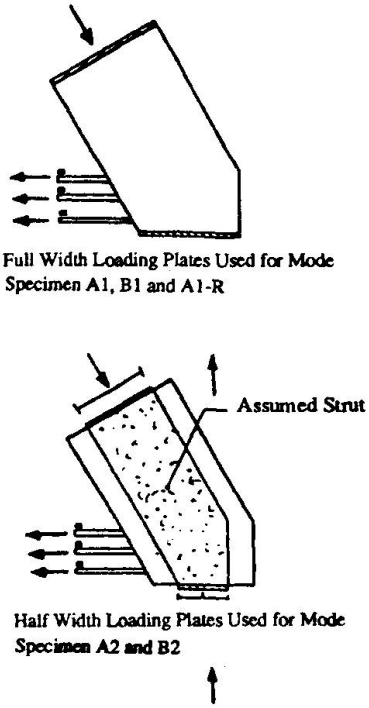

(a) Full Width Loading Plates Used for Mode Specimen A1, B1 and A1-R

(b) Half Width Loading Plates Used for Mode Specimen A2 and B2

Figure 5. General information about the tested CCT-nodes (from Ref. [4]).

3. NODE TESTS

The nodes of the STM represent the locations of change of direction of internal forces, which in the structure occurs over a certain length and width in the node region. The intersecting strut-and-tie forces have to be linked together and balanced in equilibrium in the node region. If one of the struts or ties represents a concentrated stress field (e.g. near a single load, a support or concentrated reinforcement) the deviation of forces tends to be locally concentrated and the node region is relatively small. These kind of nodes are called "singular nodes" and have to be dimensioned with special care. Evaluation of the nodal regions includes checking the nodal boundary stresses and determining reinforcement development requirements for nodes which contain tension ties. Each of these steps requires the determination of the physical boundaries of the node.

3.1 CCT Nodes

The typical critical CCT node in a dapped end beam occurs at the support as shown in Fig. 1(a). This node was isolated as shown in Fig. 1(c). In some presentations of CCT nodes, the tension reinforcement is shown as anchored by use of an external anchor plate. This is seldom found in practice. The usual detail is that straight bars, hooked bars or looped bars are used. Looped bars with confining direct pressure from the bearing plate load are preferred. Sufficient anchorage lengths have to be provided within as well as behind the node. Anchorage lengths can be assumed to begin where the compression struts meet the bars. The effective width of the compression strut can be found by assuming an effective compressive stress in the strut, $\nu_e f_c'$.

The fundamental aspects should allow the designer to determine the geometry of the CCT-node for varying reinforcement distribution and anchorage details (several layers, loops, hooks, etc.). The experimental study by Bouadi [4] provided information about the behavior and transfer of forces within the CCT-node as well as the ultimate strength. Typical test specimens are shown in Fig. 5. Test results with a concrete strength in the range from 2360 to 4680 psi showed crushing of the concrete struts only for the lower concrete strength specimens. In all other cases anchorage failure occurred. The tests indicate the of geometry of CCT nodes shown in Fig. 6. The compressive forces and the tensile force in the reinforcement were increased simultaneously. All specimens experienced post-yield failures including strut crushing, cover splitting, and gross slippage of reinforcement. Statistical examination of the specimens experiencing concrete failure indicated that if $\nu_e = 0.8$ was used, all predictions were conservative with a mean of 1.17 and a standard deviation of 0.14. The CCT node tests indicated:

(1) Specimens were controlled either by anchorage failure or compressive failure;
(2) STM strut orientation angles had been verified as correct in the dapped beam tests. Effective bearing areas based on such orientation gave consistent results for evaluating

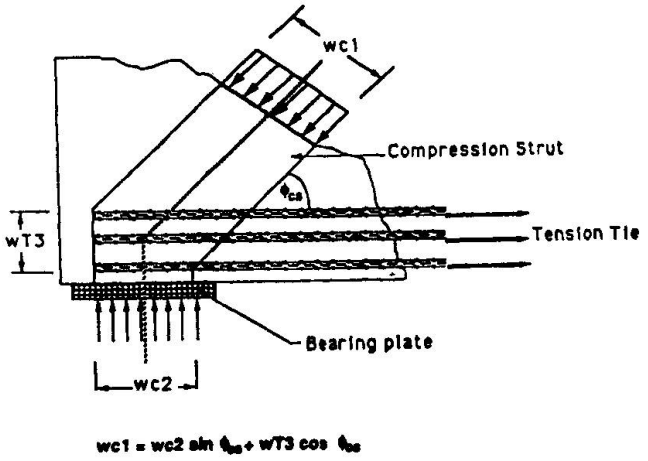

Figure 6. Anchorage detail for CCT-node with directly anchored bars.

tie anchorage and effective compressive strength factors;

(3) The effective compressive stress efficiency factor increased with reduction in bearing area size;

(4) Transverse reinforcement restrained the cracks and increased capacity 35% by preventing anchorage failure;

(5) Anchorage lengths for straight and hooked bars given in the ACI Code were found to be conservative.

3.2 CTT Nodes

The CTT-node is an intersection of a concrete compressive strut and two tensile ties. In steel trusses, bolts, welds, and gusset plates are sized to safely transfer load between the members. In contrast, a CTT-node in a concrete member must rely on anchorage, bond and other internal force transfer mechanisms to transfer strut and tie forces. Anchorage is achieved by providing proper development length or in special circumstances by attaching the reinforcement to bearing plates or other fixed components. The definition of the effective width plays an important factor in the dimensioning process. For the relatively rare case of a CTT-node with anchor plates, the widths of the plates are given as dependent constraints which tend to fix the width of the unknown compression strut. The more practical and generally occurring case is the CTT-node without a bearing plate. For this case the approach of Fig. 7 is proposed.

The efficiency factor for the CTT-node was investigated in an experimental study by Anderson [4]. Figure 8 shows typical test specimens. Other variables included types of anchorages, local confinement and concrete strength. One specimen was subjected to unequal forces in the tension ties in order to induce a different compression strut angle into the specimen. In the tests, general strut failures did not usually occur. The reinforcing anchorage detail was primarily responsible for limiting the ultimate load. However, for design purposes the actual efficiency factor for the concrete compressive strength is of interest. Only one specimen failed by concrete crushing. Using ν_e = 0.8 and taking into account the smaller bearing plate width (4") compared to the compression strut width (6.37"), the experiment/theory-ratio was computed as 1.02.

While data was collected from a relatively small number of CTT tests, the unique nature of the isolated node specimens provides interesting insight into node behavior and design.

(1) Specimens were generally able to reach the design strength which was governed by yielding of tie reinforcement. The ultimate strength of the CTT nodes was affected by concrete strength; however, internal force transfer mechanisms were more affected by the specimen geometry and placement of steel.

(2) In all the specimens, different layers of tie reinforcement were observed to strain at different rates. In the strut and tie model the reinforcement making up a single tie is

normally assumed to be uniformly strained. Major cracks appeared to reduce the available development length for some of the layers of reinforcement closest to the external surface enough to cause a deterioration in the tensile capacity of the tie.

(3) Correlations between the behavior of the node specimens and the prototype dapped beam specimen were quite good.

(4) Evaluation of the strut-and-tie model in the light of the test results indicate that
   (a) cracks were generally parallel with the angle of the compression strut;
   (b) the geometry of the strut is best defined by the strut angle and the width of the outer intersections of the layers of the reinforcement in both directions;
   (c) defining the critical section of the reinforcement by the boundaries of the compression fields appeared to produce reasonable estimates of the capacity of ties anchored through development.

(5) The splitting failures that occurred in several specimens underscored the importance of detailing the CTT-node as a three-dimensional element. Reinforcement should be provided across all planes of weakness to control cracking. Confining reinforcement normal to planes of hooks and bends is especially important.

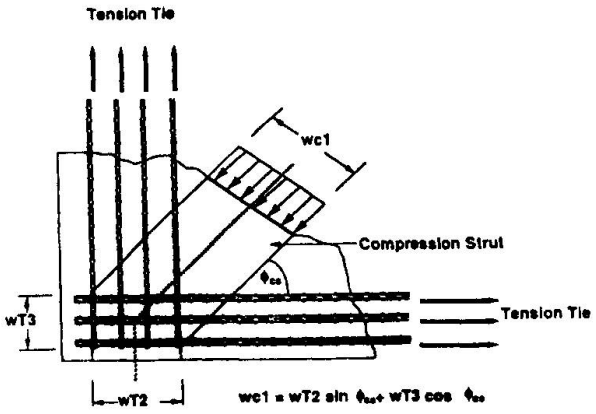

Figure 7 Geometrical approach to define the strut width for CTT-node

4. CONCLUSIONS AND RECOMMENDATIONS

The results of these limited tests show that the STM is useful design procedure for detailing structural concrete. The use of STM along with a knowledge of behavior derived from experimental research seems a good basis for developing efficient design procedures. The STM represents a rational approach which can be extended to detailing situations not covered by existing procedures.

As called for by MacGregor [3] and Marti [1], further experimental verification of other types of details is necessary. In addition, guidelines on analysis and design of nodal regions, serviceability criteria, and tie layout need development. In order to develop comprehensive design criteria for nodes, future studies should include specimens with a number of different bar spacings and amounts of tie reinforcement. Test specimens with high percentages of reinforcement and narrow web widths are also suggested so that effective concrete strength limits could be evaluated more closely. The behavior of specimens with anchor plates and straight or hooked bars needs to be examined. In addition, the effect of strut orientation should be studied more closely. In particular, the effects of skew cracks on the effective concrete strength of the compressive strut should be verified. The isolated node specimens used in this study provide much useful data but admittedly it is never possible to remove a portion of a structural element and isolate it in a manner that does not produce some change in boundary conditions. In spite of that, such node specimens offer a means of acquiring a large amount of data on detailing at a minimal cost.

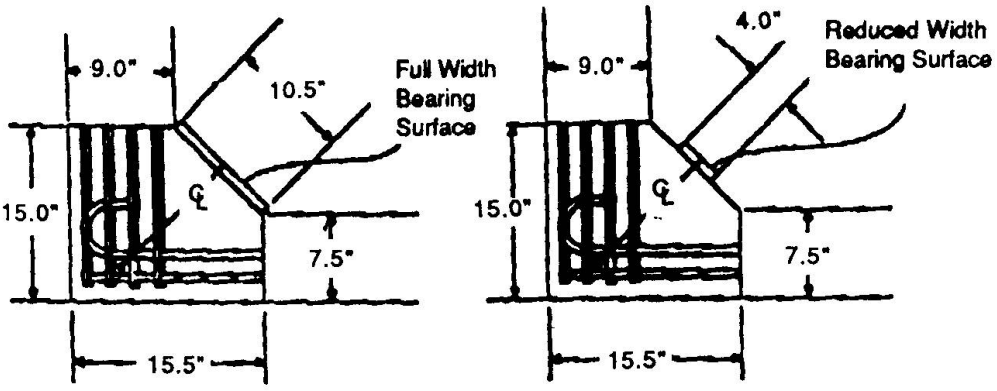

Typical Full Width Bearing Surface Specimens

Reduced Bearing Surface for Specimens HHSR and LHSR

Figure 8 Typical CTT-nodes tested (from Ref. [4]).

5. ACKNOWLEDGEMENTS

The research reported herein was carried out under the sponsorship of the Texas State Department of Highways and Public Transportation and of the Federal Highway Administration. The opinions presented are those of the authors and not necessarily those of the sponsors. Ms. Mary Lou Ralls provided excellent advice on sponsor prototype details and problems.

REFERENCES

1. MARTI, P., "Sub-Theme 2.4: Dimensioning and Detailing," Final Report, IABSE Colloquium *Structural Concrete*, Stuttgart, April 1991.
2. SCHLAICH, J., "Sub-Theme 2.2: Modelling," Final Report, IABSE Colloquium *Structural Concrete*, Stuttgart, April 1991.
3. MAC GREGOR, J.G., "Sub-Theme 2.4: Dimensioning and Detailing," Final Report, IABSE Colloquium *Structural Concrete*, Stuttgart, April 1991.
4. BARTON, D.L., ANDERSON, R.B., BOUADI, A., JIRSA, J.O., AND BREEN, J.E., An Investigation of Strut-and-Tie Models for Dapped Beam Details," Research Report 1127-1, Center for Transportation Research, February 1990.
5. BERGMEISTER, K., BREEN, J.E., JIRSA, J.O., AND KREGER, M.E., "Detailing for Structural Concrete," Research Report 1127-3F, Center for Transportation Research, October 1990.
6. SCHLAICH, J., SCHAFER, K., AND JENNEWEIN, M., "Towards a Consistent Design of Structural Concrete," PCI Journal, May-June 1987, pp. 75-150.

Design of Disturbed Regions

Conception des zones de discontinuités

Bemessung von Diskontinuitätsbereichen

Denis MITCHELL
Prof. of Civil Eng.
McGill Univ.
Montreal, PQ, Canada

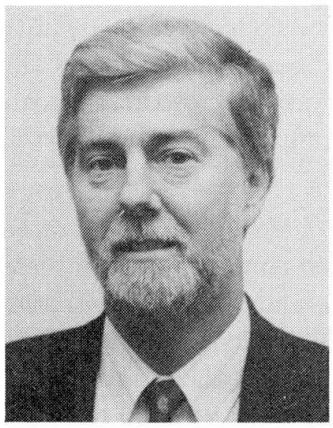

Denis Mitchell has received a number of awards from ACI, ASCE and PCI for his research on structural concrete. He is currently Chairman of the Canadian Concrete Code Committee.

William D. COOK
Res. Eng.
McGill Univ.
Montreal, PQ, Canada

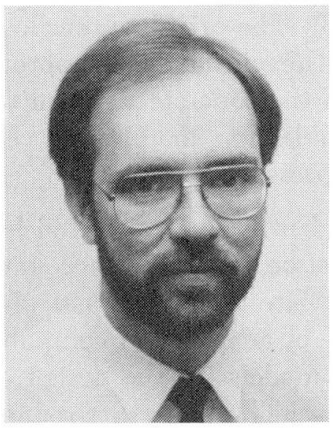

William D. Cook obtained his doctorate in Civil Engineering at McGill University in 1987. His research interests relate to nonlinear analysis of reinforced and prestressed concrete structures.

SUMMARY

The design method for disturbed regions in the Canadian concrete code is first described and the need to consider strain compatibility is explained. The transition from regions where sectional analysis is applicable to regions where strut-and-tie models apply, is discussed. Examples of the application of strut-and-tie models and non-linear finite element analysis, are presented.

RÉSUMÉ

On décrit la méthode de calcul de zones de discontinuités proposée par le Code Canadien du béton, ainsi que la nécessité de considérer la compatibilité des déformations. La transition entre des zones où l'on peut appliquer l'analyse sectionnelle et celles où l'on prend en considération l'analogie du treillis est discutée. L'application de modèles d'analogie du treillis et d'analyse non-linéaire par éléments finis est illustrée par des exemples.

ZUSAMMENFASSUNG

Das Bemessungsverfahren in der kanadischen Betonnorm für Diskontinuitätsbereiche wird beschrieben und die Notwendigkeit erläutert, die Verträglichkeit der Dehnungen zu berücksichtigen. Es wird der Übergang von den Bereichen, in denen eine Querschnittsbemessung durchgeführt werden kann, zu den Bereichen, in denen Stabwerkmodelle verwendet werden, diskutiert. Beispiele für die Anwendung der Stabwerkmodelle und nichtlinearer Finite Element Methoden werden vorgestellt.

1 INTRODUCTION

The design of a structural concrete member typically involves separating the member into two distinct zones. Regions removed from both geometric and loading discontinuities are usually designed for flexure assuming that plane sections remain plane and designed for shear assuming that the shear stresses are uniform over the nominal shear area of the cross-section. Because the plane-sections analysis for flexure satisfies both equilibrium and compatibility, engineers are able to apply this method to a large variety of loadings and cross-sectional configurations. The 1984 Canadian Concrete Standard (CSA)[1] provides the designer with a sectional design approach for shear based on the compression field model[2], which uses a variable angle for the diagonal compressive stresses in the concrete and satisfies both equilibrium and compatibility. The strain-softening of the diagonally cracked concrete is based on the influence of the principal tensile strain in reducing the compressive load carrying capacity of the concrete as developed by Vecchio and Collins[3]. The principal tensile strain is determined by considering compatibility of strains. However, this current code approach does not consider the beneficial effects of the tension that exists in the concrete between the diagonal cracks. The presence of these tensile stresses has been included in a more recent version of this shear design approach[4] and is based on the modified compression field model[3].

Regions adjacent to discontinuities caused by abrupt cross-sectional changes or concentrated loads or reactions must be designed to account for the resulting disturbed flow of forces. In these regions it is inappropriate to assume that plane sections remain plane and that shear stresses are uniform. In spite of advances in computer analysis techniques, engineers are reverting to simple strut and tie models for the design of disturbed regions, similar to those introduced by Ritter[5] and Mörsch[6] and further refined by Thürlimann *et al.*[7], Marti[8] and Schlaich *et al.*[9]. Marti[8] suggested a truss model with a limiting compressive stress in the concrete diagonals of $0.6f'_c$. Schlaich *et al.*[9] suggested choosing the geometry of the truss model such that the angles of the compressive diagonals are within $\pm 15°$ of the angle of the resultant of the compressive stresses obtained from an elastic analysis. These methods, which satisfy equilibrium, do not necessarily satisfy compatibility. The strut and tie model of the 1984 CSA Standard uses compatibility of strains in the determination of the limiting compressive stress in the cracked compressive struts.

2 STRUT AND TIE MODEL OF THE CSA STANDARD

The steps in design of a disturbed region, such as the deep beam shown in Fig. 1, are:

1. Sketch flow of forces in disturbed region and locate nodal zones which are regions bounded by struts, tension ties or bearing areas.
2. Choose dimensions of loading and reaction areas such that nodal zone stresses stay below permissible limits (i.e., $0.85\phi_c f'_c$ in nodal zones bounded by compressive struts and bearing areas, $0.75\phi_c f'_c$ in nodal zones anchoring only one tension tie and $0.60\phi_c f'_c$ in nodal zones anchoring tension ties in more than one direction).
3. Determine geometry of truss model and determine forces in struts and ties. If truss is statically indeterminate, estimate relative stiffnesses of truss members in order to solve forces in struts and ties.
4. Determine required areas of tension ties ($A_s = T/\phi_s f_y$) and check details of tension reinforcement to ensure adequate anchorage into nodal zones.

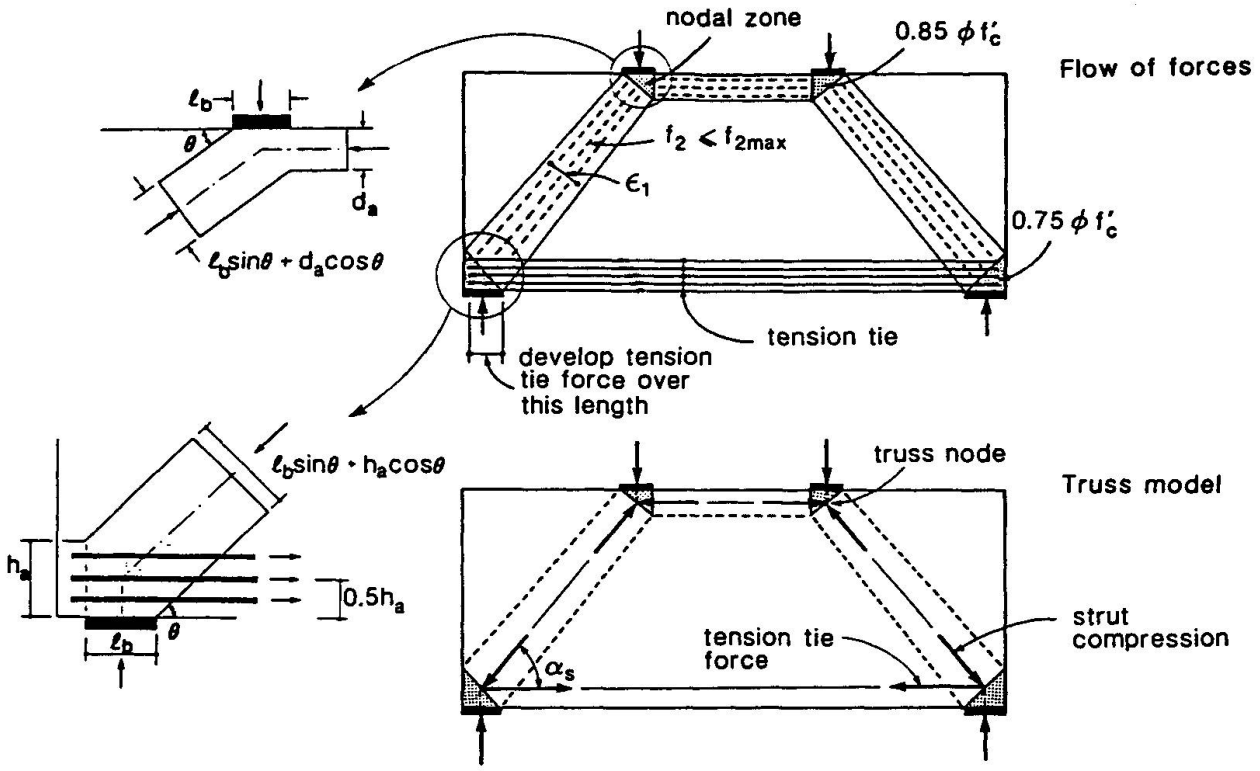

Figure 1: Strut and tie modeling of a deep beam.

5. Check strut compressive stresses from $f_2 = C/\phi_c A_c$ where A_c is effective area of strut as determined by end anchorage conditions (see Fig. 1). Check that f_2 does not exceed crushing strength, f_{2max}, of cracked concrete where:

$$f_{2max} = \frac{\lambda \phi_c f'_c}{0.8 + 170\epsilon_1} \leq 0.85 \phi_c f'_c \tag{1}$$

where ϵ_1 is the principal tensile strain and λ is a factor varying from 1.0 for normal density to 0.75 for structural low-density concrete.
Compatibility of strains is used to determine the principal tensile strain as:

$$\epsilon_1 = \epsilon_s + (\epsilon_s + 0.002) \cot^2 \alpha_s \tag{2}$$

where ϵ_s is the required strain in tension tie (usually taken as ϵ_y) and α_s is the angle between the strut and the tie crossing the strut.

Although design using strut and tie models appears simple, it takes considerable experience in choosing an appropriate model. Guidance on the use of strut and tie models is given by Schlaich *et al.*[9], Marti[8,10], MacGregor[11], Collins and Mitchell[12] and Cook and Mitchell[13].

3 SECTIONAL ANALYSIS VERSUS DISTURBED REGION ANALYSIS

Figure 2 compares the experimentally obtained shear strengths of a series of beams tested by Kani[14] with the predicted capacities from both sectional and strut and tie analyses[4]. In these tests the shear span to depth ratio, a/d, was varied from 1 to 7 and no web reinforcement was provided. At a/d ratios less than about 2.5 the resistance is governed by strut and tie

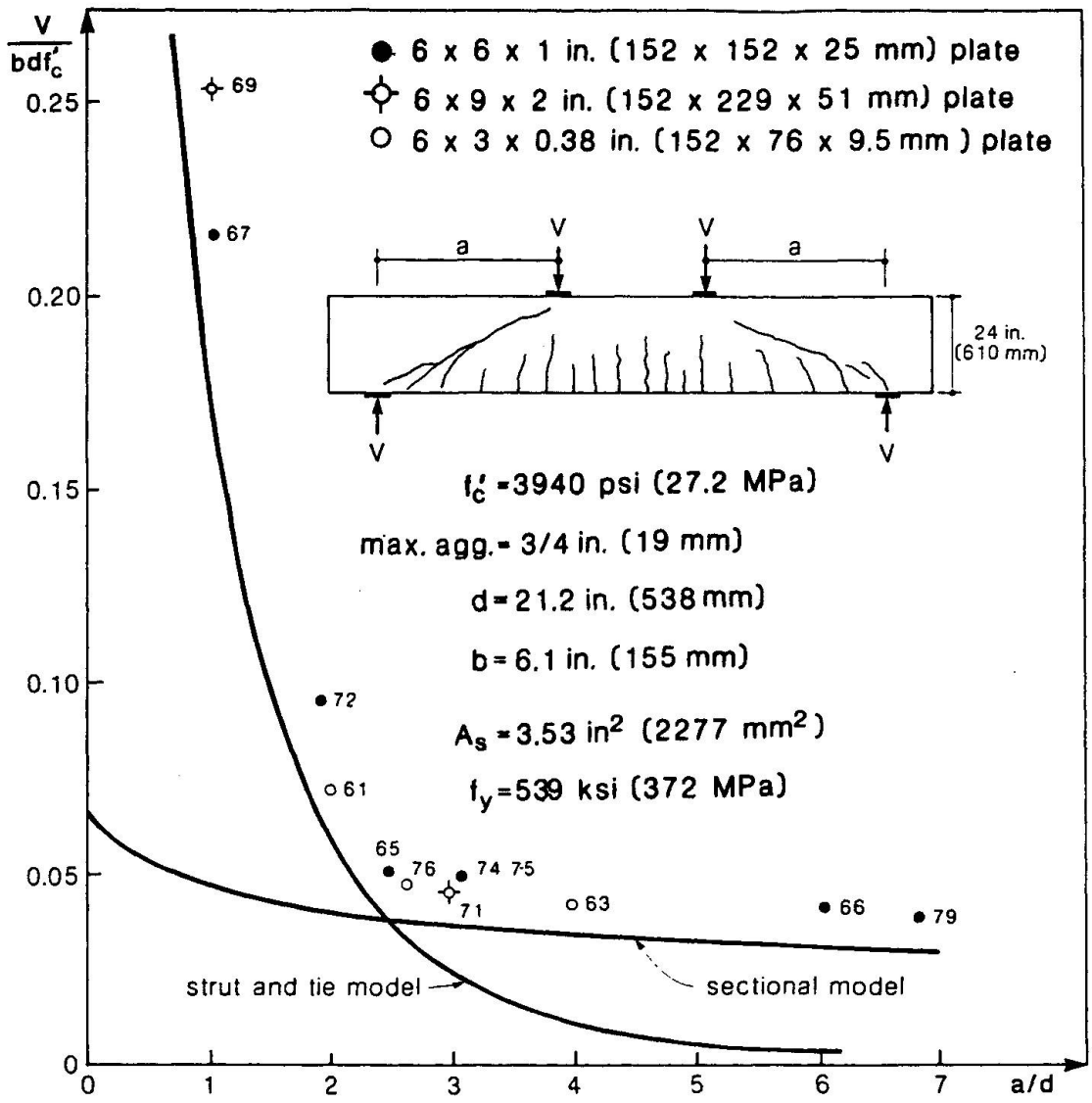

Figure 2: Predictions[4] of shear strength versus a/d ratio for tests reported by Kani[14].

action, with the resistance dropping off rapidly as a/d increases. The failures in this range were governed by crushing of the compressive struts, which were sensitive to the size of the bearing plates. Using the CSA code approach[1] in determining the strength of a member with $a/d = 2.0$ and having a 152 mm long bearing plate resulted in a value of f_{2max} of 10.2 MPa, or only $0.38f'_c$. This relatively low value of the crushing strength of the strut emphasizes the importance of considering strain compatibility in determining the strain softening effect. For a/d values greater than 2.5 the strength is governed by the conditions away from the disturbances created by the support reactions and the applied loads. Because of the significant amount of longitudinal reinforcement failure is governed by shear and the details of the support and loading bearings have little influence on the shear capacity of the member.

4 DESIGN VERSUS ANALYSIS

Elastic finite element analysis is useful for assessing the serviceability conditions of disturbed regions. It has also been used to approximate the required reinforcement for service and fac-

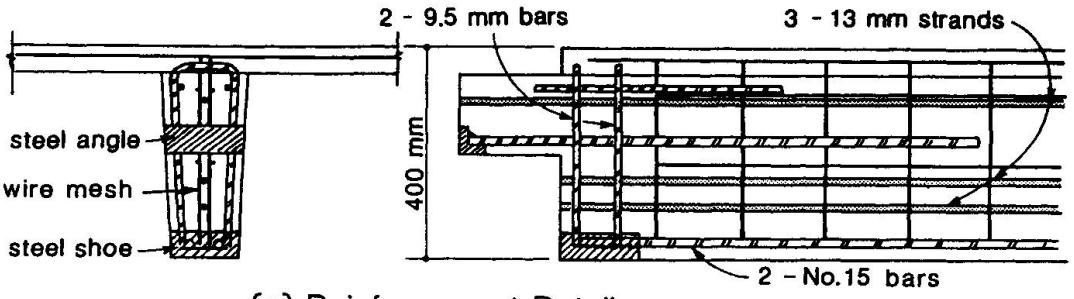

(a) Reinforcement Details

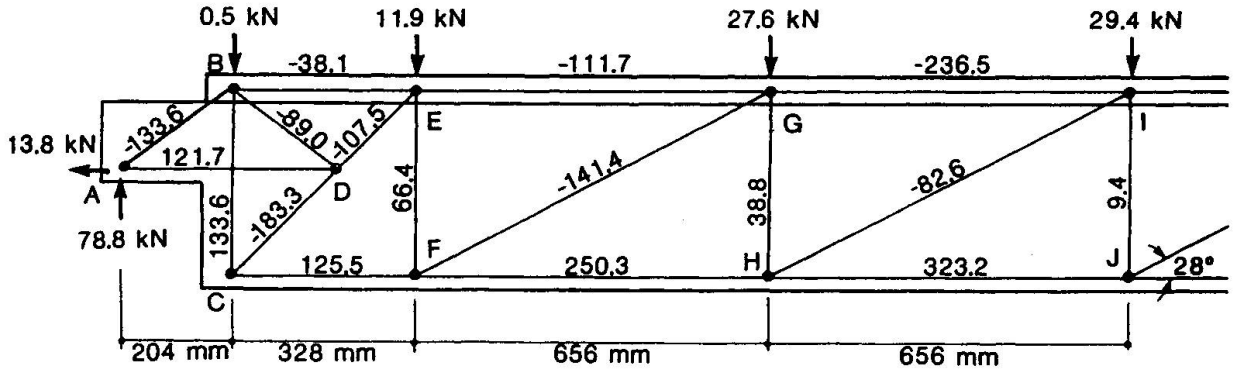

(b) Strut and Tie Model

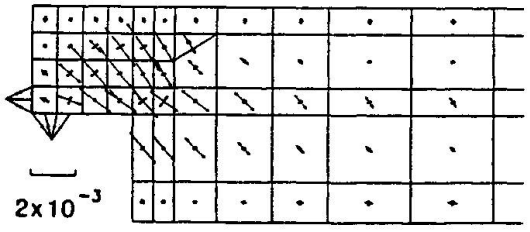

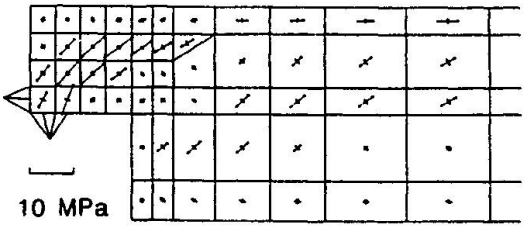

(c) Principal Concrete Strains (d) Principal Concrete Stresses

Figure 3: Analyses of thin stemmed precast pretensioned beam with dapped end[16].

tored loading conditions, however, it does not realistically predict the redistribution of stresses that takes place near ultimate. Non-linear finite element analyses[13,15], based on the modified compression field theory, naturally satisfy both equilibrium and compatibility and take into account the strain softening of the concrete compressive stress-strain relationship (see Eq. (1)). The complex transfer of forces across crack interfaces, including the influence of surface roughness and the increased tensile stresses in the reinforcement at crack locations, is approximated and the tensile stresses between the cracks (tension stiffening) is accounted for. This analysis provides the complete response through all stages of loading, including redistribution of stresses after cracking and yielding. Non-linear finite element analysis is an analysis tool, rather than a design tool, useful for verifying the behaviour of regions designed using strut and tie models.

Figure 3 shows a thin-stemmed dapped-end precast pretensioned beam tested at McGill University[16]. In order to permit the development of the strut and tie model shown (see Fig. 3b), a steel shoe was provided at the bottom of the thin stem (see Fig. 3a) and horizontal and vertical ties, welded to the shoe, provided the bottom chord and the vertical tension tie forces in the truss. Figure 3c and d show the principal concrete strains and stresses predicted by non-linear

finite element analysis. The test beam failed at an end reaction of 79.8 kN. The strut and tie and finite element predictions were 78.8 and 84.5 kN, respectively.

CONCLUSIONS

Strut and tie models, which appropriately account for compatibility in determining the compressive capacity of the struts, provide a simple design method for disturbed regions. Non-linear finite element analysis provides a more sophisticated tool for checking the design for both service and ultimate conditions.

REFERENCES

1. CSA Committee A23.3, "Design of Concrete Structures for Buildings", CAN3-A23.3-M84, Canadian Standards Association, Rexdale, Canada, 1984, 281 pp.
2. COLLINS, M.P. and MITCHELL, D., "Shear and Torsion Design of Prestressed and Non-Prestressed Concrete Beams", PCI Journal, V. 25, No. 5, Sept-Oct. 1980, pp. 32–100.
3. VECCHIO, F.J. and COLLINS, M.P., "The Modified Compression-Field Theory for Reinforced Concrete Elements Subjected to Shear", ACI Journal, V. 83, No. 2, March-April 1986, pp. 219–231.
4. COLLINS, M.P. and MITCHELL, D., "Prestressed Concrete Structures", Prentice Hall, Englewood Cliffs, NJ, USA, 1991, 766 pp.
5. RITTER, W. "The Hennebique Design Method (Die Bauweise Hennebique)", Schweizerische Bauzeitung (Zürich), V. 33, No. 7, Feb. 1899, pp. 59–61.
6. MÖRSCH, E., "Concrete-Steel Construction (Der Eisenbetonbau)", Translation of the third German Edition by E.P. Goodrich, McGraw-Hill Book Co., New York, 1909, 368 pp.
7. THÜRLIMANN, B., MARTI, P., PRALONG, J., RITZ, P., and ZIMMERLI, B., "Anwendung der Plastizitaetstheorie auf Stahlbeton", Institute for Structural Engineering, ETH Zürich, 1983, 252 pp.
8. MARTI, P., "Basic Tools of Reinforced Concrete Beam Design", ACI Journal, V. 82, No. 1, Jan.-Feb. 1985, pp. 46–56.
9. SCHLAICH, J., SCHÄFER, K., and JENNEWEIN, M., "Towards a Consistent Design of Reinforced Concrete Structures", PCI Journal, V. 32, No. 3, 1987, pp. 74–150.
10. MARTI, P., "Sub-Theme 2.4: Dimensioning and Detailing", Proceedings IABSE Colloquium on Structural Concrete, Stuttgart, April 1991.
11. MACGREGOR, J.G., "Sub-Theme 2.4: Dimensioning and Detailing", Proceedings IABSE Colloquium on Structural Concrete. Stuttgart, April 1991.
12. COLLINS, M.P. and MITCHELL, D., "Chapter 4 - Shear and Torsion", CPCA Concrete Design Handbook, Canadian Portland Cement Association, Ottawa, 1985, pp. 4-1–4-51.
13. COOK, W.D. and MITCHELL, D., "Studies of Disturbed Regions near Discontinuities in Reinforced Concrete Members", ACI Structural Journal, V. 85, No. 2, 1988, pp. 206-216.
14. KANI, M.W., HUGGINS, M.W., WITTKOPP, P.R., "Kani on Shear in Reinforced Concrete", Dept. of Civil Engineering, University of Toronto, Toronto, Canada, 1979, 225 pp.
15. ADEGHE, L.N. and COLLINS, M.P., "A Finite-Element Model for Studying Reinforced Concrete Detailing Problems", Publication No. 86-12, Dept. of Civil Engineering, University of Toronto, Toronto, Canada, Oct. 1986, 267 pp.
16. SO, K.M.P. "The Behaviour of Thin Stemmed Precast Prestressed Concrete Members with Dapped Ends", M.Eng Thesis, McGill University, Montreal, Canada, 1989, 155 pp.

Strut-Crack-and-Tie Model in Structural Concrete

Le modèle tirant-bielle-fissure en béton armé

Das Risswerkmodell – materialgerechtes Modell für Stahlbeton

Andor WINDISCH
Civil Engineer
Dyckerhoff & Widmann AG
Munich, Germany

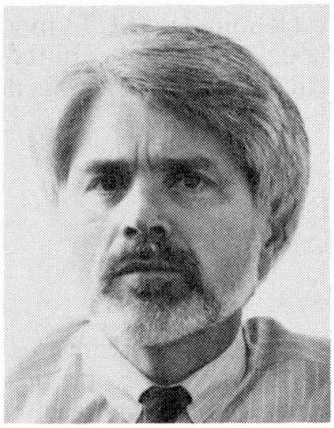

Andor Windisch, born 1942, obtained his Dr. techn. degree at the TU Budapest, Hungary in 1975. He served there as assistant professor for reinforced concrete structures until 1983. For 3 years he was research assistant at TU Stuttgart. He joined the R&D Department of a building company in 1987.

SUMMARY

The strut-crack-and-tie model, a synthesis of section-by-section design and strut-and-tie model, is presented. The geometry of the cracks and correspondingly that of the struts between cracks follow the linear elastic trajectories and can be predicted explicity. The material parameter of the model is the effective steel strength. It depends on the angle between a crack and the reinforcing bar crossing this crack. The concrete struts are assumed to be stressed biaxially. Applicability of the model to design and detailing is presented in an example.

RÉSUMÉ

Le modèle tirant-bielle-fisure est en fait une synthèse du calcul de résistance section par section et du calcul utilisant l'analogie du treillis. La géométrie des fissures, et donc des bielles en béton délimitées par ces fissures, suit les trajectoires linéaires élastiques et peut ainsi être prévue explicitement. Le paramètre de matériau du modèle est la résistance effective de l'acier, qui dépend de l'analyse formé par la fissure et la barre d'armature traversant la fissure. Les bielles de béton subissent une contrainte biaxiale. Un exemple illustre l'application de ce modèle dans le dimensionnement et les détails de construction.

ZUSAMMENFASSUNG

Das Risswerkmodell, eine Synthese der Querschnittsbemessung und des Stabwerkmodells, wird vorgestellt. Die Rissgeometrie und damit auch die Form und Richtung der dazwischenliegenden Druckstreben wird aufgrund des linear-elastischen Trajektorienbildes angenommen. Die wirksame Stahlfestigkeit, die vom Winkel zwischen Riss und Bewehrungsstab abhängt, dient als Materialparameter. Druckgurt und Druckstreben sind als zweiachsig beansprucht betrachtet. Die Anwendbarkeit des Modells zur Bemessung und zum Bewehren wird an einem Beispiel gezeigt.

1. INTRODUCTION

The section–by–section design for flexure and axial load in B regions is simple, rational and general but generally does not work in D regions. Attempts to adapt the classical 45–degree truss model to the results of shear and torsion tests made it complex, empirical and restricted.

Besides the diagonal compression field theory [1] and methods of dimensioning based on equilibrium solutions from the theory of plasticity [2] the strut–and–tie model [3] has been proposed as a unified design concept which is physical and consistent for all types of structures. Its development is not yet finished.

The paper presents the strut–crack–and–tie (SCT) model: a synthesis of the section–by–section design and the strut–and–tie model. The applicability of the SCT model at dimensioning and detailing of geometrical and statical discontinuities is demonstrated on a dapped end.

2. STRUT–CRACK–AND–TIE MODEL

2.1 Basic considerations

During loading of structural concrete (s.c.) structures first the concrete will crack. As a rule, the cracks are not straight (plain) and consist of a flexural crack and a shear crack. The loads can be increased as long as a) the reinforcement which crosses the cracks is able to carry the tensile forces which are necessary for the equilibrium in the cracked sections or b) the compressive strength of the concrete is reached in the compressive zone or in the web. S.c. structures or parts of them, where their failure is announced by yielding of the reinforcement are called normal–reinforced. Those where the reinforcement remains elastic at failure are called over–reinforced.

80–90 per cent of s.c. structures are normal reinforced. They will fail along one of their cracked sections. This section consists of a flexural–shear crack and a sliding (failure) surface across the compression zone. In case of pure bending only a flexural crack and a failure zone in the compression zone develop, their direction is perpendicular to the member's axis. In all other cases the failing sections are curved: in regions with flexure and shear they are cylindrical, while in those with torsion they are distorted. All these failing sections will be called further *sections.*

It was concluded that the load bearing capacity of normal–reinforced s.c. structures cannot be characterized neither with the concrete compressive strength nor with any reduction of this strength. The adjustment of a calculated ultimate bending moment to a test result, which was influenced by anything, will seldom function by the help of any reduction of the effective compressive strength, as it is well known, that the flexural capacity of a normal–reinforced section is quite insensitive to scatters in the concrete strength.

All these circumstances point out that the effective concrete compressive strength cannot be chosen as material parameter in any physical and consistent model for normal–reinforced s.c. structures.

In a second step a possible and reliable reason of the reduced load bearing capacity of D regions with geometrical discontinuity has been found.

Although each member in Figs. 1b–i contains the same bracket shown in Fig.1a, different additional flexural reinforcements are needed in the root sections of the brackets in cases c, d, f, g and i.

Analyzing the crack patterns of these regions it was found that at those members where additional reinforcement was needed, the direction of the flexural crack in the root section (at

the geometrical discontinuity) was not perpendicular to that of the usually horizontal flexural reinforcement (cf. Figs. 2a–i). It is well known, that reinforcing bars are less effective if they cross a crack at an angle less than 90°.

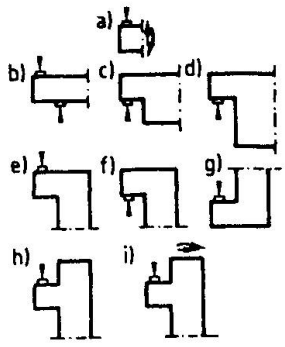

Fig. 1 D regions with the same loading but with partly different reinforcement

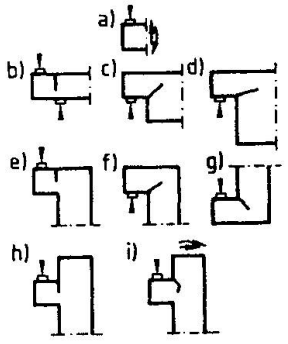

Fig. 2 Direction of flexural cracks in D regions shown in Fig. 1

The idea of the SCT model was born.

2.2 Definition of the SCT Model

The principal characteristic of the SCT model is a system of (cracked) sections. The form of the section depends on the member's geometry and the state of action effects. This form can be simply predicted. The sections are crossed by uniaxially stressed tension ties consisting of reinforcing and/or prestressing steel. The concrete compression struts between the cracks and the compression zone are stressed bi- or triaxially. The tensile strength of the concrete is an integral part of the model, its existence should be guaranteed by both structural and technological measures.

2.3 Selection of Strut–Crack–and–Tie Model

The procedure for laying out SCT models is straightforward omitting any trial and error efforts. Each designer will come with the same model which will reflect the natural load carrying mechanism of s.c. No obscure adaptation of the concrete to the strut–arrangement in the model is demanded. The designer may apply his ingenuity to find the most economic and aesthetic form of the structure.

Starting from a linear elastic analysis of uncracked members and their connections, after applying (if possible) a plastic moment redistribution, the form of the sections can be predicted directly using one and the same model. Instead of looking for the most valid model using minimum strain energy concepts etc. the most convenient reinforcement pattern (e. g. industrialized reinforcement) can be implied directly into the model.

2.4 Interaction of Flexure and Shear

The assumption that flexure and shear can be decoupled and considered separately is assumed to be the source of those troubles which are treated in both invited lectures [4], [5], e.g.:

- shear force carried by concrete
- enhanced shear strength of prestressed members
- shear strength of shear–unreinforced slabs.

If the biaxial state of stress and failure criteria resp. of the compression zone would be rediscovered [6], [7], [8], than all these aforementioned problems and many others could be solved.

In the SCT model the transversal (shear) component of the strength of the compressive zone is fully recognized. The contribution of aggregate interlock along a crack to the shear strength of a member can be easily taken into account at verification of the section's equilibrium.

SCT models indeed allow for consideration of internal forces due to shear, flexure, torsion and axial loads. As when applying this model always the equilibrium of the full member and not a single node is checked, the SCT model provides a real full–member design.

2.5 Material Strength

2.5.1 Steel in Tension

The strength of the steel in tension in ULS is taken as

$$f_{yd} = \Psi \cdot f_{yd}$$

where Ψ is an effectiveness factor, not greater than 1.0. This effectiveness factor accounts for the reduction of the useable strength of a rebar which is not perpendicular to the crack. Factor Ψ, a function of the angle α, shown in Fig. 3, was determined with extended computer calculations using realistic local bond stress – slip relationships, taking into consideration a) the distance between cracks having the characteristic crack width and b) the compatibility requirement that the crack width corresponding to $\alpha = 0$ should remain constant for any α value. The derivation of the effectiveness factor can be found in [9].

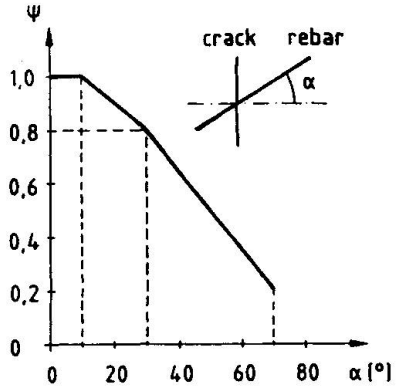

For $10° \leq \alpha = 30°$

$\Psi = 1.00 - 0.01\,(\alpha - 10°)$

for $30° \leq \alpha \leq 70°$

$\Psi = 0.80 - 0.015\,(\alpha - 30°)$

Applying the same factors at checking SLS, the proper performance of D regions can be expected, as it was confirmed by control calculations.

Fig. 3 Effectiveness factor Ψ of a skew rebar

2.5.2 Concrete

Compression struts are considered to be stressed biaxially. The components of the strength of a strut are

a) parallel to the strut's axis $D = b \cdot x \cdot f_{cd}$

b) perpendicular to it $\nu \cdot D$.

The assumption a) can be maintained in webs as well until no improved empirical verification of the opposite is available. It is felt, that the strains perpendicular to the strut will not influence very much the effective compressive strength. No evidence of any reduction in the compression zone due to the anchorage of highly stressed stirrups has been found until now. Obviously, reductions at effective web thickness due to ducts for prestressing elements but even to relative thick rebars which are not perpendicular to the strut's axis should be taken into account.

The factor ν in (b) can be deduced from the Mohr–failure–criterion in a similar way as in [6]. It gives a realistic and physical meaning to the V_c term.

No reduction of the concrete strength under loading plates or supports due to anchored tension bars is necessary. Obviously transverse reinforcement is required to "hang up" longitudinal rebars which lie outside the bearing plate, in order to avert a downward splitting of them.

2.6 D Regions

D regions classified in [3] as a) geometrical discontinuities, b) statical discontinuities and c) combination of a) and b) are interpreted in the SCT model as:

i) the flexural crack at the point of geometrical discontinuity is not perpendicular to any boundary of the region (cf. Fig. 2c, d, f, g and i)

ii) in the neighbourhood of the statical discontinuity only a part of the effective height of the member is really efficient and/or transverse reinforcement (due to bursting and spalling stresses) must be applied when the concrete stress under the loading plate is greater than f_{cd} (cf. deep beams).

Both, variation of the "efficient height", as function of the distance to the concentrated load and inclination of the flexural crack, as function of the linear elastic state of stress at the geometrical discontinuity, can be determined once and for ever and be comprised into quite simple rules.

Knowing the "efficient height" of a given section in a D region, the dimensioning to flexure can be carried out as in a B region: the beam theora can be applied. A similar procedure for deep beams has been suggested in [10].

2.7 Staggering Rule

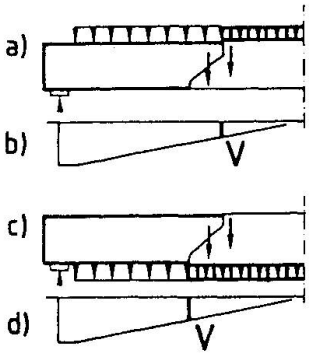

The form of the sections in both, B and D regions gives a direct interpretation of the required extension of the flexural reinforcement in presence of shear and of the staggering rules as well.

The beam shown in Fig. 4a is loaded on its top, that in Fig. 4c on its bottom. Each beam is divided in the same manner into two parts by a section. The inner forces along these sections substitute the loading on the parts at the right. The difference in the shear loads corresponding to the two sections is obvious (cf. Figs. 4b and d resp.).

Fig. 4 Staggering rule in beams loaded on their top and bottom resp.

It should be emphasised that SCT models are clearly intended to be behavioural models, thus they remain simple and transparent. The following example should verify it.

3. DAPPED END OF A PREFABRICATED GIRDER

Intensive linear elastic FE calculations showed that the inclination of the flexural crack at the reentrant corner of a dapped end can be taken as

$$\alpha = 90\, h_k / h \quad [°] \qquad (1)$$

Test results [11] confirmed the applicability of (1).

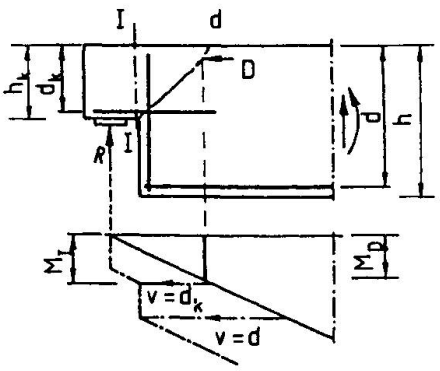

The flexural reinforcement at this corner must be dimensioned for the moment M_D (under the point of application of the compressive inner force on the section d–d shown in Fig. 5a. Applying the horizontal shifts v and v_k resp. due to the effect of the inclined shear crack, approximate the same moment is obtained under the conventional cross section I–I, which is to be dimensioned here actually.

Fig. 5 Dapped end: determination of the design moment for the corner section

At dimensioning the flexural reinforcement in this section the inclined position of the flexural crack relative to the reinforcing bars must be taken into account. If only horizontal reinforcement (A_{sh} in Fig. 6a) will be applied in the dapped end then the flexural equilibrium equation for section d–d in ULS is

$$M_D = M_I = A_{sh} \cdot \Psi_{(90° - \alpha)} \cdot f_{sd} \cdot z_k + A_{sv} \cdot \Psi_{\alpha} \cdot f_{sd} \cdot z_k \cdot \cot \alpha \qquad (2)$$

If inclined reinforcing bars (A_{ss}) will be added (Fig. 6b) then (2) must be extended with

$$A_{ss} \cdot \Psi_{(90° - \alpha - \beta)} \cdot f_{sd} \cdot z_k \cdot (\cos \beta + \sin \beta \cdot \cot \alpha) \qquad (3)$$

The flexural dimensioning of other sections on both sides of the reentrant corner can be performed in the well known manner, as each flexural crack there is perpendicular to the rebars (see Figs. 6c.)

The SCT model gives clear guidance for detailing as well: each rebar may be anchored "behind" that section, where its strength is no more required for maintaining equilibrium in ULS (see Fig. 6d).

Failure loads, calculated with a truss model [11] and SCT model are compared with test results [11] in Fig. 7. The SCT model approximates the test results better.

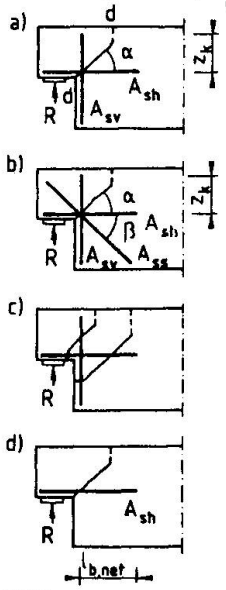

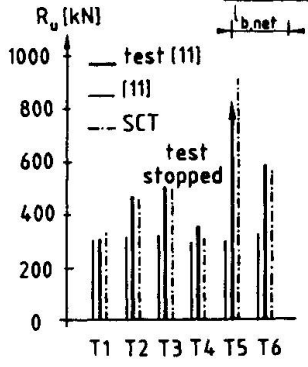

Fig. 6 Dimensioning of a dapped end a) without b) with additional inclined reinforcement at the corner c) at sections on both sides of the corner d) anchorage of the horizontal reinforcement

Fig. 7 Comparison of test results [11] with calculated failure loads

SCT models yielded excellent approximations for test results with other D regions as well [12].

REFERENCES

1. VECCHIO F.J., COLLINS M.P., The Response of R.C. to In–Plane Shear and Normal Stresses. Publ. No. 82–03. University of Toronto
2. NIELSEN M.P. et al., Concrete Plasticity, Beam Shear, .. Spec.Publ. TU Denmark, 1978
3. SCHLAICH J. et al., Towards a Consistent Design of R.C. Structures. JOURNAL PCI 1987
4. MACGREGOR J.G., Dimensioning and Detailing. Invited lecture, Sub–theme 2.4
5. MARTI P., Dimensioning and Detailing. Invited lecture, Sub–theme 2.4
6. WALTHER R., Über die Berechnung der Schubtragfähigkeit .. Beton u Stahlb. 1962.
7. KORDINA, K. et. al., Zur Schubtragfähigkeit von Stahlbeton . Beton u. Stahlb. 1987
8. ELZANATY A.H. et al., Shear Capacity of RC Beams .. ACI Journal, March–April 1986
9. WINDISCH A., Wirkungsgrad eines schiefen Bewehrungsstabs. Bauingenieur, 1991
10. LEONHARDT F., MÖNNIG E., Vorlesungen über Massivbau. Teil 2. Springer 1977
11. STEINLE A., ROSTASY P., Zum Tragverhalten ausgeklinkter Trägerenden. Beton+Fertigteiltechnik, Jun–Jul. 1975
12. WINDISCH A., Das Modell der charakteristischen Bruchquerschnitte. B. u.Stahlb. 1988

Models and Tests of Anchorage Zones of Post-Tensioning Tendons

Modèles et essais de zones d'ancrage des câbles de précontrainte

Modelle und Versuche von Verankerungszonen von Vorspannkabeln

Olivier L. BURDET
Scientific Associate
Fed. Inst. of Technology
Lausanne, Switzerland

Carin L. ROBERTS
Ph. D. candidate
Univ. of Texas
Austin, TX, USA

Gregory L. FENVES
Prof. of Civil Eng.
Univ. of California
Berkeley, CA, USA

David H. SANDERS
Prof. of Civil Eng.
Univ. of Nevada
Reno, NV, USA

John E. BREEN
Prof. of Eng.
Univ. of Texas at Austin
Austin, TX, USA

SUMMARY
This paper presents the results of an investigation of the behaviour and the design of anchorage zones of post-tensioning tendons. The analytical component is a combination of Finite Element Analysis and Strut-and-Tie Models. A total of more than 60 tests of anchorage zones are included in discussion and practical guidelines for the design proposed for incorporation in the AASHTO Bridge Design Specification are outlined.

RÉSUMÉ
Cet article présente les résultats d'un projet de recherche sur le comportement et le dimensionnement des zones d'ancrage des câbles de précontrainte. La partie analytique comprend à la fois une analyse par la méthode des éléments finis et des modèles de treillis. Au total, cet article inclut les résultats de plus de 60 tests expérimentaux de zones d'ancrage et inclut des directives pratiques qui ont été proposées pour être inclues dans la norme américaine de ponts routiers AASHTO.

ZUSAMMENFASSUNG
Im vorliegenden Bericht werden die Resultate eines Forschungsprojektes über das Verhalten und die Bemessung von Verankerungszonen von Vorspannkabeln beschrieben. Der analytische Teil beinhaltet sowohl Finite Element Berechnungen als auch Fachwerkmodelle. Die Resultate von mehr als 60 Versuchen an Verankerungszonen werden aufgeführt. Weiter enthält dieser Bericht praktische Richtlinien, die für die Aufnahme in die amerikanische Strassenbrücken-Norm AASHTO vorgeschlagen wurden.

1. Introduction

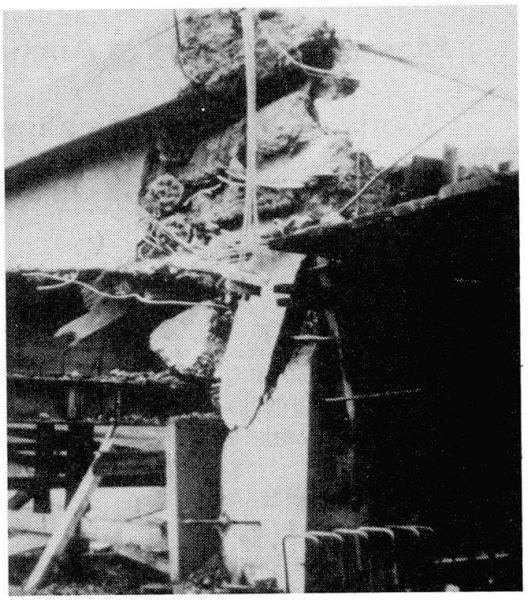

Figure 1: Failure of an Anchorage Zone in a Pedestrian Bridge during Construction

The quest for development of a consistent approach to structural concrete clearly requires a hierarchy of highly transparent design oriented analysis tools [2]. These will range from relatively traditional section mechanics principles suitable for use in B-regions to the more intuitive strut-and-tie models (STM) or more formal elastic or non-linear finite element analyses (FEA) required for the D-regions. Scordelis [12] indicates that while the latter are extremely useful, "... it is imperative that experienced and qualified structural engineers be involved in the interpretation of the results using their judgement and knowledge of structural behavior..." MacGregor [5] reiterates this need but gives special emphasis in the D-regions saying "... the details of the reinforcement in the discontinuities control the strength of these regions and hence must be considered by the structural engineer." Marti [6] suggests that in usual applications of STM, the design is rather insensitive to the assessment of the effective concrete stress, f_c. While this is true in many applications, it is clearly not true in design of post-tensioned anchorage zones. In such discontinuity zones, the very large forces transmitted to the concrete by the tendon anchorages cause very high local stresses on the concrete. The spreading of these forces through the member causes substantial transverse stresses and forces. Problems both at the serviceability limit state, with undesirable cracking, and at ultimate, with possible brittle and explosive failure of the anchorage zone need to be prevented.

Test results and failures during construction (See Figure 1) indicate that compressive stresses in unconfined nodes or at the intersection of confined nodes and unconfined struts often govern actual capacity of anchorage zones. This particular detailing application thus poses much more of a challenge to the development of detailing methods since assessing node and strut capacity is far more difficult than providing proper tie capacity through dimensioning of reinforcement.

This paper describes current progress on an on-going NCHRP sponsored study at the University of Texas at Austin to investigate the behavior of post-tensioning tendons anchorage zones, to provide guidance and to suggest specific provisions for anchorage zone design for the AASHTO Bridge Specification [1].

2. State of Stresses in an Anchorage Zone

The state of stresses in the anchorage zone of a post-tensioning tendon is very complex. Within very short distances, the stresses parallel to the tendon vary from very high compressions (often in excess of the uniaxial compressive strength of the concrete) ahead of the anchorage device to the average compressive stress induced by the post-tensioning, usually in the vicinity of $0.45f_c'$. Perpendicular to the axis, the stresses vary from very high compressive stresses under the device to tensile stresses which often exceed the tensile capacity of the concrete at a certain distance from the anchorage. Figure 2 identifies the major areas of tensile stresses in a simple anchorage zone. The tensile force caused by the lateral spreading of the tendon force from the anchorage device to the entire cross section is often called bursting force in the literature. The force parallel to the concrete surface has in the past often been called spalling force. Because this term implies that this force can cause spalling of the concrete, which is not the case because the force acts parallel to the face of the concrete, and not perpendicular to it, it is more appropriate to call it *edge tension force*. Edge tension forces also occur between anchorages acting on the same concrete surface, and on faces parallel to the axis of the tendon.

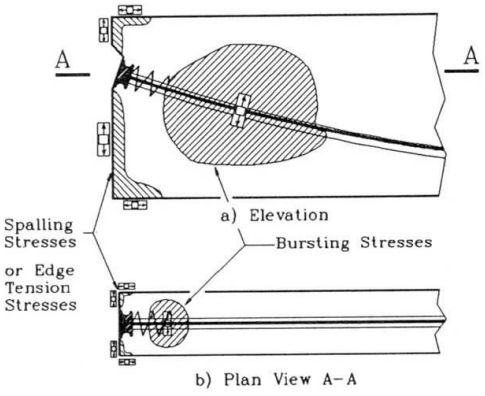

Figure 2: Tensile Stresses in the Anchorage Zone

3. Local Zone - General Zone Concept and Modes of Failure

As a consequence of the complex state of stresses, various modes of failure have been observed for anchorage zones. Aside from failures caused by insufficient material properties or lack of equilibrium, the failures of anchorage zones can be categorized as follows:

- Local compression failure, in which the failure occurs at a very short distance from the anchorage device, and is caused by lack of confinement in the area immediately surrounding the anchorage device.
- Compression failure, similar to the previous mode failure, but with the difference that the failure occurs at a larger distance from the anchorage device, which is itself sufficiently confined.
- Tension failure, in which the reinforcement provided to resist the tensile force induced by the spreading of the concentrated tendon load is insufficient.

Figure 3 shows two regions in the anchorage zone. The *local zone*, in the immediate vicinity of the anchorage device, is highly dependant on the post-tensioning system and is the responsibility of the supplier of the anchorage device. The *general zone* is more remote from the anchorage device and is less influenced by the post-tensioning system. It is the responsibility of the structural engineer. Of the three modes of failure described above, the first one occurs in the local zone, the second mode of failure occurs in the general zone, most often at the interface with the local zone, and the third mode of failure occurs in the general zone.

In order for anchorage devices to be deemed satisfactory, they need to either meet maximum bearing stress and minimum stiffness requirements or to be tested following a prescribed testing procedure described in Section 4. The distinction between local and general zone gives flexibility to the constructor, who can choose the anchorage device and the post-tensioning system, without jeopardizing the integrity of the structure, and without unduly complicating the work of the design engineer.

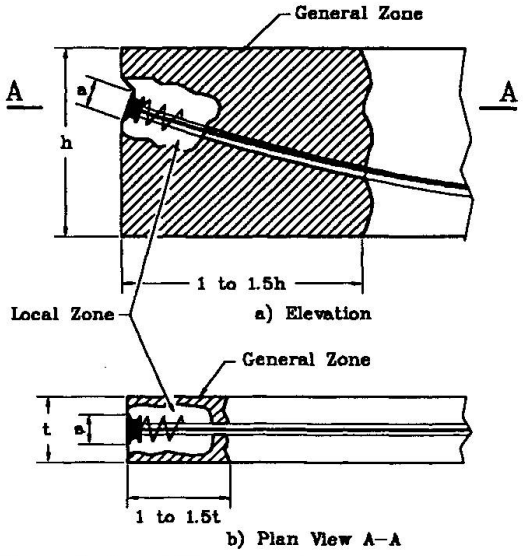

Figure 3: Local Zone and General Zone

4. Local Zone Tests by Roberts

A part of the NCHRP Anchorage Zone research project consisted in an investigation focusing on the behavior of local anchorage zones both at service state and at ultimate. The purpose of this study by Roberts [9] was to define the test procedures and compliance criteria for the testing of anchorage devices. Roberts tested 31 local zone test specimens. The behavior of local anchorage zones was found to be sensitive to the type and amount of confining reinforcement, as well as to the cover provided around the anchorage device. Existing formulae by Richart [8] and Nyogi [7] were enhanced to give a better prediction of the strength of a local zone. Cyclic testing of local zones gives results similar to extended (48 hours) testing, and is more representative of the behavior of anchorage zones under field conditions than monotonic testing. A standardized testing procedure for the local zone was proposed by Roberts for introduction in the AASHTO Bridge Specification.

5. Finite Element Analysis and Strut-and-Tie Models

It is nor practical to test all possible general zone configurations, therefore the design of the general zone must be approached in a different manner than the local zone. The number of variables affecting the design of the anchorage zone remains large even though the local zone has been addressed. A survey of the current design practice in the United States by Sanders [10] showed that the post-tensioning industry is very creative. Tendons often present an eccentricity, an inclination and a curvature in the anchorage zone. Multiple tendons are commonly used, in groups of two to six tendons. Transverse post-tensioning and transverse reactions are often present in the anchorage zone. Special geometries are used to introduce the post-tensioning force to the section, using for example blisters or ribs. The first phase did not consider the expanding field of external post-tensioning. The project was set up to use a combination of elastic finite element analysis, strut-and-tie models and physical tests. Linear elastic finite element analysis offers the advantage of being a well known method of obtaining the internal state of stresses in a body. As pointed out by

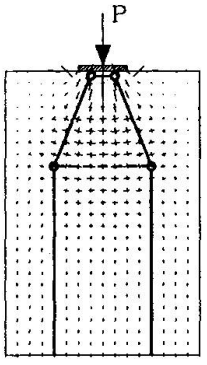

Figure 4: Simple Strut-and-Tie Model with Elastic Stress Vectors

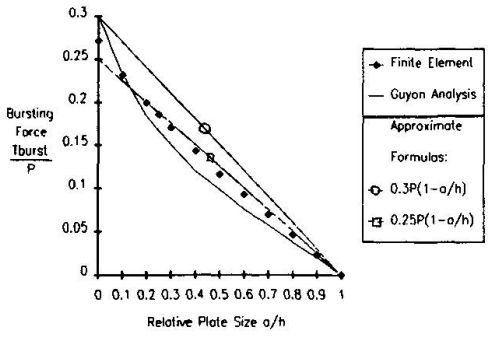

Figure 5: Bursting Force for Concentric Tendons

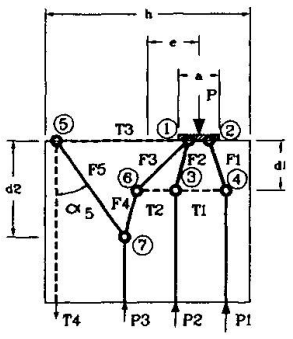

Figure 6: Strut-and-Tie Model of an Eccentric Anchorage Zone

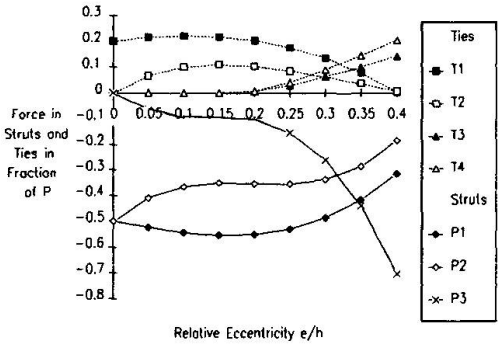

Figure 7: Forces in the Struts and Ties as a Function of the Eccentricity

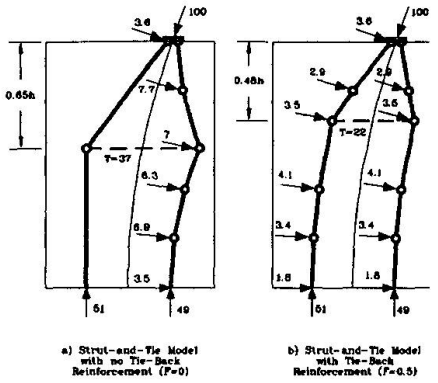

Figure 8: Strut-and-Tie Model of an Anchorage Zone with a Curved Tendon, Eccentricity 0.25h and Initial Inclination 20 degrees

Schlaich [11], the elastic state of stresses constitutes a good starting point for the development of strut-and-tie models. Of special interest is the representation of the principal stress vectors shown in Figure 4. These vectors give a good idea of the flow of forces through the anchorage zone and are helpful in assessing the adequacy of a strut-and-tie model. The physical test specimens by Sanders [10] were used to demonstrate the validity of the models and to calibrate the design formulae.

Figure 5 shows the bursting force obtained by integrating the elastic stresses perpendicular to the tendon path, along with the force obtained from the simple strut-and-tie model shown in Figure 4. As can be observed, the correlation is quite good. The figure also shows Guyon's equation [4] for the same force.

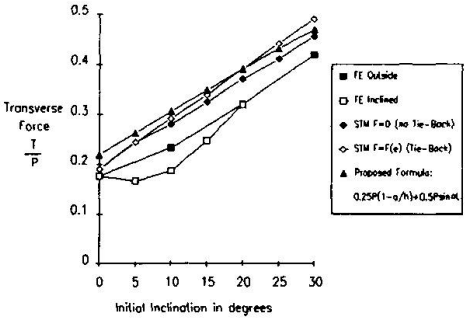

Figure 9: Transverse Bursting Force as a Function of the Initial Inclination for an Initial Eccentricity of 0.25h

The real power of the strut-and-tie model is its ability to model a wide range of anchorage zone configurations. Figure 6 shows a strut-and-tie model for an anchorage zone with an eccentric load. Figure 7 shows the forces in the various members as a function of the eccentricity.

Figure 8 shows two possible strut-and-tie models for an anchorage zone with an eccentricity, an inclination and a curvature of the tendon. If no tie-back reinforcement is provided, all the tendon deviation forces are transmitted to the strut on the inside of the tendon, and the external strut is straight between the reinforcement bars. If tie-back reinforcement is provided, the tendon deviation forces are distributed to both compression struts. If the force in the tie-back reinforcement is added to the bursting force, it is found that the sum is approximately equal to the bursting force in the case without tie-back reinforcement. Figure 9 shows the variation of the bursting force as a function of the initial inclination. The figure also shows the results obtained from the finite element analysis and the values predicted by an approximate formula as outlined in Section 6. In a simplified fashion, the increase in tensile force caused by the inclination of the tendon can be approximated as one half of the net shear on the general zone summing the effect of external loads and the transverse component of the post-tensioning force. This corresponds to the intuitive idea that roughly half of the force is resisted by each compression strut.

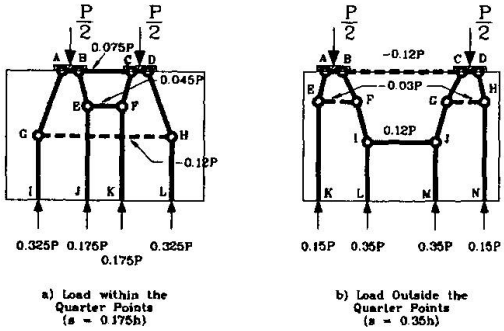

Figure 10: Examples of Strut-and-Tie Models with two Tendons

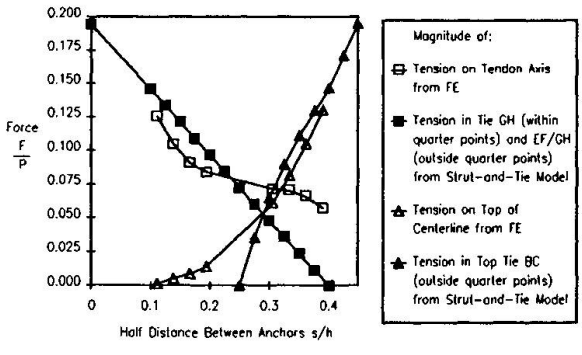

Figure 11: Tension Forces in an Anchorage Zone with Two Tendons

The effect of groups of tendons was investigated, and it was found that, for rectangular sections with straight tendons, the largest tensile forces are induced when only two tendons are used. Figure 10 shows the two basic configurations for two anchorages. If both tendons act within the kern of the section, the state of stresses is similar to that induced by a single anchorage device. As the tendons move outside the kern, an increasingly large edge tension force is induced between the anchorage devices close to the surface of the concrete. Figure 11 shows the edge tension force between the anchorages as a function of the spacing of the anchorages.
Because the compressive stresses in the immediate vicinity of the anchorage device are usually higher than the uniaxial compressive strength of the concrete f'_c, the verification of the capacity of the concrete compression struts is critical. Most authors assume that the limiting stress in the concrete struts is some fraction of f'_c, which is too constraining for anchorage zones. Sanders [10] incorporated the effect of confining reinforcement in a strut-and-tie model. For most practical cases, however, the checks involved in such calculations are beyond the capabilities of the engineer. Therefore, the local zone acceptance tests are relied on for determining the adequacy of the confined node. The critical section for the verification of the compressive stresses in the concrete struts is defined at a certain distance from the anchorage device (in general at one times the lateral dimension of the anchorage device). This allows one to check the compressive stresses in the concrete against the conventional value of $0.70f'_c$ which is commonly accepted for strut-and-tie models.

6. Design Method for Anchorage Zones

The goal of the NCHRP Anchorage Zones research project is the elaboration of a clear, consistent and easily applicable method for the design of anchorage zones of post-tensioning cables. Assuming that the engineer has a good knowledge of the location and magnitude of the force for each tendon, some idea of the size of the anchorage device that will be required to transmit the force and the assurance that the anchorage device used satisfies the testing requirements of Section 4, guidelines for the design of the general anchorage zone are needed. A number of procedures are suggested in the proposed AASHTO revisions. Two general procedures are allowed. One is a detailed elastic analysis such as a valid finite element analysis (FEA). Rules are provided for integrating tensile stresses and selecting appropriate limiting stress values. The second procedure allowed is the strut-and-tie model (STM). Since this equilibrium based procedure is not sensitive to compatibility induced stresses at service load levels, such as edge tension, or spalling stresses around anchorages, certain guidelines are provided requiring supplemental spalling crack control reinforcement. Recognizing that either FEA or STM solutions may require considerable extra effort for the design of some relatively simple but common applications, an approximate procedure is also included. This procedure was developed from the results of FEA and STM parametric studies [3]. It uses relatively simple formulae to determine the magnitude and location of the bursting force and to check the compressive stress at the interface between the local zone and the general zone. It is limited to the case of a single anchorage, or of a single group of closely spaced anchorages acting on a rectangular cross section.

7. Evaluation of the Methodology based on Test Results by Sanders

Sanders [10] conducted a series of 36 tests of anchorage zones. In the specimens modelling single tendon anchorage zones, the reinforcement patterns and the tendon eccentricity, inclination and curvature were varied. Tests of anchorage zones with multiple tendons were also conducted, with the prime variable being the spacing between the anchors. The cracking load of 31 of the specimens by Sanders was estimated based on the elastic stress distribution obtained from a two-dimensional Finite Element Analysis. and the tensile strength of the concrete measured from split-cylinder tests. The average ratio of actual to predicted cracking load is 0.91, with a standard deviation of 0.22. Figure 12 shows the ultimate load reached by the same series of specimens, along with the ultimate load predicted using strut-and-tie models based on elastic stress resultants at the end of the general zone. The average ratio of predicted to ultimate is 1.44, with a standard deviation of 0.44. Sanders [10] developed enhancements to the cracking load prediction, including the effect of the reduction of the tensile strength of the concrete caused by the three-dimensional state of stresses in the anchorage zone. Taking this modification into account, the average ratio of actual to predicted cracking load becomes 1.05 for all tests, with a standard deviation of 0.20. For the ultimate load, Sanders also developed an enhanced STM which includes the effect of a limited plastification of the concrete in the immediate vicinity of the anchorage device. Taking this modification of the model into account brings the average ratio of the predicted ultimate load to the actual ultimate load to 1.19, with a standard deviation of 0.19.
One of the most notable observations made during the evaluation of the test results is the fact that in the large majority of the cases, the capacity of the anchorage zone is controlled by the strength of the compression struts at the interface between the local zone and the general zone. At this location the concrete has no confinement, and is exposed to very large compressive stresses. Thus, increasing the reinforcement of the general anchorage zone will in many case lead to little or no improvement of the overall strength of the anchorage zone. This is confirmed by the observation of Stone and Breen [13], who noted that increasing the amount of orthogonal reinforcement

(the reinforcement provided in the general zone) is not nearly as effective as using longer and heavier spirals, which confine the local zone and have the effect of displacing the interface between the local zone and the general zone to an area of lower compressive stresses. For design purposes, it is in any case advisable to remember that the stresses in the concrete struts often control the design. Also notable is the effect of tensile stresses existing in the anchorage zone. The resistance these stresses provide is usually neglected in the design, but it nevertheless plays an important role in the behavior of anchorage zones. In several cases it was observed that the strength of the anchorage zone exceeded that predicted based on the capacity of the tension ties alone. Burdet [3] suggests that this additional strength is caused by the fact that a part of the concrete at the base of the specimens remained uncracked up to failure, thus providing an additional tensile capacity to resist bursting forces.

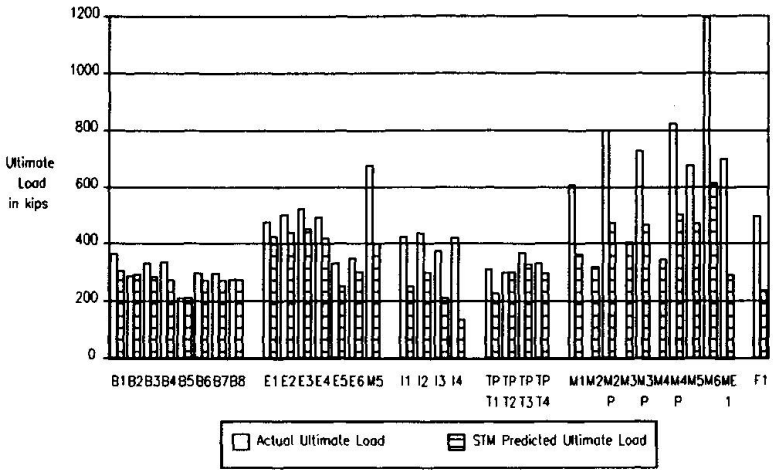

Figure 12: Actual Ultimate Load and Predicted Ultimate Load for Sanders' Test Specimens (1 kip = 4.54 kN)

8. Conclusions

The analysis, behavior and design of anchorage zones of post-tensioning tendons was investigated using a combination of Finite Element Analysis, Strut-and-Tie Models and experimental test specimens. This combination allowed minimization of the number of required experimental specimens and generalization the results in the form of simple design formulae. A consistent design methodology allowing use of finite element analyses, strut-and-tie models, and for certain frequently occurring cases, relatively simple design formulae was developed and has been proposed for inclusion in the AASHTO Bridge Design Specification. A standard testing procedure for anchorage devices and their necessary confinement was also proposed.

The cracking loads computed based on the elastic stresses and the split cylinder strength of the concrete are slightly smaller than the actual cracking loads, possibly because of the detrimental effect of the transverse compression. The ultimate capacity of anchorage zones can be conservatively predicted using the Strut-and-Tie Model. This investigation clearly indicates the critical nature of the compressive struts in anchorage zones. This differs from many other D-region applications in which the struts are not as criotical.

References

[1] American Association of State Highway Transportation Officials (AASHTO),"Standard Specification for Highway Bridges", 13th edition, 1983.

[2] Breen, J.E., "Why Structural Concrete," Final Report IABSE Colloquium on Structural Concrete, Stuttgart, April 1991.

[3] Burdet, O.L., "Analysis and Design of Anchorage Zones in Post-Tensioned Concrete Bridges," PhD dissertation, University of Texas at Austin, May 1990.

[4] Guyon, Y., "Prestressed Concrete," John Wiley and Sons, New York, 1953

[5] MacGregor, J.G., "Sub-Theme 2.4 - Dimensioning and Detailing," Final Report IABSE Colloquium on Structural Concrete, Stuttgart, April 1991.

[6] Marti, P., "Sub-Theme 2.4 - Dimensioning and Detailing," Final Report IABSE Colloquium on Structural Concrete, Stuttgart, April 1991.

[7] Nyiogi, S.K., "Bearing Strength of Reinforced Concrete Blocks," ASCE Structural Division Journal, Vol. 101, No ST5, May 1975.

[8] Richart, F.E., Brandtzaeg, A., and Brown, R.L., "A Study of the Failure of Concrete under Combined Compressive Stresses," Research Bulletin No 185, University of Illinois Engineering Experimental Station, 1928.

[9] Roberts, C.L., "Behavior and Design of the Local Anchorage Zone in Post-Tensioned Concrete," MS thesis, University of Texas at Austin, May 1990.

[10] Sanders, D.H., "Design and Behavior of Post-Tensioned Concrete Anchorage Zones," PhD dissertation, University of Texas at Austin, August 1990.

[11] Schlaich, J., Schäfer, K., Jennewein, M., "Towards a Consistent Design of Structural Concrete," PCI Journal, Vol. 32, No 3, May-June 1987, pp 74-151.

[12] Scordelis, A.C., "Analysis of Structural Concrete Systems," Final Report IABSE Colloquium on Structural Concrete, Stuttgart, April 1991.

[13] Stone, W.C., Breen, J.E., "Behavior of Post-Tensioned Girder Anchorage Zones," Center for Transportation Research Report No 208-2, University of Texas at Austin, January 1981.

Dimensioning of the Nodes and Development of Reinforcement

Dimensionnement nodal et développement de l'armature

Bemessung von Knoten und Entwicklung von Bewehrungen

Konrad BERGMEISTER
Research Associate
Univ. of Stuttgart
Stuttgart, Germany

John E. BREEN
Prof. of Civil Eng.
Univ. of Texas at Austin
Austin, TX, USA

James O. JIRSA
Prof. of Civil Eng.
Univ. of Texas at Austin
Austin, TX, USA

SUMMARY

This paper presents a proposal for the dimensioning process of nodal zones. Based on test results an efficiency factor for cylinder compressive strength from 20 to 80 MPa is proposed. In order to optimize the nodes, some geometrical constraints as well as an equation for the development length for straight bars under lateral pressure (CCT-, CTT-nodes), are also presented.

RÉSUMÉ

Cet article présente une proposition de dimensionnement des zones nodales. Basé sur des résultats d'essais, un facteur d'efficacité pour la résistance en compression de cylindres en béton de 20 à 80 MPa est présenté. On propose aussi quelques restricitions géométriques, ainsi qu'une équation pour les longueurs d'ancrage des barres droites soumises à effort tranchant, et ceci en vue de l'optimisation des nœuds.

ZUSAMMENFASSUNG

In dieser Veröffentlichung wird die Bemessung von Knotenbereichen aufgezeigt. Aufbauend auf Versuchen wird ein Vorschlag für die Wirksamkeit der Zylinderdruckfestigkeit von 20 bis 80 MPa vorgestellt. Sowohl geometrische Bedingungen als auch eine Gleichung für die Verankerungslänge von geraden Bewehrungsstäben mit Querpressung (CCT-, CTT-Knoten) sollen zur Optimierung von Knotenbereichen beitragen.

1. INTRODUCTION

Recent advances in the understanding of the behavior of concrete structures have resulted in more sophisticated methods of analysis. Computer based methods enable the elastic- and inelastic analysis of highly indeterminate and non-linear structures. For the majority of structures however it is unnecessary and inefficient to replicate the entire structure as a strut-and-tie-model (STM). Rather, it is more convenient and common practice to first carry out a general structural analysis, and then to subdivide the given structure into B-regions and D-regions [1]. It utilizes the well-known principle of Saint Venant which provides that local stresses may be assumed negligible at a distance h_D. For practical applications the following approaches as illustrated in Fig. 1 are suggested, and the total area of zone 2 + zone 1 + zone 2 is the effective D-region [2].

2. NODE BACKGROUND

D-regions usually contain either smeared or singular nodes. The singular nodes are more critical and need more attention. The following dimensioning and anchorage requirements must be applied to either smeared or singular nodes. The stress peaks in smeared nodes are less critical because a greater amount of surrounding concrete is normally available. The node of the STM represent the location of change of direction of internal forces. Evaluation of the nodal zones includes checking the nodal boundary stresses an determining reinforcement development requirements for nodes which contain tension ties.

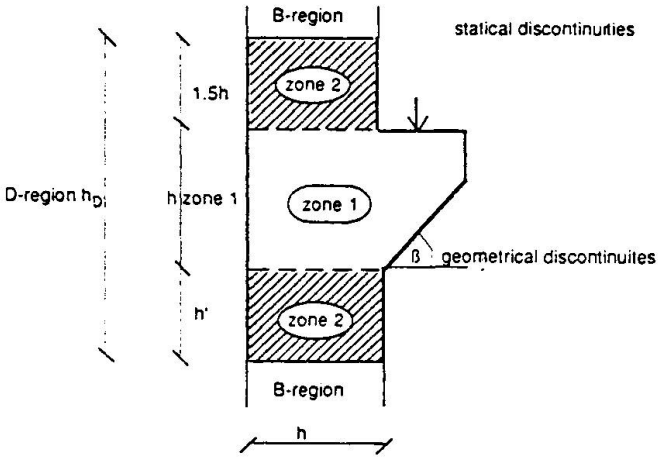

Fig. 1 Suggested subdivison of structure

2.1 Concrete efficiency factor

In general, the effective strength, f_{ce}, available for use in the struts is chosen as some fraction of the concrete compressive strength, f_c. It is given as the product of an efficiency factor, v_e, and the 28 day cylinder compressive strength. The efficiency factor should take into account the following parameters:

- multiaxial state of stress
- disturbances from cracks
- disturbances from reinforcement
- friction forces
- aggregate interlock after cracking
- dowel forces
- time dependence

$$f_{ce} = f_c \cdot v_e \qquad (1)$$

Various proposals for the efficiency factor have been presented. They are usually based on tests of continuous compression fields generated either in thin-web beams or thin

shear panels, although some appear to be based largely on engineering judgement. Empirical relations for the concrete efficiency factor of concrete struts in beam webs as suggested by Nielsen et al. [3], Ramirez and Breen [4], Collins and Mitchell [5] are summarized below:

- Nielsen et al. [3]: $\nu_e = 0.7 - f_c / 200$ $f_c <$ 60 MPa (2)
- Ramirez, Breen [4]: $\nu_e = 2.82 / \sqrt{f_c}$ $\sigma_c < 2.5\sqrt{f_c}$ MPa (3)
- Collins, Mitchell [5]: $\nu_e = 1 / (0.8 + 170\ \varepsilon_1)$ (4)

$$\varepsilon_1 = \varepsilon_x + (\varepsilon_x + 0.002)\cot^2\theta_{cs} \quad \varepsilon_x = 0.002$$

Marti [6] suggested as a reasonable average value for the nodal zone $\nu_e = 0.6$. Schlaich et al. [1] propose values between 0.4 (extraordinary cracks) and 1.0 (undisturbed).

In many applications, substantial confining reinforcement may be present so as to greatly increase the efficiency factor for concrete in compression.
A total of 122 tests have been evaluated using the following approach [2]
(see Fig. 2):

$$f_{ce3} = \nu_e\, f_c\, (A/A_b)^{0.5} + (A_{core}/A_b)\, f_{lat}\, (1 - s/d) \quad \text{[MPa]} \quad (5)$$

$$\nu_e = 0.5 + 1.25 / \sqrt{f_c} \quad \text{[/]} \quad (6)$$

f_{ce3} = confined concrete strength [MPa]
d = equivalent diameter = side length of confined square core [mm]

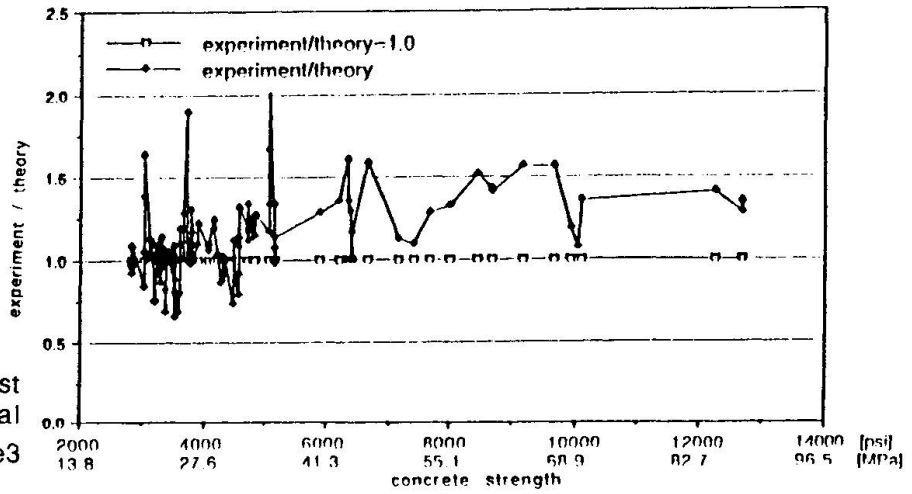

Fig. 2 Comparison of test results with theoretical approaches for predicting f_{ce3}

The proposed equation for the effective confinement strength is a generally conservative and safe approach. The 5%-fractile (m-2σ = 1.124−2*0.238) would be 0.65 which is also the minimum actual test value. The efficiency factor may be used with a concrete strength of up to 80 MPa.

2.3 Anchorage requirements in the nodal zone

All nodal zones are influenced by the tension tie anchorage details. If the resistance to applied tensile force is provided by bearing plates and does not rely appreciably upon bond stresses, then the tie actually provides a compression strut in terms of its action on the nodal zone (positive anchorage details). However, such positive anchorages are not

necessarily required nor are they always desirable or practical construction alternatives for anchoring tensile ties. In CCT- and CTT-nodes the reinforcing bars are under lateral pressure from the compressive strut. When lateral pressure is applied, the bond strength increases approximately in proportion to the square root of the lateral pressure. In addition, the distance between the bearing plate and the reinforcing bar, "e", has an important effect as shown in the study by Lormanometee [7]. Various experimental studies were evaluated to develop a formulation for a possible reduction of the development length for a reinforcement bar under lateral pressure. Only tests in which failure occurred before the bars yielded were included. The lateral pressure acts similar to the action of transverse reinforcement. Based on a comprehensive review of a broad range of test results [2], the development length,"l_d", with transverse reinforcement,A_{tr}, and lateral pressure,f_n, can be expressed as follows:

$$l_d = \frac{d_b \{(3 f_s / [(f_c')^{0.5}] - 50\}}{\{1.2 + 3c/d_b + (A_{tr} f_{yt})/(3.4 s d_b) + [(f_n)^{0.5} (2.4 - e^2/58000)]\}} \quad [mm] \qquad (7)$$

$$(A_{tr} f_{yt}) / (3.4 s d_b) \leq 3.0 \qquad (8)$$

$$0 \leq [(f_n)^{0.5} (2.4 - e^2/58000)] \leq 6.0 \qquad (9)$$

d_b	=	bar diameter	[mm]
f_s	=	stress in the bar at the critical section	[MPa]
f_{yt}	=	yield strength	[MPa]
s	=	spacing	[mm]

The proposed equation take the lateral pressure into account to a distance e = 350 mm.

3. CHECKING AND DIMENSIONING NODES

3.1 Checking and dimensioning CCC-, CCT- and CTT-nodes

The following equation is proposed for confined concrete strength:

a) Unconfined nodes without bearing plates:

$$\sigma \leq f_{ce} / \gamma \qquad (10)$$

$$f_{ce} = \nu_e f_c \leq 2.5 f_c \qquad (11)$$

b) Confined nodes

$$f_{ce3} = [(\nu_e f_c (A/A_b)^{0.5} + (A_{core}/A_b) f_{lat} (1 - s/d)^2)] \leq 2.5 f_c \qquad (12)$$

α = 4.0 for spiral confinement
= 2.0 for square confinement with longitudinal reinforcement
= 1.0 for square confinement without longitudinal reinforcement

$$f_{lat} = \text{lateral pressure} = 2 f_y A_s / (d s) \qquad (13)$$

c) Unconfined nodes with bearing plates (e.g CCT- and CTT-nodes)
For CCT- and CTT- nodes the width of the strut can be found by considering geometrical constraints such as bearing plates and by assuming that the effective

width of the tensile tie is governed by the dimensions from the inside to the outside reinforcement layer.

$$f_{ce3} = \nu_e f_c (A/A_b)^{0.5} \leq 2.5 f_c \quad (14)$$

$$A/A_b \leq 4 \quad (15)$$

d) Triaxially confined nodes
The increase in strength due to three-dimensional states of compressive stresses may be taken into account if the simultaneously acting transverse compressive stresses are considered reliable. This may be particularly appropriate if supplementary transverse prestressing is applied.

$$f_{ce3} = 2.5 f_c$$

In order to optimize the CCT-node both stresses at the C_1 and C_2 faces should be the same (hydrostatic stress). Fig. 3 shows the geometric inter-relation of the strut width, w_{1C}, the tie width w_{T3}, and the angle ϕ_{cs}. If the reinforcement is welded or bolted to the anchor plate, the stress configuration in the node is similar to that in a CCC-node.

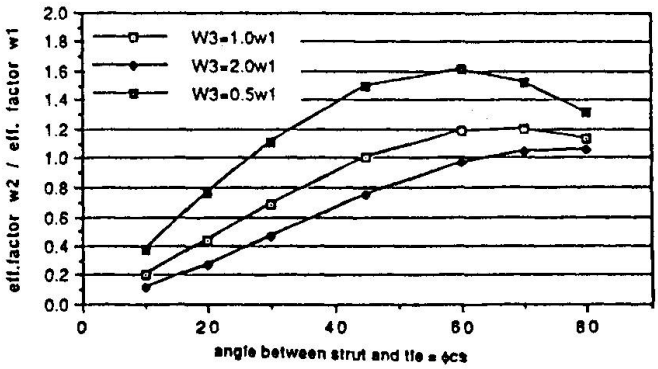

Fig. 3 Dependency of ν_e for CCT-node

When designing a CTT-node the reinforcement in both ties should yield at the same time. Since the compression strut,w2, is dependent on the tension tie widths,w1, and w3, the optimal concrete efficiency is given by the angle with the largest compression strut w2.

Tests by Bouadi [8] with CCT-nodes have shown that confining reinforcement has only a low effect (≈2%) on the failure load. Similarly, for the CTT-node (tests by Anderson [8]) in which the transverse reinforcement anchorage hooks were turned nearly parallel to the longitudinal bars (but not closed), the ultimate load decreased by only 4% compared with closed confining reinforcement.

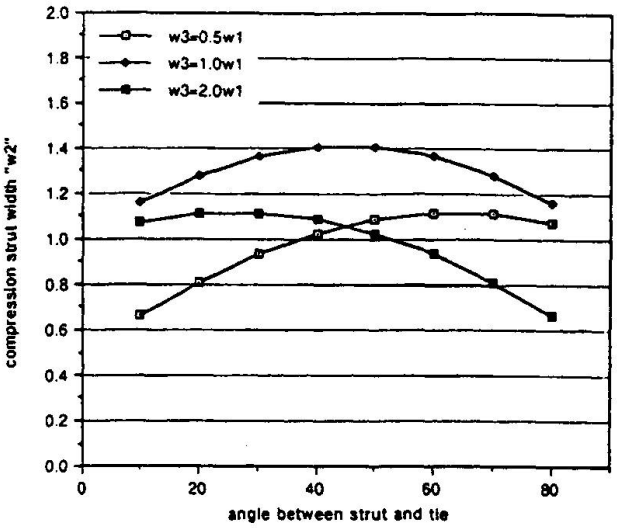

Fig. 3 Dependency of ν_e for CTT-node

By using vertically oriented hooks instead of long bars for the anchorage, the ultimate load decreased by 8% for CCT-nodes. This decrease is probably not significant given the other uncertainties in the design process. The advantage of hooks is that the required anchorage length can be minimized. Using a transverse U for the second tie in CTT-nodes provided lateral confinement, but prying action at the 90° bend can produce splitting cracks. In order to control splitting cracks of the end cover it is suggested that the longitudinal reinforcement be extended a short distance (≈s/2 or 50 mm) past the transverse reinforcement.

3.2 Checking and Dimensioning TTT - nodes

For TTT-nodes it must be evident that satisfactory behavior and adequate strength can be attained only by the efficient interaction of concrete and steel.

In details where the length available for end anchorage may be so short that only special devices can ensure the development of the required bar strength. For TTT-nodes the largest tensile tie should be anchored with looped - or hooked bars (Fig. 4). The stirrup spacing "s" must be so selected that the cover will not break away between two stirrups when the curved bar tends to straighten.

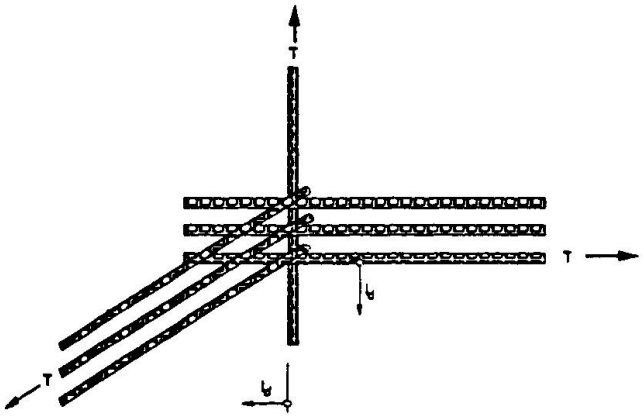

Fig. 4 TTT-node with looped bar

4. CONCLUSIONS

Some guidelines are given for the dimensioning process for the nodal zones. More research on this topic is needed as well as improved guidance for the serviceability control.
In order to satisfy the requirements of the theory of plasticity, a model must be in equilibrium under the applied loads. However, if the selected strut and- tie- model is to fully develop, the load carrying capacity of the strut- and- tie- elements and the rotational capacity of the nodes must not be exceeded before the ties yield. In addition the accepted standards for bar spacing, minimum reinforcement to control creep and thermal stresses should be applied.

REFERENCES

1. SCHLAICH, J.; SCHÄFER, K.: Konstruieren im Stahlbetonbau (Design for Concrete Structures). Betonkalender, 1989, pp. 563-715
2. BERGMEISTER, K.; BREEN, J.E.; JIRSA, J.O.; KREGER, M.E.: Detailing for Structural Concrete. Research Report 1127-3F, Center for Transportation Research, October, 1990
3. NIELSEN, M.; BRAESTRUP, N.; JENSEN, BACH. F.: Concrete Plasticity: Beam Shear-Shear in Joints - Punching Shear. Specialpublication - Dansk Selskab for Bygningsstatik, Lyngby, 1978, 129 pp.
4. RAMIREZ, J.; BREEN, J.: Proposed Design Procedures for Shear and Torsion in Reinforced and Prestressed Concrete. Research Report 248-4F, Center for Transportation Research, 1983
5. MITCHELL, D.; COLLINS, M.: Diagonal Compression Field Theory - A rational Model for Structural Concrete in pure Torsion. ACI-Journal, August, 1974
6. MARTI, P.: Dimensioning and Detailing, Final Report, IABSE Colloquium Structural Concrete, Stuttgart, April, 1991
7. LORMANOMETEE, S.: Bond Strength of Deformed Reinforcing Bar under Lateral Pressure. Master's Thesis, The University of Texas at Austin, 1974
8. BARTON, D.L.; ANDERSON, R.B.; BOUADI, A.; JIRSA, J.O.; BREEN, J.E.: An Investigation of Strut- and Tie Models for Dapped Beam Details. Research Report 1127-1, Center for Transportation Research, February 1990

Current Design Methods for Frame Connections

Méthodes ordinaires de dimensionnement des connexions des cadres

Gewöhnliche Entwurfsmethoden für Rahmenknoten

S.J. PANTAZOPOULOU
Assist. Prof.
Univ. of Toronto
Toronto, ON, Canada

S.J. Pantazopoulou holds a Civil Eng. degree from the National Techn. Univ. of Athens, and M.Sc. and Ph.D. degrees from the Univ. of California at Berkeley. She is a member of ACI Committee 368 and associate member of the joint ACI-ASCE Committee 352.

John F. BONACCI
Assist. Prof.
Univ. of Toronto
Toronto, ON, Canada

John F. Bonacci received B.S., M.Sc. and Ph.D. degrees in Civil Eng. at the Univ. of Illinois-Urbana. He is a member of the joint ACI-ASCE Committee 352 and ACI Committee 408. He is also an associate member of the joint ACI-ASCE Committee 442.

SUMMARY

Current requirements for lateral load design of beam-column joints are either on equilibrium considerations (CEB and New Zealand Codes), or are empirically derived from experimental data (ACI Code). As a result, deformations associated with the design limit states are not considered in evaluating the performance of connections. An alternative approach, satisfying both equilibrium and compatibility requirements is discussed in this paper. The proposed model incorporates the effects of axial load, reduction of concrete compressive strength resulting from diagonal tension, and the influence of indeterminacy which arises in statically redundant structures. Design limits for joint shear stress obtained from the model are compared with those adopted by Design Codes.

RÉSUMÉ

Les codes couramment utilisés pour le dimensionnement sous charge latérale des joints poutres-colonnes sont soit basés sur des principes d'équilibre (CEB et normes de Nouvelle-Zélande), soit dérivés de valeurs expérimentales (Code ACI). Les déformations associées aux états limites de dimensionnement ne sont pas considérées comme véritable résultat lors de l'évaluation de performance des connexions. Une approche alternative satisfaisant à la fois l'équilibre et les conditions de compatibilité est discutée dans cette étude. Le modèle proposé tient compte des effets d'une charge axiale, de la diminution de la résistance à la compression du béton sous l'effet de tensions diagonales, ainsi que de l'indétermination caractérisant les structures hyperstatiques. Les limites de dimensionnement caractérisant les joints soumis à l'effort tranchant obtenues par ce modèle sont comparées à celles adoptées par les codes officiels.

ZUSAMMENFASSUNG

Die derzeit gültigen Anforderungen für die Bemessung von Knoten in seitlich belasteten Rahmen sind entweder auf Gleichgewichtbetrachtungen aufgebaut (CEB und Neuseeland Vorschriften) oder sie wurden empirisch hergeleitet (ACI-Vorschriften). Daraus folgt, dass die mit den Bemessungsgrenzwerten verbundenen Verformungen bei der Beurteilung des Verhaltens der Knoten nicht berücksichtigt werden. Eine alternative Methode, die Gleichgewichts- und Verträglichkeitsbedingungen einschliesst, wird in diesem Beitrag besprochen. Das vorgestellte Modell berücksichtigt den Einfluss der Normalkraft, die Verringerung der Druckfestigkeit des Betons infolge Querzug und den Einfluss der statischen Unbestimmheit von Tragwerken.

1. INTRODUCTION

Requirements for lateral-load design of reinforced concrete (RC) beam-column joints currently implemented in design codes worldwide [1, 2, 3] are based on extensive experimental studies of the inelastic behavior of individual RC frame connections. Because of the complexities associated with controlling tests of statically indeterminate systems, most of the experiments included in the data bases of the various codes have been carried out on highly idealized statically determinate assemblies modelling beam-column connections of frame structures [4, 5, 6, 7].

Forces considered for joint design are illustrated in Fig. 1a. In most contemporary design codes, the magnitudes of these forces are associated with a beam flexural hinging mechanism, implying that beams and columns are dimensioned first. Because a large portion of the forces loading the joint are introduced by bond stresses that develop between concrete and reinforcement, codes require that the magnitude of bond stresses be regulated by controlling the size of longitudinal bar diameter with respect the available development length (column or beam depth). In the following discussion, it will be assumed that the development length requirements are satisfied apriori, and that bond deterioration is not significant (referring both to the derivations and the experimental data discussed in this paper).

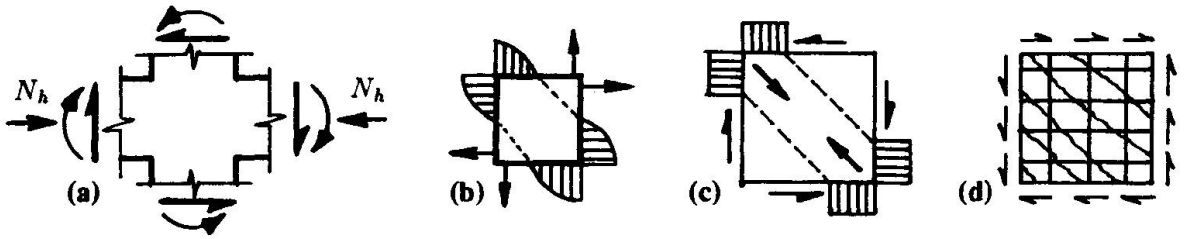

Fig. 1 Shear mechanisms adopted by design codes

Dimensioning and detailing of beam-column joints according to the current design practice is directly linked to evaluation of the so-called joint shear index. This index, which is an estimate of the horizontal and/or vertical joint shear stress, is computed using one of two alternative approaches. The first approach, adopted by the joint ACI-ASCE Committee 352 [1], is characteristic of North American practice. In this approach, the joint-shear index is computed only for a horizontal plane, and is limited by allowable stresses (empirically derived from experiments). The allowable stresses amount to $0.083\ \lambda\sqrt{f'_c}$, (MPa), where λ is 20, 15 and 12 for interior, exterior and corner joints respectively. Furthermore, it has been proposed that development of the concrete strength in the compressed diagonal (Fig. 1b) is facilitated by confining of the concrete core, with closed hoops or other members that frame in to the connection, such as transverse beams and floor slabs [5]. Lateral reinforcement provided in the joint region is the same as that provided in the column critical regions.

The second approach [8], currently adopted by the CEB Model Code [2] and the N. Zealand Code [3], considers both horizontal and vertical joint shear stresses. These stresses, in combination with the normal forces that act at the faces of the joint (Fig. 1a), constitute a loading system for which an admissible state of equilibrium is said to develop from the superposition of a diagonal strut mechanism and a truss mechanism (Fig. 1c, 1d). For the purpose of design, the ultimate joint shear resistance is established by considering the formation of diagonal tension failure inside the joint. For conservatism, the concrete contribution to shear resistance associated with main-strut action (Fig. 1c) is accounted for when the axial force in the column is significant. It has been proposed [8] that axial load improves joint performance by reducing the inclination (from vertical) at which the main-strut mechanism develops. In this model, intermediate horizontal reinforcement is an essential part of the shear-resisting mechanism, comprising the horizontal chords of the idealized truss shown in Fig. 1d. With reference to the role of stirrups or hoops in the overall behavior of beam-column joints, it has been suggested recently that the emphasis which the ACI 352 recommendations place on the confining action of tie reinforcement or other members framing into joint is misleading because the mechanisms of confinement in the critical regions of columns are different from those associated with shear action [9].

The sharp contrast between the two approaches effects different views regarding the definition of acceptable levels of performance, and, to a certain extent, two different interpretations of available experimental evidence as it pertains to the mechanics of joints. Of the two methods, the first is clearly empirical and the latter is based on an admissible equilibrium solution. A consequence of both is that deformations of the joint are not considered in the design process. From the point of view

of structural performance, the amount of deformation required for the joint to develop its resistance is as significant as the magnitude of the resistance. It is therefore desirable that both quantities be reflected in design recommendations.

Although the need for deformation based design criteria for joints has been stated [5], their development has been impeded by the realization that load and deformation demand on the beam-column joints of frames with complex structural configurations is greatly influenced by the three-dimensional effects of the response, and the ability of statically indeterminate structures to redistribute forces. Joint deformation and member expansion are generally unrestrained in statically determinate assemblies, like those used in most experimental studies of joint behavior. Therefore, deformation performance criteria (usually expressed in terms of displacement ductility for the assemblage) quoted by experimentalists in establishing allowable values for joint shear do not directly apply in the case of indeterminate frame structures because of the significant amount of restraint to joint deformation that continuity can cause.

To identify the important parameters that control the behavior of joints, it is instructive to review the available experimental evidence. Early tests conducted in the 1960's on isolated connection specimens illustrated that joint reinforcement in the form of horizontal stirrups, in combination with uniformly distributed longitudinal column reinforcement (so as to form a closed cage), significantly enhanced the shear resistance of joints [4]. Since then, a large amount of research has been conducted, with an aim towards establishing relationships between the degree of deterioration of shear resistance under cyclic loads and the amount of lateral reinforcement provided in the joint. Recent tests (as part of a U.S. - Japan - N. Zealand - China cooperative research effort) of connection specimens simulating Japanese, U.S. and N. Zealand practice (of which the first and last pose the lowest and highest requirements of joint reinforcement, respectively), clearly demonstrate that there is an upper limit in the amount of joint reinforcement, beyond which the overall resistance of a connection is not significantly affected [5]. This manifests the obvious fact that, although large amounts of joint reinforcement can increase the available shear resistance of the joint, this additional strength is not likely to be usable because the demand on the joint is eventually limited by the flexural resistance of adjacent members. All reported specimens (which were designed to fail in beam yielding and had very favorable bond conditions) demonstrated similar overall resistance, with the only significant differences being apparent stiffness of the connections and the amount of deformation. Increased amounts of lateral steel delayed the initiation and propagation of cracking in the joint, and reduced the amount of joint distortion that occurred under a given level of joint shear stress. These results suggest that an important consequence of adding joint reinforcement is an increase of joint stiffness.

Based on this experimental evidence, it is possible to idealize joints as two-dimensional (2-D) panels reinforced in two orthogonal directions, and acted upon by in-plane stresses. However, contrary to familiar 2-D panels, the concrete stiffness contribution is not independent of that of the reinforcement. This is supported by experimental evidence obtained from tests of beam-column joints in which the closed stirrups were replaced by longitudinal beam reinforcement that was uniformly distributed along the height and anchored outside of the joint [7]. Although the joints in these specimens were able to resist the shear demanded to develop beam hinging, a rapid deterioration of joint shear resistance was observed with cycling. Evidently, the stiffening action of closed stirrups occurs not only in the direction of the load but in the perpendicular direction as well, making the confining role of stirrups a more transparent phenomenon. Therefore, the experimental evidence suggests that stirrups contribute to the shear resistance of joints directly (by resisting part of the joint shear), and indirectly (by confining the concrete core, thus enhancing its diagonal compressive strength). However, these two functions are not independent or mutually exclusive of each other - a point that fuels the current debate between differing design philosophies.

From tests of interior beam-column joints with transverse beams, it has been established even joints without any stirrup reinforcement can perform satisfactorily within realistic levels of lateral displacement [5]. This suggests that transverse beams at interior connections and closed hoop reinforcement affect the behavior of joints in a similar manner, by restraining volumetric expansion, which eventually leads to deterioration of joint shear resistance. It has been suggested that this is result of insufficient modeling of boundary conditions in the experimental models, since the enhancement of joint performance occurred only when transverse beams were free of load during the tests. Indeed, experiments in which transverse beams were loaded have been carried out, and in these cases transverse beams had negligible confining contribution. Nevertheless, tests conducted on indeterminate specimens have shown that the excessive deformation that would occur in the beam plastic hinge regions if the assembly was statically determinate, is partially restrained by the presence of adjacent

members. This restraint has been measured experimentally as internal axial forces that developed in beams experiencing inelastic deformation near the connection. The internal forces, N_3 and N_h (Fig. 1a), represent the reactions of adjacent columns to the lateral displacement required to accommodate beam expansion. Because of the presence of these internal actions, the confining effect of transverse beams on the joint is likely to be significant in actual (indeterminate) structures, where each connection is restrained by the presence of adjacent frames.

With respect the overall displacements of beam-column connections, experiments have shown that a satisfactory joint performance is always accompanied by minimal contribution of joint distortion to the overall lateral drift of the structure (joint performance is deemed satisfactory if cracking is controlled and deterioration of resistance does not occur). In statically determinate assemblies of typical proportions, joint distortion accounted for approximately 25% of the total displacement at low levels of lateral drift. At higher displacement levels (corresponding to approximately 2% interstorey drift, which is often considered a design limit), experimental data suggest that the contribution of joint distortion to total drift became less than 15%, when beams developed sustained flexural hinging as a result of sufficiently reinforced joints or joints with low shear stresses (stresses below values associated with cracking of concrete). In contrast, the contribution of joint distortion to the total drift has been observed to increase with increasing magnitude of total displacement, reaching 40% in cases of joints with insufficient hoop reinforcement or excessive levels of joint shear stress (stresses exceeding the empirical limits in the ACI-ASCE 352 Recommendations [1]). This information suggests an opportunity to link connection design to overall structural response. But any such design approach must consider joint deformations as well as internal forces. No current design basis does so explicitly.

2. EQUILIBRIUM AND KINEMATICS OF JOINTS

In this section it is assumed that the joint is properly detailed and that reinforcement is present in quantities sufficient to provide adequate crack control; stresses and strains are averaged over the dimensions of the entire joint [10].

2.1 Equilibrium

Average stresses in the joint are depicted in Fig. 1. Shear stresses are introduced by direct member action and by the bond that develops between the main reinforcement and the joint core concrete. Shear stress, v, is assumed to be uniformly distributed over the boundaries of the joint (Eqn. 1, Table 1). Eqns. 2 and 3 establish equilibrium in the vertical l and horizontal t directions at the center of the joint. σ_l and σ_t represent the average vertical and horizontal compressive stresses of the concrete. ρ_l, ρ_t are the available amounts of vertical and horizontal reinforcement (where $\rho_t = \rho_b + \rho_s$, for which ρ_b and ρ_s are the percentages of horizontal beam reinforcement and horizontal stirrups in the joint, respectively). The corresponding average stresses in the reinforcement are f_l and f_t. Dimensions of the joint (depth, width and height), are denoted by d_w, b and h ; N_v is the column axial force. N_h represents the beam axial force, which results from partial restraint to beam expansion provided by adjacent columns in indeterminate frames.

$v = \frac{V_h}{bd_w} = \frac{V_v}{bh}$ (1)	$\sigma_t = -\rho_t f_t - \frac{N_h}{bh}$ (3)	$\sigma_1 - \sigma_t = v \tan\theta$	$\sigma_t = -v \tan\theta$ (6)
$\sigma_l = -\rho_l f_l - \frac{N_v}{bd_w}$ (2)	$\sigma = \begin{pmatrix} \sigma_t & v & 0 \\ v & \sigma_l & 0 \\ 0 & 0 & \sigma_3 \end{pmatrix}$ (4)	$\sigma_1 - \sigma_l = \frac{v}{\tan\theta}$ (5)	$\sigma_l = -\frac{v}{\tan\theta}$ $\sigma_2 = -v(\tan\theta + \frac{1}{\tan\theta})$

Table 1 Joint equilibrium equations

Furthermore, if the joint reinforcement is of the closed-hoop type, the concrete of the joint is subjected to passive confining stress $\sigma_3 = -\rho_s f_3$. Here, f_3 represents the hoop stress in direction normal to the plane of action of the applied shear force. Eqn. 4 describes the average stress tensor associated with the joint. The maximum principal stress, σ_1, associated with the stress tensor must not exceed the tensile capacity of concrete. If, for the sake of simplicity, it is assumed that this capacity is negligible then, since in any plane stresses are either negative (compressive) or zero, it is evident that $\sigma_2 = \sigma_l + \sigma_t$ (conservation of the first invariant, given that σ_1 is assumed zero). The elements of the stress tensor in the (t, l) coordinate system are related to the principal stresses via Eqns. 5 (Table 1); expressions for σ_t, σ_l and σ_2 in terms of the applied shear stress v are obtained from Eqns. 5 upon substitution of $\sigma_1 = 0$ (Eqns. 6).

2.2 Kinematics

We assume that the overall geometry of the joint after deformation is described by the average angle of shear distortion, γ, and by the average longitudinal and transverse strains denoted by ϵ_l and ϵ_t respectively. Equation 7 (Table 2) describes the tensor of average strains as defined in the (t, l) system. Some useful relations between the entries of the tensor expressed in various coordinate systems are also given in Table 2. The direction of principal strains, which enters the terms of Eqn. 8 is generally unknown. Considering the behavior before yielding of hoops in the joint (of primary interest from the design point of view), it is assumed that, if the reinforcement has not yielded, the direction of principal strains (α) is closely related to that of stresses (θ). If $\theta = \alpha$ is adopted, then it is possible to express θ in terms of the values of stress in Table 1. To do this, $\tan\theta$ is written in terms of strains (Eqn. 8). Strains are substituted with the ratios σ_2/E_c, f_l/E_s, f_t/E_s; v is replaced by $(-\sigma_t/\tan\theta) = [\rho_t f_t + (N_h/bh)/\tan\theta]$. This procedure leads to a quadratic equation for $\tan\theta$ (Eqn. 9), where $n = E_s/E_c$, while the strain ratio $r = e_h/\epsilon_t$ reflects the amount of lateral restraint to joint growth, which is likely to be significant for indeterminate structures. It is evident from Eqn. 9 that such restraint plays the same role algebraically as horizontal joint reinforcement, which is parallel to experimental observation of improved joint performance when transverse beams were present in tests of interior connections. The quantities $e_v = N_v/E_c b d_w$ and $e_h = N_h/E_c h b$ have units of strain, and represent the deformations occurring in the joint under purely axial forces.

$$\epsilon = \begin{pmatrix} \epsilon_t & 0.5\gamma \\ 0.5\gamma & \epsilon_l \end{pmatrix} \qquad \epsilon_1 + \epsilon_2 = \epsilon_l + \epsilon_t \tag{7}$$

$$\gamma = \frac{2(\epsilon_1 - \epsilon_t)}{\tan\alpha} = 2(\epsilon_1 - \epsilon_l)\tan\alpha \qquad \tan^2\alpha = \frac{\epsilon_1 - \epsilon_t}{\epsilon_1 - \epsilon_l} = \frac{\epsilon_2 - \epsilon_l}{\epsilon_2 - \epsilon_t} \tag{8}$$

$$\frac{1 + \frac{1}{n\rho_t} - \frac{r}{n\rho_t(n\rho_t + r)}}{1 + \frac{1}{n\rho_l}} \tan^4\theta + \frac{e_v/\epsilon_t}{(1 + n\rho_l)(n\rho_t + r)} \tan^2\theta - 1 = 0 \tag{9}$$

2.2.1 Behavior before yielding of joint reinforcement

Before yielding of the horizontal joint reinforcement, the magnitude of joint shear stress is related to hoop strain by Eqn. 10 (Table 3). In a similar manner, expressions for the remaining elements of the strain tensor may be obtained as seen in Table 3. The expression for the principal tensile strain (ϵ_1) indicates that the strain is not only affected by the amount of joint shear stress, but also that it increases with increasing vertical axial load, while the influence of lateral restraint on the joint is the reverse. This effect is significant, because the magnitude of diagonal (principal) compression that can develop in the core concrete decreases with increasing magnitude of the tensile strain in the perpendicular direction.

$$\epsilon_t = \frac{1}{\rho_t E_s}\left(v\tan\theta - \frac{N_h}{bh}\right) \qquad \epsilon_l = \frac{1}{\rho_l E_s}\left(\frac{v}{\tan\theta} - \frac{N_v}{bd_w}\right) \tag{10}$$

$$\gamma = \frac{2}{E_s(1 - \tan^2\theta)}\left[v\frac{\tan^2\theta\rho_l - \rho_t}{\rho_l\rho_t} + \left(\frac{N_v}{bd_w\rho_l} - \frac{N_h}{bh\rho_t}\right)\tan\theta\right]$$

$$\epsilon_1 = \frac{1}{E_s(1 - \tan^2\theta)}\left[v\tan\theta\frac{\rho_l - \rho_t}{\rho_l\rho_t} - \frac{N_h}{bh\rho_t} + \frac{N_v\tan^2\theta}{bd_w\rho_l}\right] \tag{11}$$

Eqn. 11a provides a relationship between average joint shear stress and the amount of associated joint distortion. It is evident from the above that column axial load promotes joint distortion, while restraining horizontal loads reduce the amount of distortion at a given level of shear stress.

2.2.2 Behavior after yielding of joint reinforcement

Upon yielding of the joint hoops, the pattern of deformation in the joint is likely to change noticeably. In terms of stresses, it is evident from Eqn. 3 that $\sigma_t = -\rho_t f_y - (N_h/bh) = -v\tan\theta$, which can be solved for the angle of principal stresses $\tan\theta$: $(\tan\theta = [\rho_t f_y + N_h/bh]/v)$. This result can be used to obtain expressions for the average longitudinal (vertical) stress, the average nonzero principal stress, and the amount of hoop strain, ϵ_t, in terms of the joint shear v (Eqns. 12, 13, Table 4).

$$\sigma_l = -\frac{v^2}{\rho_t f_y + N_h/bh} \; ; \; \sigma_2 = -\rho_t f_y - \frac{N_h}{bh} - \frac{v^2}{\rho_t f_y + N_h/bh} \tag{12}$$

$$\epsilon_t = \frac{1 + \frac{1}{n\rho_l}}{E_c\left[\rho_t f_y + e_h E_c\right]^3} v^4 - \frac{e_v v^2}{n\rho_l\left[\rho_t f_y + e_h E_c\right]^2} - \frac{\rho_t f_y + e_h E_c}{E_c} \tag{13}$$

Thus, a dramatic increase occurs in the values of σ_l, σ_2 and ϵ_t, for small increases in the value of joint shear after yielding of hoops, since all terms (except v) in Eqns. 12 and 13 remain constant thereafter.

3. MECHANISMS CONTROLLING SHEAR RESISTANCE

The shear resistance of a joint is likely to be limited by the occurrence of one of two possible mechanisms: (1) bond failure of the main reinforcement, which is responsible for introducing the shear stresses, v, to the joint, or (2) yielding of joint reinforcement. Of these, case (1) was excluded in this study by assuming that pertinent development length requirements are satisfied. For case (2), it has been shown that after initiation of yielding of joint hoops, a substantial increase in the values of σ_1 and σ_2 will occur. Thus, hoop yielding is is likely to be succeeded by either a) yielding of the longitudinal column reinforcement, or b) crushing in the principal direction of concrete compressive stresses. Upper limits to the shear capacity associated with these two mechanisms can be established as follows: for case 2(a), the stress in the longitudinal steel reaches the yielding stress, f_y. Thus,

$$\sigma_l = -\rho_l f_y - \frac{N_v}{bd_w} = -\frac{v^2}{\rho_t f_y + N_h/bh} \text{ therefore, } v_n = \sqrt{\left\{\rho_t f_y + \frac{N_h}{bh}\right\}\left\{\rho_l f_y + \frac{N_v}{bd_w}\right\}} \tag{14}$$

For case 2(b), failure occurs when the principal compressive stress, σ_2, reaches the crushing strength of concrete, f_{max}. This crushing strength, however, depends upon the amount of restraint to volumetric expansion, which here is represented by stress σ_3. Furthermore, f_{max} also depends on the amount of tensile deformation in the perpendicular direction, characterized by ϵ_1 [11]. It is assumed here that the relationship between stress and strain along the principal compressive direction can be described by [11],

$$\sigma_2 = f_{max}\left[2\frac{\epsilon_2}{\epsilon_{max}} - (\frac{\epsilon_2}{\epsilon_{max}})^2\right] \text{ where, } \left\{\begin{array}{l} f_{max} = \alpha f_c' \\ \epsilon_{max} = \alpha\epsilon_o \end{array}\right\} \text{ and, } \alpha = \frac{K}{0.8 + 0.34\epsilon_1/\epsilon_o} \tag{15}$$

where, $K = 1 + \rho_s(f_y/f_c')$. Upon substitution of Eqn. 15 in Eqn. 12, the following alternative expression for the limiting joint shear stress is established:

$$v_n = \sqrt{|(f_{max} + \rho_t f_y + N_h/bh)(\rho_t f_y + N_h/bh)|} \tag{16}$$

4. STUDY OF PARAMETERS IN PROPOSED FORMULATION

In this section, the proposed formulation is used to investigate the influence of various connection-design parameters on conditions corresponding to yielding of hoop reinforcement. Equation 10 can be solved for the amount of shear stress, and Eqn. 11 the corresponding shear distortion, that a joint will tolerate before horizontal reinforcement yields. The "design" variables considered for this hypothetical case study are summarized in Table 5. For this example, the ratio of beam reinforcement (ρ_s) was set at 0.015 (top and bottom combined).

To apply the equations for the purposes of this parameter study, two simplifying assumptions were made:

1. The term E_c is actually a function of ϵ_2, which means that Eqn. 9 should be solved iteratively for the angle θ. Instead, E_c was taken as the secant modulus at the point of peak stress for an assumed parabolic concrete compressive stress–strain relationship (Eqn. 15).

2. The particular response condition examined here corresponds to tensile yield of hoop reinforcement. To account for hoop "pre–strain" that would exist in the presence of vertical axial force, N_v, Poisson's ratio was taken equal to 0.2 to give the expression $\epsilon_t(available) = f_{yh}/E_s - 0.2e_v$ for use in Eqns. 9, 10, and 11.

The influence that each of the variables considered had on tolerable shear before hoop yield is summarized in Table 5. Only cases for which failure by crushing or vertical yield did not occur before hoop yield are included in this analysis of parametric influences. It can be observed that increasing hoop yield stress ($f_{yt}(hoops)$), amount of hoop reinforcement (ρ_s), and beam axial stress ($N_h/f_c'bh$) had similar effects of increasing both tolerable shear distortion and shear stress (Fig. 2a-2c). Indeed, these were the only parameters that resulted in significant and consistent increase of overall joint capacity as limited by hoop yield. By comparison, the proposed formulation shows (Fig. 2d) that column axial stress ($N_v/f_c'bd_w$) had less of an effect on the shear distortion or stress the joint sustained before hoops yielded.

Design Variable	Nominal Value for Study	Range of Values for Study	Effect of increase of variable	
			$v/\sqrt{f_c'}$ @ hoop yield	γ @ hoop yield
f_c'	35 MPa	20 - 100 MPa	Nonlinear decrease	Nonlinear decrease
f_{yt} (hoops)	400 MPa	300 - 600 MPa	Strong linear increase	Strong linear increase
ρ_l	0.04	0.01 - 0.08	Slight nonlinear increase	Slight nonlinear decrease
ρ_s	0.003	0 - 0.010	Linear increase	Linear increase
$N_v/f_c'bd_w$	0.05	0 - 0.25	Slight linear increase	Slight linear decrease
$N_h/f_c'bh$	0.02	0 - 0.25	Linear increase	Linear increase

Table 5 Summary of design parameter study

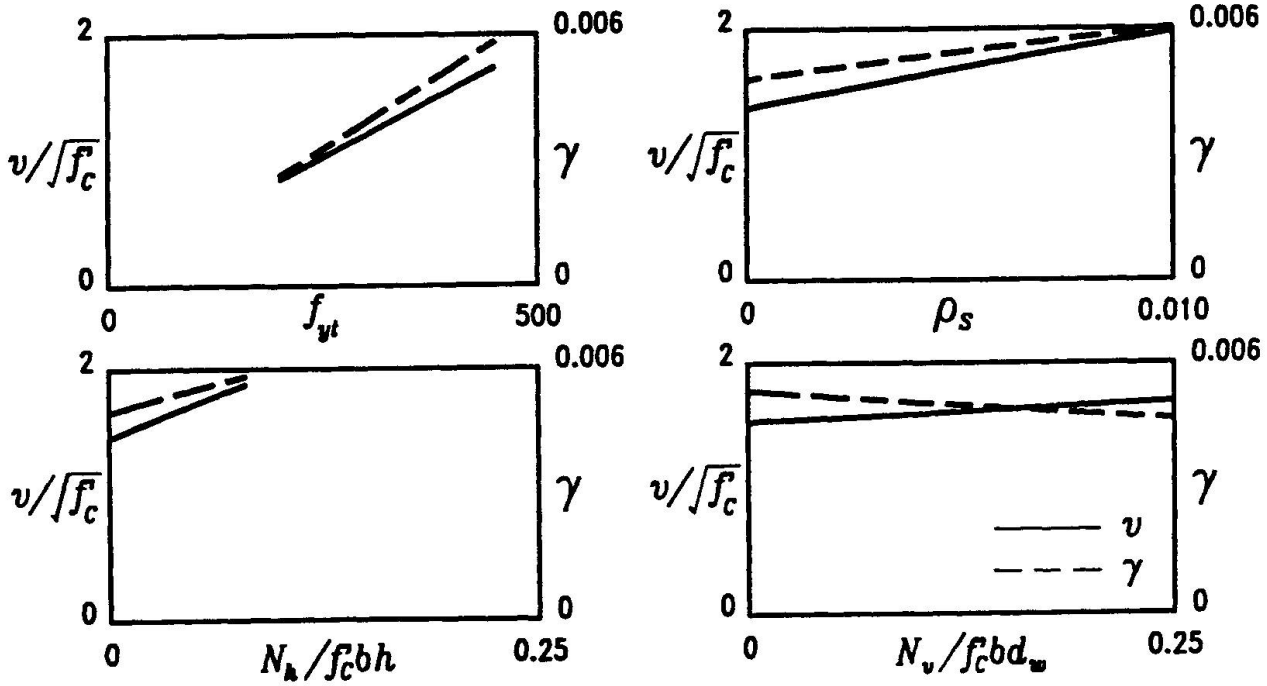

Fig. 2 Results of parametric study

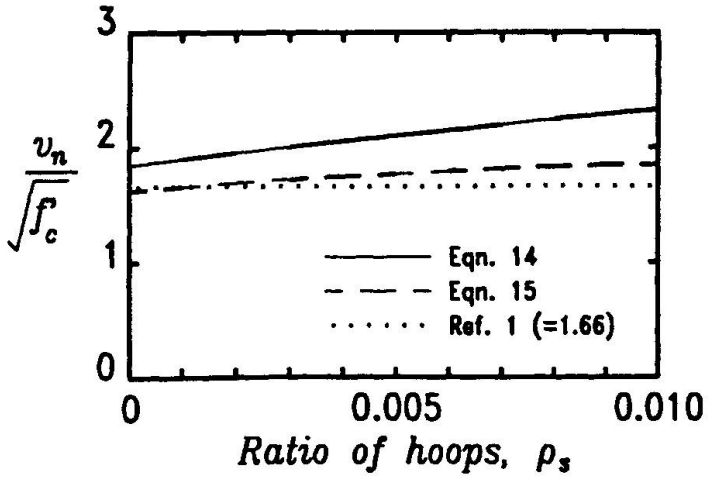

Fig. 3 Shear resistance after hoop yield

Shear capacities associated with connection failure by yield of vertical reinforcement (Eqn. 14) or concrete crushing along the principal diagonal (Eqn. 16) after hoop yield are plotted against the ratio of hoop reinforcement for the sample problem in Fig. 3. For this particular example, it can be observed that capacity will be limited by concrete compression and that, for any ratio of hoops, it is about equal to the value recommended by ACI-ASCE Committee 352 [1]. From the terms of Eqns. 14 and 16, it is apparent that axial stress in the column and beam play an active role, along with the quantity of hoop reinforcement, in determining the shear capacity of connections.

From the terms of Eqns. 14 and 16, it is apparent that axial stress in the column and beam play an active role, along with the quantity of hoop reinforcement, in determining the shear capacity of connections.

5. CONCLUSIONS

At the root of this Colloquium is the pursuit of generalized approaches for design of structural concrete [12, 13]. Connections in framed structures are a good example of a specific problem in need of unified interpretation– as evidenced by the slowly converging, but still diverse, viewpoints recently presented to the American Concrete Institute by researchers from Japan, New Zealand, and the United States [ACI Fall Convention 1989, San Diego]. In this paper, consideration of both the kinematics and equilibrium of a joint resulted in a comprehensive model that makes it possible to gauge the influence of any design variable at any stage of response and provides design equations for joint shear capacity. While the latter is possible from approaches based strictly on equilibrium and empirical summary, the former can only be achieved by attempting to consider joint deformations. The point is transparent to the particular structural element considered in this paper.

ACKNOWLEDGEMENTS

The work presented in this paper was carried out at the University of Toronto, Canada. Financial support for the study was provided by NSERC grants No. OGP0042033 and OGP0042154.

REFERENCES

1. ACI-ASCE COMMITTEE 352, Recommendations for Design of Beam-Column Joints in Monolithic Reinforced Concrete Structures. American Concrete Institute, Detroit, 1985, 18 pp.

2. CEB-FIP Model Code for Seismic Design of Concrete Structures. Bulletin d'Information No. 160, Paris, 1983, 117 pp.

3. STANDARDS ASSOCIATION OF NEW ZEALAND. Code of Practice for the Design of Concrete Structures. Part 1, 127 pp. and Part 2, 156 pp. Wellington 1982.

4. HANSON N. W. and CONNER H. W., Seismic Resistance of Reinforced Concrete Beam-Column Joints. Proceedings, ASCE, V. 93, ST5, Oct. 1967, pp. 533-560.

5. KUROSE Y., Recent Studies on Reinforced Concrete Beam Column Joints in Japan. PMFSEL Report No. 87-8, Phil M. Ferguson Structural Engineering Laboratory, Department of Civil Engineering, The University of Texas at Austin, December 1987, and references thereof.

6. MEINHEIT D. F. and JIRSA J. O., Shear Strength of R.C. Beam-Column Connections. Proceedings, ASCE, V. 107, ST11, Nov. 1981, pp. 2227-2244.

7. WONG P. K. C., PRIESTLEY M. J. N. and PARK R., Seismic Resistance of Frames with Vertically Distributed Longitudinal Reinforcement in Beams. ACI Structural Journal, Vol. 87, No. 4, July-August 1990, pp. 488-498.

8. PAULAY T., PARK R. and PRIESTLEY M. J. N., Reinforced Concrete Beam-Column Joints Under Seismic Actions. ACI Journal, Proceedings V. 75, No. 11, Nov. 1978, pp. 585-593.

9. PAULAY T., Equilibrium Criteria for Reinforced Concrete Beam-Column Joints. ACI Sructural Journal, V. 86, No. 6, November-December 1989.

10. COLLINS M. P., Towards a Rational Theory for RC Members in Shear. ASCE Structures Journal, Vol. 104, No. ST4, April, 1978, pp. 649-666.

11. VECCHIO F.J. and COLLINS M.P., The Modified Compression-Field Theory for Reinforced Concrete Elements Subjected to Shear. ACI Journal, March-April 1986, pp. 219-231.

12. MacGREGOR J. G., Dimensioning and Detailing. Sub-Theme 2.4, Proceedings, IABSE Colloquium, Stuttgart, 1991.

13. MARTI P., Dimensioning and Detailing. Sub-Theme 2.4, Proceedings, IABSE Colloquium, Stuttgart, 1991.

Evaluation of the Rotation Capacity of «D» Regions

Capacité de rotation des zones «D»

Schätzung der Rotationsfähigkeit von «D»-Zonen

Gian Michele CALVI
Researcher
Univ. of Pavia
Pavia, Italy

Gian Michele Calvi received his Master of Science from the University of California, Berkeley, and his Ph.D. from the Politecnico di Milano. His main research interests are related to the seismic design of reinforced concrete and masonry structures, having been active both in the experimental and numerical fields.

Ester CANTU'
Researcher
Univ. of Pavia
Pavia, Italy

Ester Cantu', born in 1952, graduated in Civil Engineering at the University of Pavia. She is a researcher at the Department of Structural Mechanics of the University of Pavia. Her research field concerns masonry and reinforced concrete structures.

Guido MAGENES
Grad. Res. Assist.
Univ. of Pavia
Pavia, Italy

Guido Magenes, born in 1963, obtained his Civil Engineering degree at the University of Pavia and his M.Sc. degree at the University of California, San Diego. His research interests are related to structural concrete and masonry.

SUMMARY
The main objective of this paper is to discuss the effectiveness of some currently applied models in predicting the real rotation capacity of concrete slabs reinforced with welded wire meshes, as a functional of steel properties, reinforcement percentage and load condition. Comparisons are made with the experimental results obtained from 36 tests performed at the University of Pavia. Attention is given to the implications of the results for design codes and practical detailing.

RÉSUMÉ
L'objectif principal de cet article est de discuter l'efficacité de quelques modèles appliqués actuellement pour prévoir la capacité de rotation des dalles en béton armées de treillis, en fonction des propriétés de l'acier, du pourcentage d'armature et des conditions de mise en charge. Des comparaissons sont faites avec les résultats expérimentaux obtenus à partir de 36 essais effectués à l'université de Pavie. On portera son attention sur les conséquences de ces résultats sur les normes de dimensionnement, ainsi que sur les détails constructifs.

ZUSAMMENFASSUNG
Hauptgegenstand dieser Arbeit ist, die Effektivität einiger allgemein angewandter Modelle zu diskutieren, die die tatsächliche Rotationsfähigkeit von mit geschweissten Betonstahlbalken bewehrten Betonplatten als Funktion der Materialeigenschaften des Stahles, des Bewehrungsgehaltes und der Belastung ausdrücken. Es werden Vergleiche mit Ergebnissen aus 36 Versuchen, die an der Universität von Pavia durchgeführt wurden, angestellt. Die Einbindung dieser Ergebnisse in Normen und in die Praxis wird betrachtet.

1. PRELIMINARY REMARKS

The CEB Model Code 78 [1] allowed the redistribution of the bending moments calculated from a linear analysis if some ductility requirements were met by the critical sections.
The available plastic rotation was computed as a function of the neutral axis position according to the experimental results obtained from about 350 tests performed in the sixties [2,3].
Most of these tests had been performed on specimens reinforced with mild steel bars, with very good elongation capacity and large overstrength after yielding.
More recently it has become more and more common in Europe to produce steel with lower elongation capacity and lower overstrength, due to different production processes (cold worked steel) and weldability requirements (welded wire meshes). The applicability of the older results has been therefore questioned and discussed on the base of numerical analyses [4,5].
The plastic rotation capacity available for redistribution purposes has been consequently reviewed in the most recent codes [6,7], adding a second parameter to be considered: the elongation capacity of the steel.

The main objective of this paper is to discuss the ability of current numerical models to predict the real rotation capacity of plastic hinge regions and to examine the implications on codes of practice. Particular attention will be paid to the case of welded wire meshes, for a number of reasons: the steel is usually cold worked and has a lower elongation capacity; the steel percentages are often small; the bond between steel and concrete and the crack pattern can be strongly affected by the presence of the transversal bars.

2. FACTORS AFFECTING THE PLASTIC ROTATION CAPACITY

The basic parameter used in design codes to determine the available rotation capacity of a D region is the neutral axis depth (x/d) [1,6,7]. It has to be noted that the CEB MC 90 recognizes a decreasing rotation capacity if the neutral axis is too high, which means that the steel mechanical percentage is too low. The neutral axis depth is a very comprehensive parameter because it summarizes the effect of the section geometry and of some mechanical properties of the material.

Nevertheless the most recent codes are assuming a second parameter, i.e. the steel elongation capacity. The reason for which the influence of steel elongation was not considered in the past is simply due to the good uniform quality of the steel used up to the seventies.

A third parameter which is implicitly recognized as important is the ratio of the ultimate strength (f_{su}) to the yielding strength (f_{sy}) of the steel: a higher ratio allowes a larger region in which the yielding moment is attained, and the theoretical plastic rotation is consequently higher. Actually only a minimum for this ratio is given by the codes, but a tendency to the production of steel with less and less f_{su}/f_{sy} does exist, particularly for what concerns welded wire meshes.

It is also well known that the bond between steel and concrete plays an important role for the determination of the available rotation capacity, but there has not been in the past any transposition of this fact in the codes of practice. If this may be acceptable for deformed bars (but the bond is in this case proportional to the bar diameter), in the case of smooth bars the

spreading of the yielded region of the bar can significantly affect the rotation capacity. In this case the distance between transversal bars may become the fundamental parameter.

Finally it has to be reminded that the beam slenderness (length over depth, l/d) governs the relation between fiber deformation, section curvature and overall rotation, therefore if the maximum fiber deformation is given (i. e. the steel elongation capacity and the bond relations) the available rotation is proportional to the beam slenderness. Also if the depth of a beam is kept constant the theoretical length of the plastic hinge (distance between the points at which the yielding moment is attained) increases with increasing span. The beam slenderness is usually taken into account in the codes by means of some limit value of slenderness for which the given relations are applicable.

3. MODELS TO PREDICT THE AVAILABLE ROTATION CAPACITY

The most commonly used models able to predict the plastic rotation capacity of D regions are based on a few common hypotheses and follow some common steps:

- plane sections are supposed to remain plane;
- the sections are divided into layers, each of them being characterized by the appropriate stress - strain relation;
- the sectional moment - curvature relations are then constructed by imposing increasing curvatures, getting strains and stresses and computing the corresponding bending moments;
- for a given bending moment diagram is then possible to compute the total rotation integrating the section curvatures on the desired length.

The key issue of such models is a refined consideration of the tension stiffening effect of the concrete around the bars from crack to crack. For this purpose some bond stress-slip relation is needed [8], together with some model to predict the position of the cracks.
If the tension stiffening effect is not considered a rotation for the case of so called "naked" bars is obtained, which is generally always greater than the real rotation. The difference in the curvature for the two cases are qualitatively shown in fig. 1.

Some possible plastic penetration beyond the limit of the yielding moment should also be considered.

A fundamental problem which is far from being solved is to decide if, in which cases, and for what amount a translation of the bending moment diagram has to be considered, as required by the well known "truss analogy". In [4] it is suggested to consider a translation if some shear cracking is expected.

If only one crack is present in the yielded region and if the reinforcement percentage is low (i. e. the neutral axis depth is very small), a simplified model could be used to estimate the maximum available plastic rotation.
The beam could be considered as a combination of two rigid bodies, connected by a hinge in the compressed zone of the critical section and by a deformable steel element at the level of the tensile reinforcement. The length of the steel element should be defined on the base of the distance at which a perfect bond is believed to have been reached.

4. EXPERIMENTAL RESULTS

Tests on thirty six slabs reinforced with welded wire mesh have been recently completed at the Laboratory of the Department of Structural Mechanics of the University of Pavia. The specimens had the same rectangular section (440 mm x 160 mm), slenderness of about 14 and were casted with the same concrete. The spacing of the transversal bars was normally set at 150 mm. All the details on materials, geometry and results are presented in [9]. The variable parameters were as follows.

Steel properties

Three types of steel were used, with different stress-strain relations and different bond characteristics. The main differences can be identified in the mean ultimate elongation capacity (ε_u equal to 3.45, 4.36 and 7.99 %) and in the surface of the wires (smooth or deformed).

Reinforcement percentage

The geometrical percentages of the tensile steel were 0.23, 0.38 and 0.64 %, corresponding to neutral axis depth approximately equal to 0.09 d, 0.12 d and 0.17 d. The steel at the compressed edge was kept constant (geometrical percentage 0.23 %).

Applied load

The load was either concentrated at midspan or divided into four equal loads.

The main results in term of available plastic rotation are given in fig. 2: the experimentally measured rotations are systematically higher than the corresponding values accepted in the CEB MC 90, but the ratio between available and accepted plastic rotation does not seem to be uniform.
The trends given by the CEB are roughly confirmed, but the steel with higher elongation capacity seems to be much more sensitive to a decrease of the reinforcement percentage and of the bar diameters.
The smooth wire meshes deserve a special mention because of the good uniform behaviour.

A comparison of numerical and experimental results is presented in fig. 3.
The numerical model was not refined and did not consider the tension stiffening effect; the complete stress-strain curve of the steel was used.
The numerical simulations should have therefore sistematically overestimated the available rotation. This is not the case for some specimens with smooth bars (LiB) and with the more ductile deformed bars (NeA). For these cases the introduction of a tension stiffening effect in the model would have further underestimated the available plastic rotation. While the substantial approximation of the same values for the experimental and numerical results could have been predicted in the case of smooth bars (i.e. in this case the bond could be neglected), the results obtained from NeA type steel still deserve some explanation.

The tension stiffening effect is experimentally very clear, as shown in fig. 4, where the moment-curvature diagrams for different regions of a beam are shown. It is also clear that only in one crack the steel has been able to reach yielding: the yielded length depends therefore on the bond stress-slip relation rather than on the distance between the points at which the yielding moment is attained. This consideration explains why the numerical predictions are generally too high in the case of smaller deformed bars: in this case the bond is much higher.

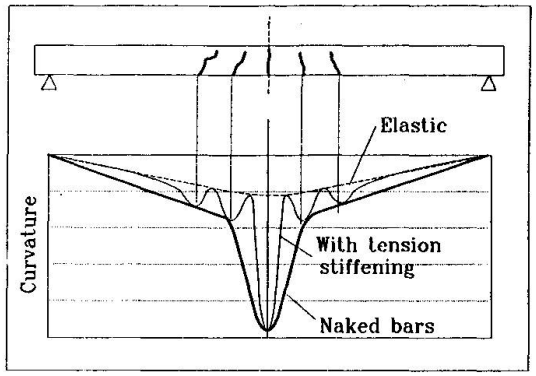

Fig.1 - Comparison of typical curvatures with and without considering the tension stiffening effect

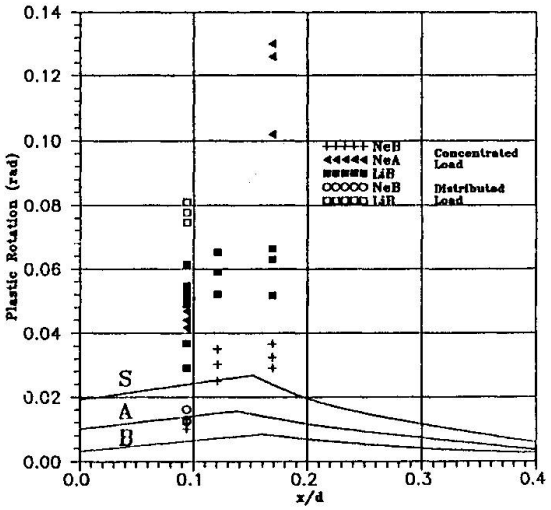

Fig.2 - Experimental plastic rotation vs. the CEB MC 90 design curves

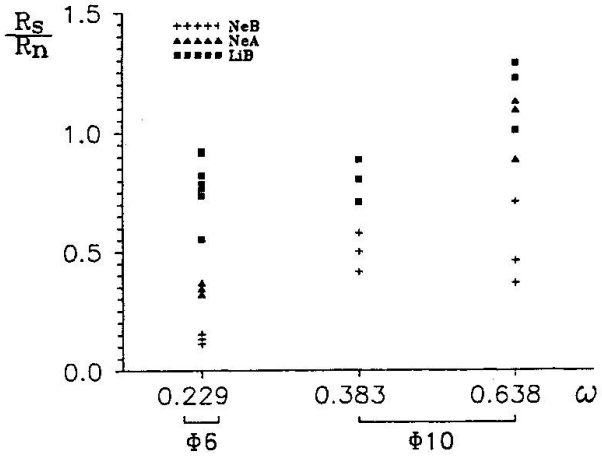

Fig.3 - Ratio between experimental and numerical ("naked bars" with bending moment diagram traslation) rotations as a function of steel percentage (bar diam.) and quality

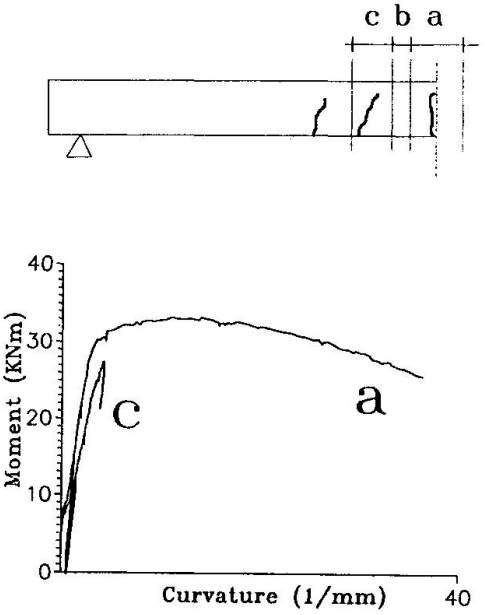

Fig.4 - Evidence of the tension stiffening effect from the experimental results

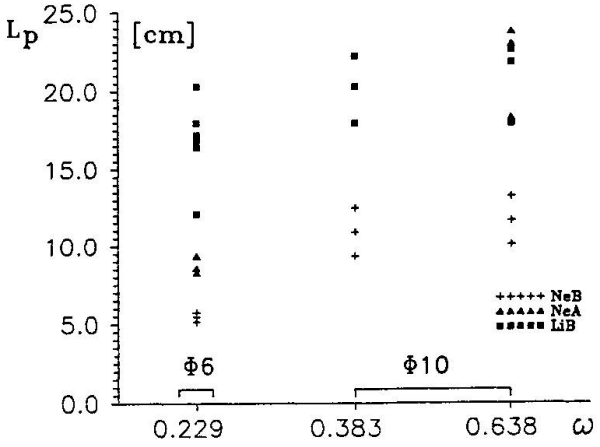

Fig.5 - Yielded lenghts required by the "rigid bodies model" as a function of steel percentage (bar diam.) and quality

The simplified model previously mentioned has been also applied to check the implications of the experimental results. In fig. 5 the lengths of the bars that should have fully yielded to match the experimental results are shown.
In the case of deformed bars, the bond is clearly playing the fundamental role, with required plastic length approximately proportional to the bar diameter.
In the case of smooth bars the required plastic length is about constant, confirming the negligibility of bond stress-slip relations with respect to the mechanical restraints offered by the transversal bars.

5. IMPLICATIONS FOR DESIGN CODES AND CONCLUSIONS

The importance of bond relations in the evaluation of the available rotation capacity in D regions has been generally neglected by codes and this is particularly dangerous in the case of small diameter bars, for which also the mechanical properties of the steel are usually worse.
On the opposite, from experimental results it appears that the use of smooth bars could assure a series of advantages if a mechanical bond is anyway guaranteed by the presence of transversal welded wires.
The definition of minimum values of reinforcement and minimum bar diameters seems to be particularly important in the case of deformed bars, when some plastic rotation is required, even if a good elongation capacity of the steel is provided.

ACKNOWLEDGEMENTS

The experimental tests discussed in this paper have been funded by the Italian Society of Steel Producers (Federacciai). The authors wish also to express their gratitude to Prof. G. Macchi for his support and suggestions.

REFERENCES

[1] CEB-FIP, Model Code for Concrete Structures, Bulletin d'Information CEB No. 124/125, 1978
[2] MACCHI G., Ductility Condition for Simplified Design without Check of Ductility, Bulletin d'Information CEB No. 105, 1976
[3] SIVIERO E., Rotation Capacity of Monodimensional Members in Structural Concrete, ibidem
[4] ELIGEHAUSEN R., LANGER P., Rotation Capacity of Plastic Hinges and Allowable Degree of Moment Redistribution, Bulletin d'Information CEB No. 175, 1987
[5] COSENZA E., GRECO C., PECCE M., Plastic Rotation and Required Ductility in R. C. Continuous Beams, L'Industria Italiana del Cemento, 1, 1990 (in italian)
[6] COMMISSION OF THE EUROPEAN COMMUNITIES, Eurocode No. 2, Common Unified Rules for Concrete Structures, Final Draft, 1988
[7] CEB-FIP, Model Code 1990, First Draft, Bulletin d'Information CEB No. 195/196, 1990
[8] ELIGEHAUSEN R., POPOV E. P., BERTERO V. V., Local Bond Stress-Slip Relationship of Deformed Bars under Generalized Excitations, Report No. UCB/EERC 83/23, University of California, Berkeley, 1983
[9] CALVI G. M., CANTU' E., MACCHI G., MAGENES G., Experimental Investigation on the Rotation Capacity of Concrete Slabs Reinforced with Welded Wire Meshes, Rapporto N. 33, Dipartimento di Meccanica Strutturale dell'Universita' di Pavia, 1990

Ductility of Structural Concrete

Ductilité du béton structurel

Duktilität des Konstruktionsbetons

Igor TERTEA
Prof. Dr.
Polytechn. Inst.
Cluj-Napoca, Romania

Igor Tertea, received his Dipl. Eng. and the Dr. Eng. degrees from the Polytechn. Inst. of Timişoara, Romania, and is since 1956 Professor of reinforced and prestressed concrete at the Polytechn. Inst. of Cluj-Napoca, Romania. He is the author of several publications.

Traian ONET
Prof. Dr.
Polytechn. Inst.
Cluj-Napoca, Romania

Traian Onet, born 1937, received his Dipl. Eng. and the Dr. Eng. degrees from the Polytechn. Inst. of Cluj-Napoca, Romania. He is since 1965 Professor of reinforced and prestressed concrete at the same Institute, and author of several books and publications on reinforced and prestressed concrete.

SUMMARY

The paper presents the ductility computation for B regions and the main parameters influencing the ductility of structural concrete as seen from the correlation of the numerical tests with experimental results.

RÉSUMÉ

Cet article présente une méthode de calcul des zones B, ainsi que les paramètres influençant la ductilité du béton, résultant d'une corrélation entre résultats numériques et expérimentaux.

ZUSAMMENFASSUNG

Der Artikel stellt ein Rechnungsverfahren für die Duktilität der B-Bereiche vor und zeigt die wesentlichen Einflüsse auf die Duktilität von Konstruktionsbeton auf, die aus Vergleichen von numerischen Berechnungen mit Versuchsergebnissen gewonnen werden.

1. INTRODUCTION

In accordance with the ideas expressed in the introductory reports by J.E. Breen and A.S.G. Bruggeling, as well as with the considerations contained in the lectures of J.G. MacGregor and P. Marti, we shoud emphasize the fact that one of the fundamental requirements of structural concrete elements design is the provision of a proper ductility. In fact, one of the most important advantages of structural concrete is offered by the possibility to design the required sectional or/and structural ductility, in accordance with the building's emplacement and the nature of actions.

The above assertion is valid only for the portions of the structural elements subjected to bending moments with or without axial load (B regions), for which there are already clear design models permiting a qualitative and especially a quantitative ductility computation [1,2,4].

For the portions subjected to combined action of bending moment and shear force (D regions) design model recently proposed (full-member design procedure) does not refer to ductility but in case of inclined crack width limitation.

2. DUCTILITY COMPUTATION FOR B REGIONS

The design model used by the authors [4,5] does not essentially differ from that proposed by A.S.G. Bruggeling [1], in which the prestressing can simply be regarded as an artificial loading, from the point of view of load capacity.

For the ductility computation the following assumptions are made:

a) The stress - strain curve of concrete is a parabolic one (Fig.1) and takes into consideration the concrete confinement by transverse reinforcement.

b) The stress - strain diagram for nonprestressed steel is bilinear (corresponding to elasto-plastic behaviour).

c) The stress - strain diagram for prestressing steel is linear for $\sigma_p \leq 0{,}6\ f_{pu}$ and five degree parabolic over this value.

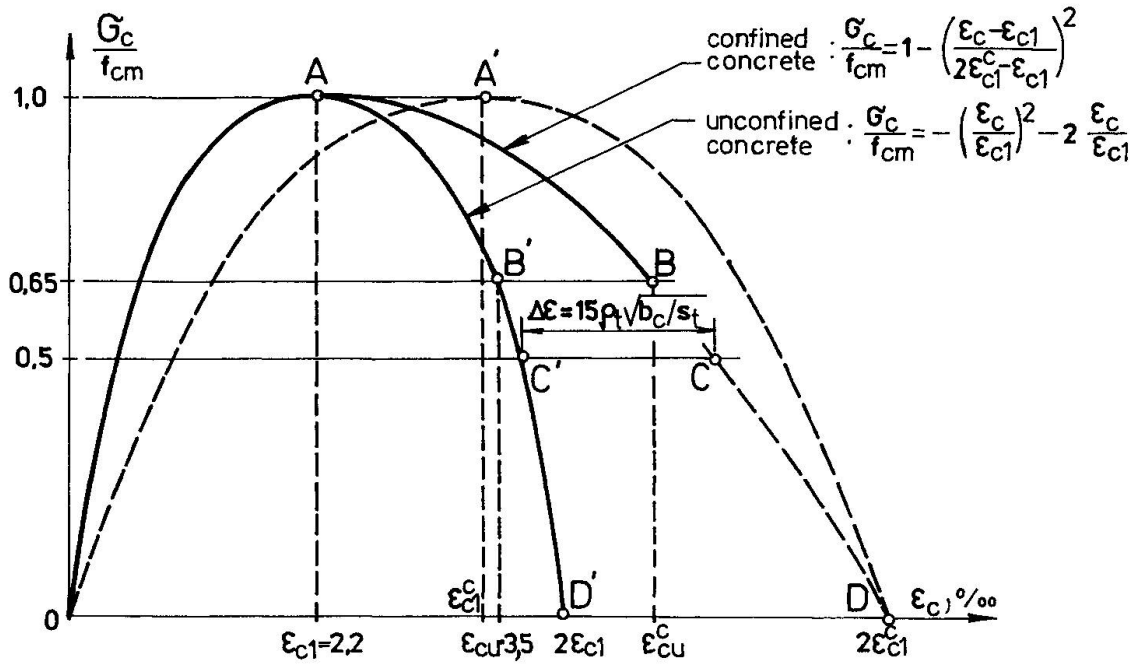

Fig. 1

d) Active and passive reinforcement yield at the same time.

e) Plane sections before flexure remain plane after flexure.

f) The prestressing effect, after losses, is similar to external forces P_{∞} and P'_{∞} (corresponding to the reinforcements A_p and A'_p).

g) There is a good bond between concrete and reinforcements.

h) The cross sectional stress and strain distribution at yield point of reinforcement and at fracture of concrete are represented in Fig.2a and Fig.2b respectively.

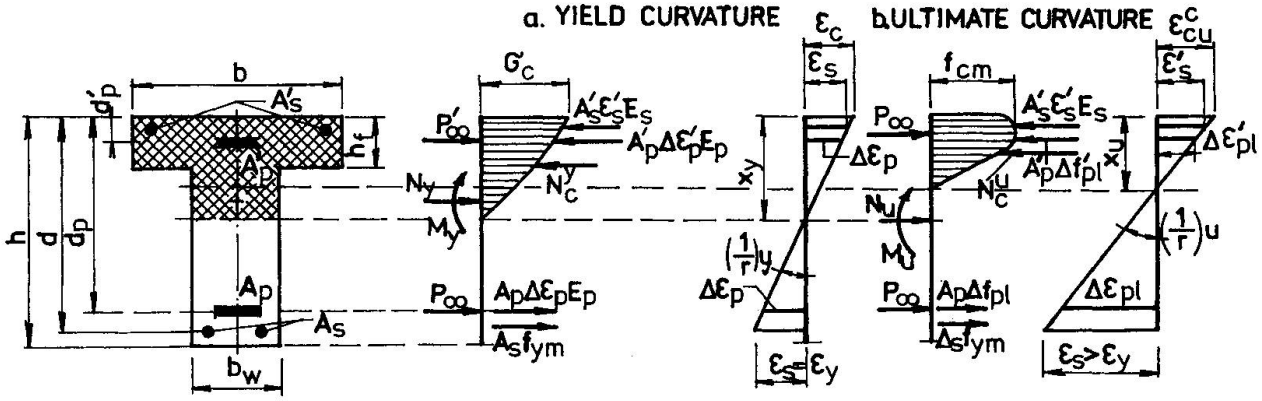

Fig. 2

The ductility ratio for a structural concrete section subjected to bending with axial load can be computed as follows:

$$D = \frac{\varepsilon_{cu}^{c}(1 - \xi_y)E_s}{\xi_u f_{ym}} = \frac{\varepsilon_{cu}^{c}(\delta - \xi_y)E_p}{\xi_u(f_{0.2m} - \sigma_{p\infty})} \qquad (1)$$

where $\xi_y = \frac{x_y}{d}$ and $\xi_u = \frac{x_u}{d}$.

The values of ξ_y and ξ_u are the solutions of the equations:

$$A \xi_y^3 + B \xi_y^2 + C \xi_y + D = 0 \qquad (2)$$

$$E \xi_u^3 + F \xi_u^2 + G \xi_u + H = 0 \qquad (3)$$

where the coefficients have the expressions from Appendix, for one of possible situations depending on section characteristics.

Design procedure is programmable. The set of numerical program [4] is providing the possibility to print the diagrams for estimating the ductility ratio depending on different parameters.

3.PARAMETERS INFLUENCING THE STRUCTURAL CONCRETE DUCTILITY

Numerical tests using the above mentioned programs have been correlated with experimental results obtained in Reinforced Concrete Laboratory of Politechnical Institute of Cluj and also with in other laboratories and we got the following conclusions:

- The ductility of structural concrete sections is drastically diminished by increasing the axial forces intensity (external action effects and/or prestressing effect) which accompany the bending moment. The curvature ductility may be improved by reducing the prestressing degree or (at a given prestressing degree) by proper transverse reinforcement [3,5].
- The beams with unbonded prestressing reinforcement have a greater ductility in comparison with those with bonded prestressing reinforcement.

- The passive or active reinforcement of compressive zone has a favourable influence on ductility due to beneficial effect of the concrete confinement.
- The higher the ratio of passive reinforcement (ρ_w) (at the same quantity of the total reinforcement) and the less the quality of this reinforcement, the greater the value of ductility.
- The effect of small number of repeated loading cycles on the ductility was insignificant.

REFERENCES

1. BRUGGELING A.S.G., Structural concrete: Science into practice. Heron, vol.32, no.2., 1987.
2. COHN M.Z., TRINH J.K.L., Précontrainte partielle: De la théorie a la pratique. Annales de l'ITBTP, no.444, mai 1986, pp. 90 - 115.
3. ONEŢ T., AL-DABBEEK J.N.S., New Data Regarding the Transverse Reinforcement Effect on Ductility of Structural Concrete Elements (in Romanian). The XIV-th Concrete Conference, vol.1, Cluj-Napoca, 1988.
4. ONEŢ T., TERTEA I., Ductility of Structural Concrete (in Romanian). Construcţii, nr.11-12, 1988, pp.72 - 77.
5. TERTEA I., ONEŢ T., Ductility of Partially Prestressed Concrete. International Symposium "Nonlinearity and Continuity in Prestressed Concrete", University of Waterloo, Ontario, Canada, 1983.

APPENDIX

$$\boxed{\varepsilon'_s \geq \varepsilon_y}$$

$$A = \frac{1}{3}\frac{\varepsilon_y}{\varepsilon_{c1}}\left(3+\frac{\varepsilon_y}{\varepsilon_{c1}}\right)$$

$$B = (\alpha+\alpha_p)-(\alpha'-\alpha'_p)-\frac{\varepsilon_y}{\varepsilon_{c1}}+\frac{\varepsilon_y}{\varepsilon_{c1}}\frac{h_f}{d}\left(\frac{b}{b_w}-1\right)\left(2+\frac{\varepsilon_y}{\varepsilon_{c1}}\right)+n_y$$

$$C = -2\alpha-\alpha_p\left(1+\frac{d}{d_p}\right)+2\alpha'-\alpha'_p\left(1+\frac{d'_p}{d}\right)-$$

$$-\frac{\varepsilon_y}{\varepsilon_{c1}}\frac{h_f}{d}\left(\frac{b}{b_w}-1\right)\left(2+\frac{h_f}{d}+\frac{h_f}{d}\frac{\varepsilon_y}{\varepsilon_{c1}}\right)-2n_y$$

$$D = \alpha+\alpha_p\frac{d}{d_p}-\alpha'+\alpha'_p\frac{d'_p}{d}+\frac{\varepsilon_y}{\varepsilon_{c1}}\frac{h_f^2}{d^2}\left(\frac{b}{b_w}-1\right)\left(1+\frac{1}{3}\frac{h_f}{d}\frac{\varepsilon_y}{\varepsilon_{c1}}\right)+n_y$$

$$\alpha = \varrho_w\frac{f_{ym}}{f_{cm}}\ ;\ \alpha' = \varrho'_w\frac{f_{ym}}{f_{cm}}\ ;\ \alpha_p = \varrho_{wp}\frac{\varepsilon_y E_p}{f_{cm}}\ ;\ \alpha'_p = \varrho'_{wp}\frac{\varepsilon_y E_p}{f_{cm}}\ ;$$

$$\varrho_w = \frac{A_s}{b_w d}\ ;\ \varrho'_w = \frac{A'_s}{b_w d}\ ;\ \varrho_{wp} = \frac{A_p}{b_w d}\ ;\ \varrho'_{wp} = \frac{A'_p}{b_w d}\ ;$$

$$n_y = \frac{N_y + P_\infty + P'_\infty}{b_w d f_{cm}}\ .$$

$$\boxed{\varepsilon'_s \geq \varepsilon_y\ ;\ \xi_u > \frac{h_f}{d} > \xi_u\left(1-\frac{\varepsilon_{c1}}{\varepsilon^c_{cu}}\right)}$$

$$E = \frac{1}{3}\frac{b}{b_w}\frac{\varepsilon_{c1}}{\varepsilon^c_{cu}}\left[1-\left(\frac{\varepsilon_{c1}}{2\varepsilon^c_{c1}-\varepsilon_{c1}}\right)^2\right]+\left(\frac{b}{b_w}-1\right)\left[\frac{\varepsilon^c_{cu}}{\varepsilon_{c1}}-\frac{1}{3}\left(\frac{\varepsilon^c_{cu}}{\varepsilon_{c1}}\right)^2\right]-$$

$$-\frac{b}{b_w}\left[1-\frac{1}{3}\left(\frac{\varepsilon^c_{cu}}{2\varepsilon^c_{c1}-\varepsilon_{c1}}\right)^2+\frac{\varepsilon^c_{cu}\varepsilon_{c1}}{(2\varepsilon^c_{c1}-\varepsilon_{c1})^2}-\left(\frac{\varepsilon_{c1}}{2\varepsilon^c_{c1}-\varepsilon_{c1}}\right)^2\right]$$

$$F = \alpha+\alpha_{pu}-\alpha'-\alpha'_{pu}-\frac{h_f}{d}\frac{\varepsilon^c_{cu}}{\varepsilon_y}\left(\frac{b}{b_w}-1\right)\left(2-\frac{\varepsilon^c_{cu}}{\varepsilon_{c1}}\right)+n_u$$

$$G = \frac{\varepsilon^c_{cu}}{\varepsilon_{c1}}\frac{h_f^2}{d^2}\left(\frac{b}{b_w}-1\right)\left(1-\frac{\varepsilon^c_{cu}}{\varepsilon_{c1}}\right)$$

$$H = \frac{1}{3}\frac{h_f^3}{d^3}\left(\frac{b}{b_w}-1\right)\left(\frac{\varepsilon^c_{cu}}{\varepsilon_{c1}}\right)^2$$

$$\alpha_{pu} = \varrho_{wp}\frac{\Delta f_{pl}}{f_{cm}}\ ;\ \alpha'_{pu} = \varrho'_{wp}\frac{\Delta f'_{pl}}{f_{cm}}\ ;\ n_u = \frac{N_u + P_\infty + P'_\infty}{b_w d f_{cm}}\ .$$

Conclusions from Tests on Corbels

Conclusions d'essais sur des consoles courtes

Folgerungen aus Versuchen an Konsolen

Wolfgang ZELLER
Dipl.-Ing.
Univ. Karlsruhe
Karlsruhe, Germany

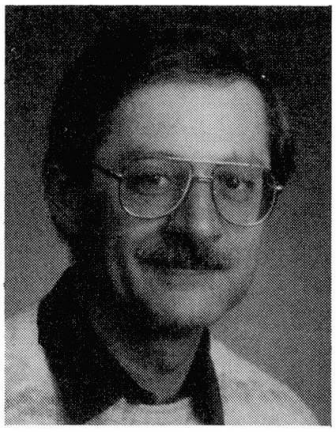

Wolfgang Zeller, born 1942, received his engineering degree from the University of Karlsruhe, Germany. Formerly he was concerned with prestressed concrete bridge construction in a consulting firm and later took up a position as a teaching assistant at the University of Karlsruhe. Presently, he is engaged in research on bridge bearings and corbels.

SUMMARY
Results of tests on reinforced concrete corbels are presented. Load-carrying behaviour after diagonal splitting is explained using a refined strut-and-tie model.

RÉSUMÉ
On présente les résultats d'essais réalisés sur des consoles courtes. Le comportement après la fissuration dans la bielle comprimée est discuté à l'aide d'un modèle de treillis modifié.

ZUSAMMENFASSUNG
Es werden Ergebnisse von Versuchen an Konsolen vorgestellt. An einem verfeinerten Fachwerkmodell wird das Tragverhalten nach dem Auftreten von Spaltrissen erläutert.

1. INTRODUCTION

Research on corbels has been an ongoing concern at the University of Karlsruhe since the early 1960's when Franz/Niedenhoff [1] suggested the simple strut-and-tie model to design reinforced concrete corbels. Tests in the late 1970's [2] have shown that heavily reinforced concrete corbels, with an a/d ratio of 1.0, require not only horizontal but, also, vertical stirrups to prevent failure caused by diagonal splitting in the compression strut. This is due to transversal tensile stresses. More recent tests described in this paper are concerned with investigating the behaviour of the compression strut and the stirrup reinforcement used for different corbel designs.

2. TESTS

Two double corbels with a/d ratios of 0.5 and 1.0, respectively, were loaded to failure (Fig. 1). The tension reinforcement A_s consists of horizontal loops, having equal cross sections for both specimens. Horizontal stirrups were used for corbels K1 to K3 to carry the transverse tensile stresses present in the compression strut. These had an amount of reinforcement equal to 1/3, 1/2 and 1/3 respectively, of the reinforcement A_s. Vertical stirrups were arranged in corbel K4 to resist the transverse tensile stresses. Steel reinforcement strains and concrete strains were measured with electrical resistant strain gauges. Table 1 gives details of the corbel design and failure loads.

Failure modes

Corbel K1 : The horizontal stirrup reinforcement first yielded and deformed extensively after the formation of wide inclined cracks, followed by crushing of the concrete in the compression strut at the column corner. Stresses in the ties were below the yield limit. A special device was then used to strengthen this corbel before the adjoining corbel K2 could be tested to failure.

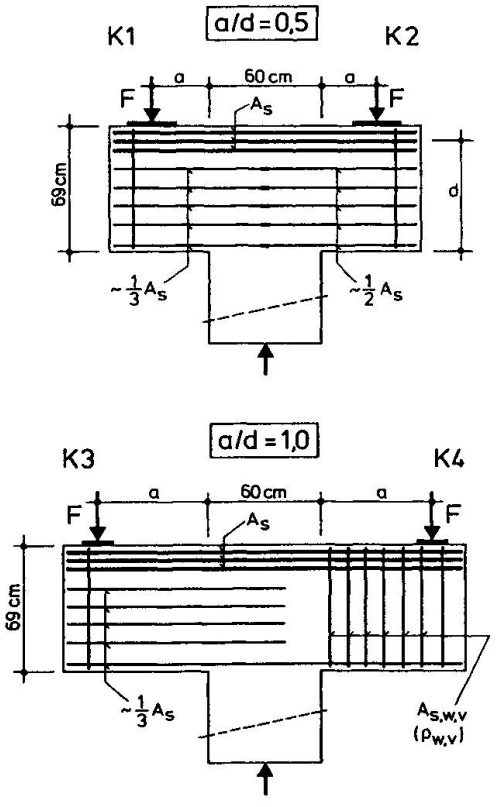

Fig. 1 : Corbel details: reinforcement and dimensions

Corbel No		K 1	K 2	K 3	K 4	units
Ratio	a/d	0,5		1,0		-
Span	a	30		60		cm
Effective depth	d	60		60		cm
Width	b	30		30		cm
Steel						
Tension	A_s	15,5		15,5		cm^2
reinforcement	f_y	~500		~500		N/mm^2
	ρ_l	0,86		0,86		%
Stirrups	A_{swh}/A_s	~1/3	~1/2	~1/3	-	-
(horizontal)	ρ_{wh}	0,38	0,55	0,39	-	%
Stirrups (vertical)	ρ_{wh}	-	-	-	0,37	%
Concrete	f_c	24,5		22,5		MN/m^2
Failure	F_u	948	>1000	455	683	kN
	$\tau_u = F_u/bd$	5,26	>5,55	2,53	3,79	MN/m^2
	τ_u / f_c	0,215	>0,227	0,112	0,169	-

Tab. 1: Experimental test results

Corbel K2 : A maximum load of 1000 kN was reached before the strengthened corbel K1 failed once again. At this load level the stresses in the horizontal stirrups of corbel K2 were just below the yield limit of the steel. The concrete strains in the compression zone at the column corner reached values greater than 4 $^{o}/_{oo}$, suggesting that this corbel would not be able to carry much higher loads.

Corbel K3 : Failure occurred suddenly by diagonal splitting of the compression strut. This was immediately followed by concrete crushing in the zone at the column corner.

Corbel K4 : This corbel failed progressively by crushing of the concrete in the compression zone after extensive yielding of the tension reinforcement (flexural tension failure). Most of the vertical stirrups also exceeded their yield limit.

Crack development

Vertical flexural cracks in the column area began to appear first at very low load levels. These cracks were followed by the formation of inclined cracks at higher load levels and then diagonal splitting cracks which developed near the bearing plate and propagated into the compression zone. The splitting crack widths were geater than those of the flexural cracks. Fig. 2a shows a typical crack pattern of specimen K3 /K4.

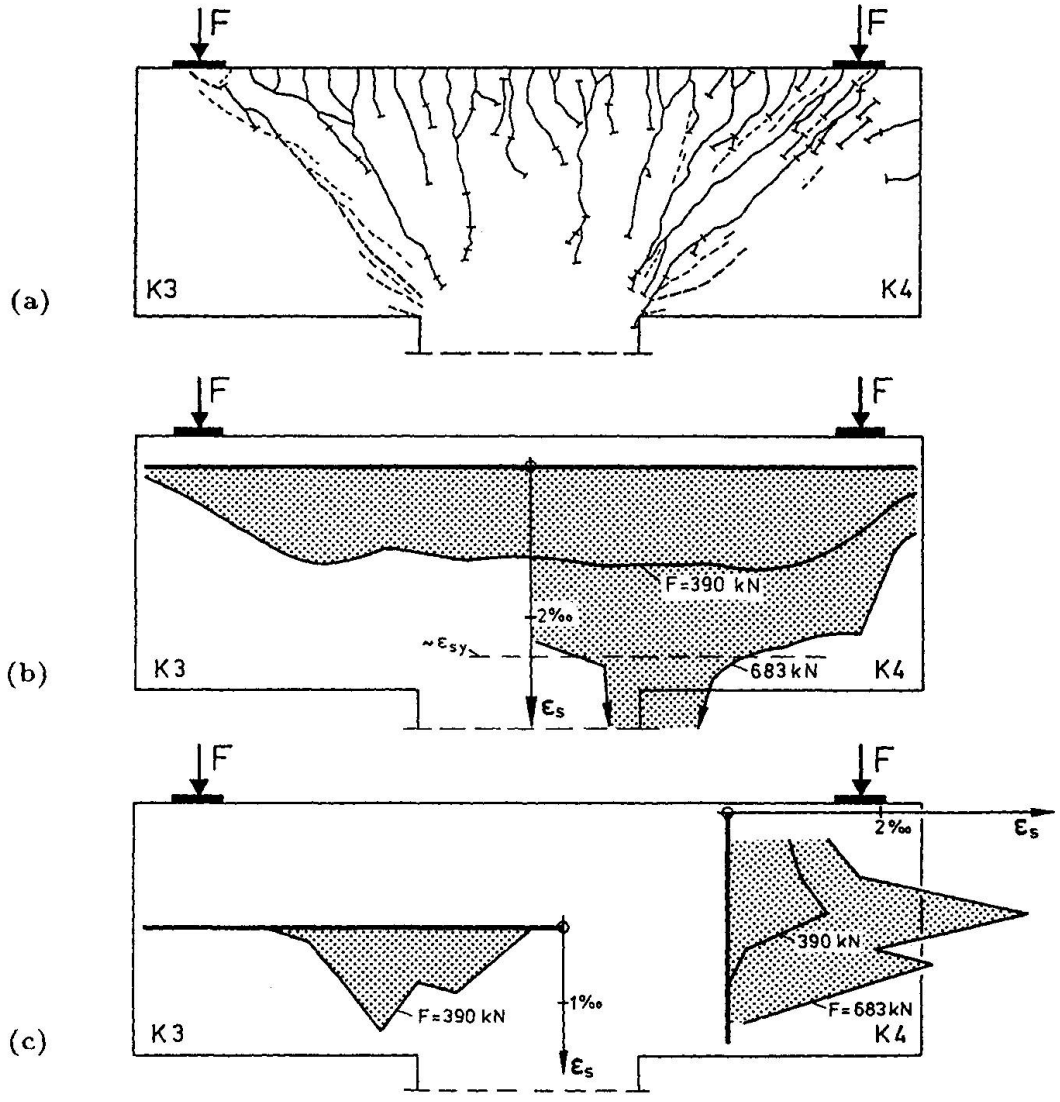

Fig. 2 : Corbels K3 and K4 (a/d = 1.0) : (a) crack pattern; (b) and (c) strain distribution in the tie reinforcement and in both a horizontal and vertical stirrup

Strain measurements

The distribution of the tension tie reinforcement was fairly uniform between the two load bearing plates for corbels K1/K2. However, this was not quite the same case for specimen K3/K4 (Fig. 2b). The maximum strains in both the vertical and horizontal stirrups always occurred in the compression strut area where the bars crossed the splitting cracks (Fig. 2c).

The distribution of concrete strains and stresses is shown in Fig. 3. Stresses are determined from the measured strains and a uniaxial cylinder stress-strain response exhibiting strain softening. Stresses in the compression struts were greatest at the column corner.

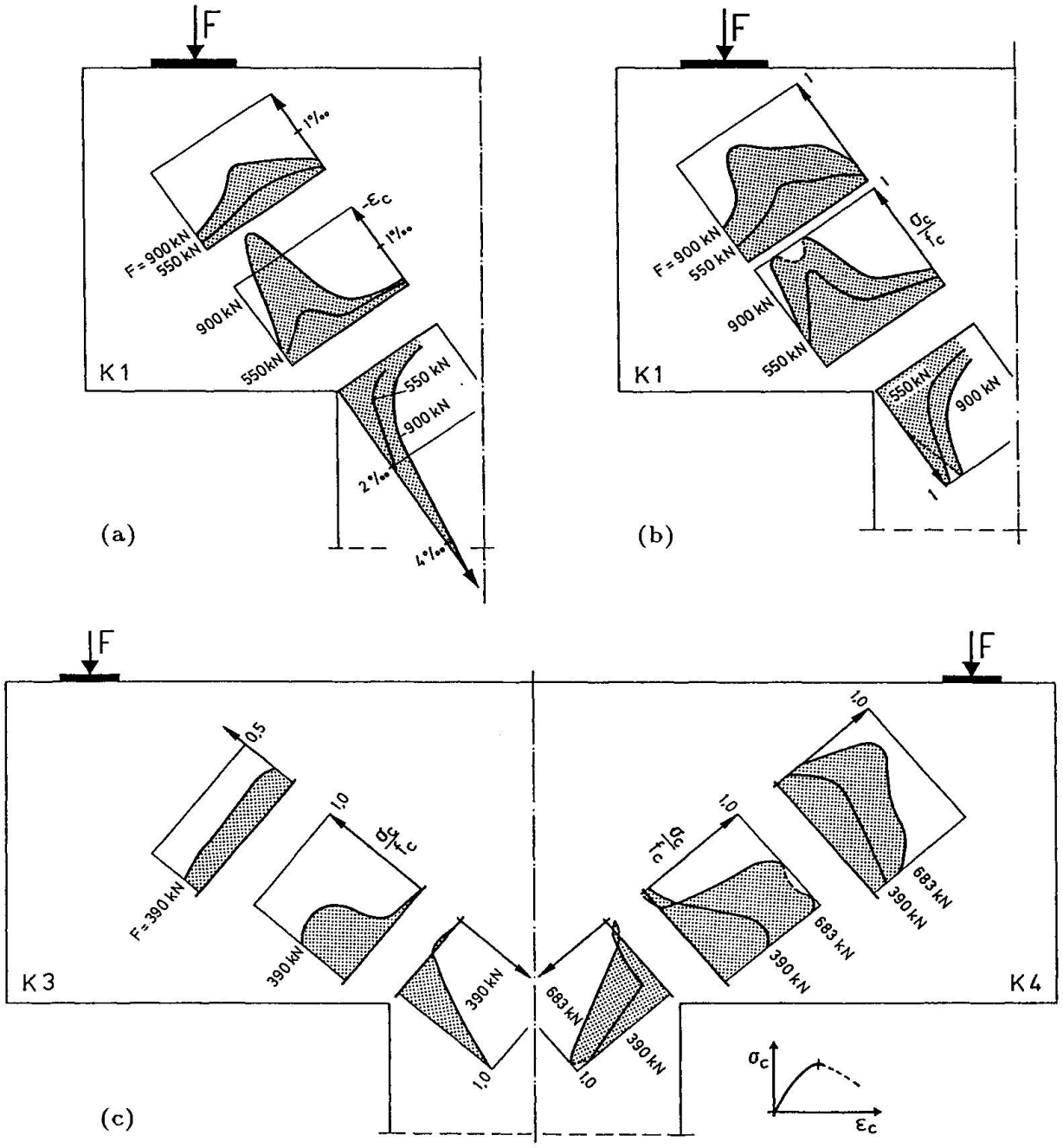

Fig. 3 : Concrete compression strain and stress distribution in corbels K1 and K3/K4

3. DISCUSSION

Results from tests on the corbels demonstrate that stirrups are needed to account for the tranverse tensile forces which develop in the compression strut. The horizontal stirrups used in corbel K1 (a/d = 0.5) were not sufficient to prevent crushing of the concrete in the column corner because of extensive yielding in the stirrups. The same behaviour is assumed for corbel K2. Recall that the stirrup reinforcement used in these corbels was equal to either 1/3 or 1/2 of the tension tie reinforcement. The horizontal stirrups used in corbel K3, having a larger aspect ratio a/d = 1.0, were not very effective, while the vertical stirrups used in corbel K4 resulted in a much higher failure load. The flexural tension failure observed for this corbel was caused by yielding of the tension reinforcement. Hence, corbels should be designed with enough vertical stirrups to allow for this type of failure.

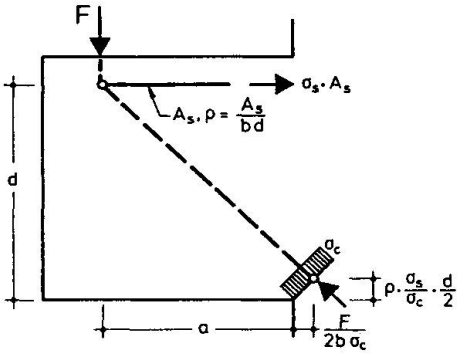

Fig. 4: Simple strut-and-tie model

The simple strut-and-tie model (Fig. 4) is not useful when diagonal splitting occurs. Fig. 5 shows a refined model which is able to analyse post-crack behaviour up to failure. Behaviour at the column corner is only considered since failure should always happen here if the loading node is properly detailed. Rotations occur primarily as a result of deformation in both the tie and transverse tension strut. Rotation on side 1 is greater than that of side 2. Since the struts are not really pinned at the column node, rotation is restrained and consequently strains are greater on side 1. Hence, tensile tie and stirrup reinforcement influence the strains in strut 1 by affecting the rotation of the system. The concrete strains obviously increase greatly when the tranverse tension strut begins to yield, resulting in failure of the concrete.

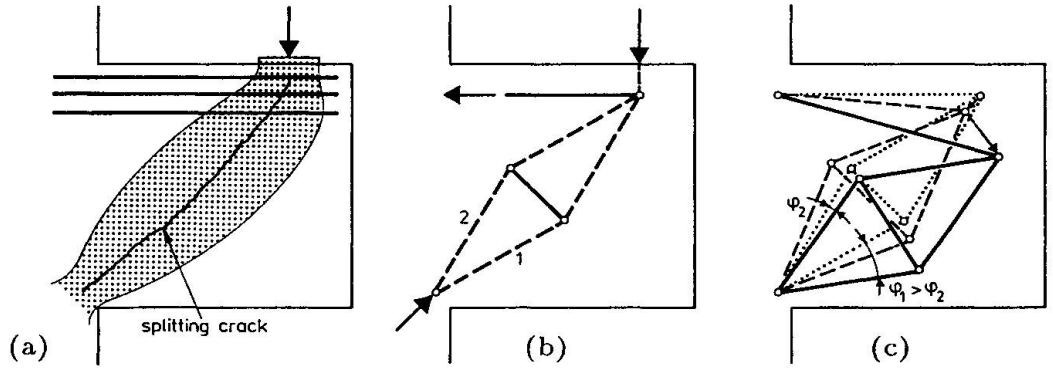

Fig. 5 : Strut-and-tie model explaining diagonal splitting; (a) bottle compression field; (b) refined model; (c) deformation and rotation

Further theoretical research has shown that the magnitude of the tensile splitting force depends on (1) the width of the compression strut at the column corner node and (2) the dimension of the bearing plate and depth of the tension main bars at the loading node.

The width of the compression zone is influenced by the amount of the tensile and the splitting reinforcement. Additionally, the splitting force increases with larger a/d ratios and is not proportional to the force in the main tension bars, as commonly suggested. This assumption leads to an amount of tensile splitting reinforcement which is too small, especially for corbels whith a small a/d ratio.

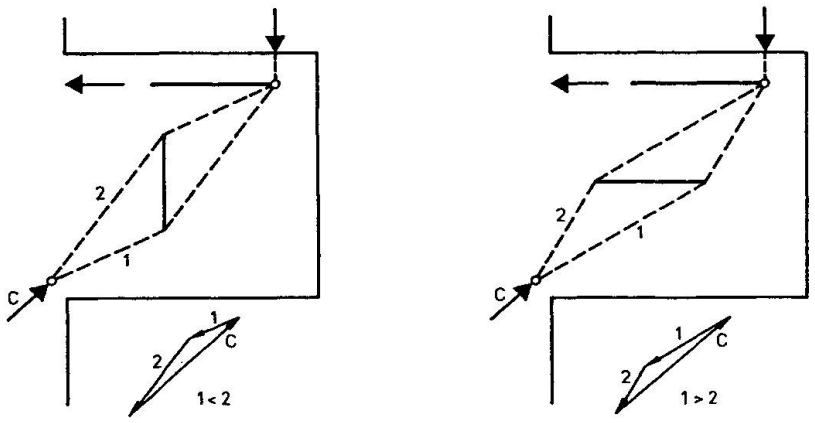

Fig. 6: Strut-and-tie models for corbels reinforced with horizontal or vertical stirrups

The amount of stirrup reinforcement also increases when the orientation of this reinforcement differs from the splitting tensile force vector which is approximately perpendicular to the direct compression strut. In this case, vertical stirrups are more sufficient when the angle of the compression strut is lower than 45°. Conversely, horizontal stirrups are better when the angle exceeds 45°, as is the case for corbels with a/d ratios smaller than about 0.7 to 0.9. Fig. 6 illustrates that when the direction of the splitting reinforcement deviates from the tensile force vector, then not only the splitting forces change but, also, the compresson forces in the column corner.

The tests and analysis described in this paper have shown that the bearing capacity of corbels is greatly influenced by the arrangement of the splitting tension reinforcement, and that the simple strut-and-tie model was not able to account for the actual stresses in the compression zone after diagonal splitting occurred.

4. REFERENCES

[1] FRANZ, G., NIEDENHOFF, H.: Die Bewehrung von Konsolen und gedrungenen Balken, Beton- und Stahlbetonbau 1963, H. 5, S. 112 - 120

[2] EIBL, J., ZELLER, W.: Bruchversuche an Stahlbetonkonsolen bei Veränderung des Bewehrungsgrades, Abschlußbericht 1983, Institut für Massivbau und Baustofftechnologie, Universität Karlsruhe

Dimensioning of the Cable-Stayed Helgeland Bridge

Dimensionnement du pont à haubans de Helgeland

Bemessung der Helgeland Schrägkabelbrücke

H.S. SVENSSON
Sen. Superv. Eng.
Leonhardt, Andrä & Partner
Stuttgart, Germany

Dipl.-Ing. Holger S. Svensson, P.E., P. Eng., born in 1945, received his Diploma in Structural Engineering from Stuttgart University in 1969. He was responsible for the design of several long-span cable-stayed bridges in different countries.

S. HOPF
Sen. Project Eng.
Leonhardt, Andrä & Partner
Stuttgart, Germany

Dipl.-Ing. Siegfried Hopf, born in 1953, received his Diploma in Structural Engineering fromStuttgart University in 1978. He has extensive experience in the design and construction of long-span bridges.

I. KOVACS
Sen. Project Eng.
Leonhardt, Andrä & Partner
Stuttgart, Germany

Dr.-Ing. Imre Kovács, born in 1943, received his Doctorate in Structural Engineering from Stuttgart University in 1973. He has wide experience in all aspects of the dynamic analysis of structures.

SUMMARY
The dimensioning of this cable-stayed bridge with a main span of 425 m and a very slender beam was governed not only by static loads, but also to a great extent by the high dynamic wind loads during construction and after completion. Non-linear effects played an important role in the determination of the stiffness of the structural concrete members.

RÉSUMÉ
Le dimensionnement de ce pont haubané en béton dont la portée principale est de 425 m et dont le tablier est très élancé, a été effectué en tenant compte non seulement des sollicitation de type statique, mais essentiellement des charges dynamiques dues au vent. Les effets non-linéaires jouent un rôle très important sur la détermination de la rigidité des éléments structuraux en béton.

ZUSAMMENFASSUNG
Die Bemessung dieser Beton-Schrägseilbrücke mit einer Hauptspannweite von 425 m und einem sehr schlanken Balken wurde nicht nur durch die statischen Lasten bestimmt, sondern weitgehend auch durch die hohen dynamischen Windlasten während des Baus und nach Fertigstellung. Nichtlineare Effekte spielten eine grosse Rolle bei der Bestimmung der Steifigkeit der tragenden Betonteile.

1. INTRODUCTION

The bridge is located near the town of Sandnessjoen, close to the Polar Circle in Northern Norway. Construction started in April 1989, completion is anticipated for September 1991. A general description is provided in Ref. [1], the layout is shown in Fig. 1.

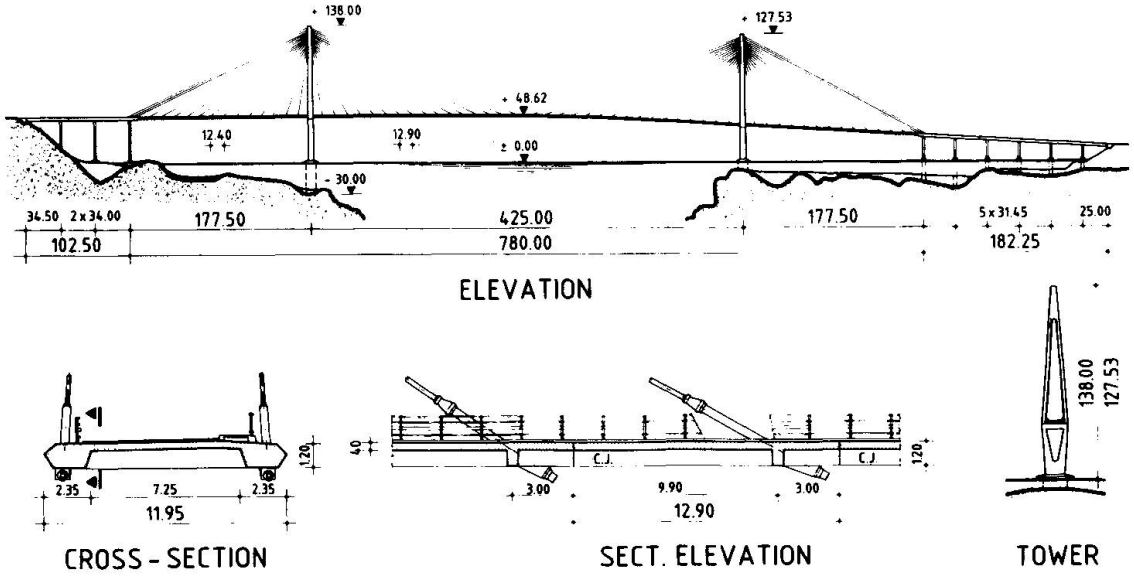

Fig. 1: General Layout

2. DIMENSIONING AND DETAILING

2.1 Towerheads

Three basic tower shapes were investigated: H-, diamond- and A-shapes. The modfied diamond shape was found most suitable, combining economy, esthetics and structural characteristics.
The upper legs are rectangular boxes with 40 cm wall thickness, temporarily post-tensioned during erection with external tendons.

For the cable anchorage area at the tower head a comparison between solid cross sections with overcrossing backstays and forestays, a composite structure, and boxes indicated that concrete box sections with wall thicknesses of 0.42 m and 1.00 m are most economical and have the advantages of anchor head protection from the environment and easy inspection access, see Fig. 2.

At the tower head a large number of concentrated cable forces are introduced. The different models for distributing these forces must be evaluated very carefully, all forces must be followed until they are equally distributed over the cross section, all deviation and tie forces must be taken by steel - rebars or post-tensioned bars - all concrete struts must be checked for compression. Special care must be taken for the design of the nodal zones where the forces are introduced or where several struts and/or ties are intersecting.

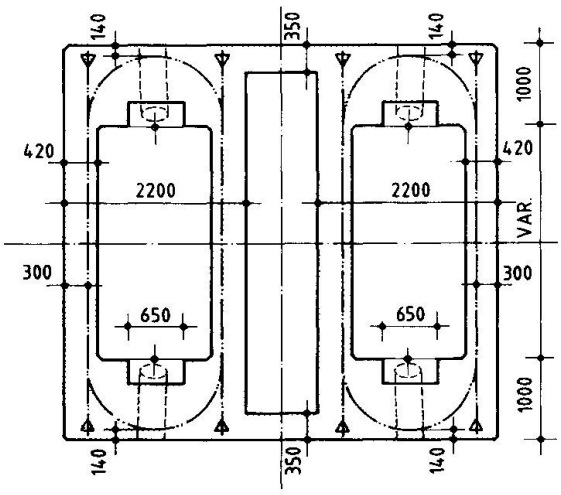

Fig. 2: Section through Towerhead

The system shown in Fig. 2 has been proven to be easy to construct. The number of post-tensioning anchorages is reduced to a minimum, thus reducing the usual congestion in this region. The cable forces are confined by loop tendons, spaced at the same distances as the stays (1.50 m). The question, how much tension is lost along the tight loops due to friction has been investigated in a 1:1 model. With a smooth lubricated duct the standard friction and wobble factors have been confirmed.

The design has been done for different models:
a) truss action (see Fig. 3 and 4)
b) arch action (see Fig. 5)
c) frame action
d) punching.

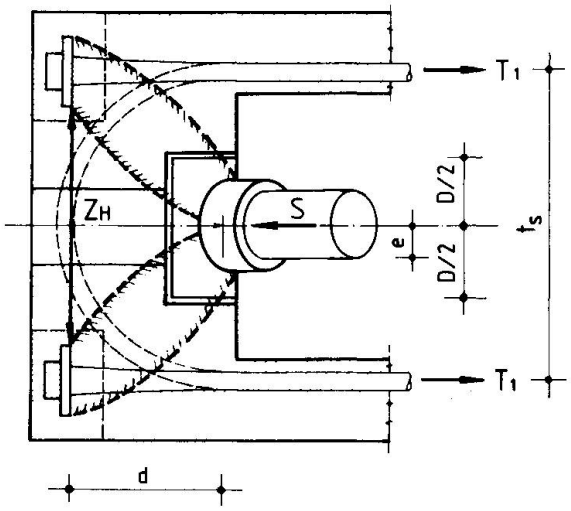

Fig. 3: Truss Action at Towerhead in plan

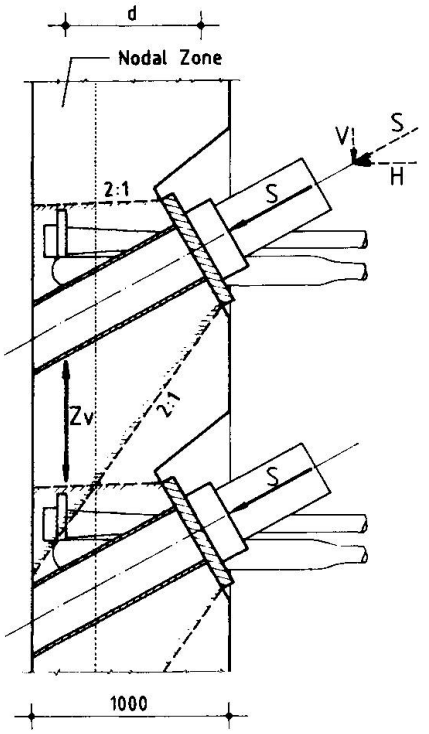

Fig. 4: Truss Action at Towerhead in elevation

a) and b) give each a contribution to the required mild reinforcement, a) more to the horizontal and vertical part outside the loops, b) to the vertical part inside the loop. Local forces have to be covered by separate reinforcement like tie back reinforcement at the loops. The nodal zone is designed as vertical beam acting in tension and bending. It ties together the anchors and gives the possibility to distribute the splitting reinforcement over the total depth of the punching cone. c) and d) are additional investigations which took into account e.g. the double box structure in the upper region.

The reinforcement is designed to satisfy all models a) to d). After the cable forces are introduced into the short walls they must be distributed into the long wall. This design has been done with a multiple truss model.

It was decided by the contractor to use slipforming for all parts of the tower, including the anchorage regions. This was necessary due to the severe wind conditions with very strong, unexpected gusts, during which nobody wanted to take the risk of lifting the more exposed jumping forms.

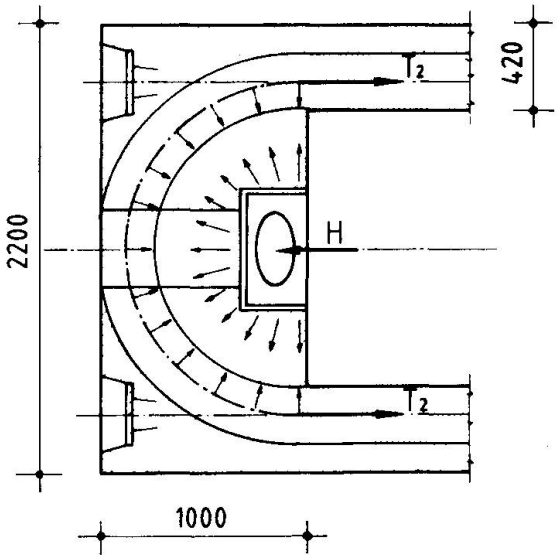

Fig. 5: Arch Action at Towerhead

This slipforming had a very stromg influence on the final rebar arrangement and detailing, especially in the anchorage area. The anchorage pipes have been welded on the ground to a steel frame, lifted up to the tower and bolted to the previous frame in the short walls. All the reinforcement had to be placed around these frames. This was achieved by a very accurate planning of each single bar location.

2.2 Deck Edge Beams

The required two lanes of traffic and a walkway resulted in a beam width of only 11.95 m, which leads to the remarkable slenderness in plan of 1:35.6. For the severe wind conditions the shallow, aerodynamically shaped 1.20 m deep cross-section was developed with a slenderness in elevation of 1:354. Non-linear effects in both directions were investigated using realistic non-linear stress-strain relationships.

Partial prestress was chosen for the beam in both directions to enhance its ductility. Straight tendons in the edge beams are continuous over the full length of the bridge and are coupled in every construction joint. Additional continuity tendons are threaded into empty ducts after completion of the beam across the mid-quarter of the main span. Full depth cross girders are provided at the cable anchorpoints. They contain the only transverse prestress. The reinforced 0.40 m thick roadway slab spans 7.25 m transversely and 12.2 m longitudinally.

The final design was governed by
a) dead plus live load action forces
b) action forces from dynamic wind
c) action forces during construction.

In a) the non-linear effect was taken into account with an estimated reduction of the E-Modulus by 2/3 because in ULS the stress level is above the linear branch of the stress-strain curve. Due to the slenderness of the bridge deck, the non-linear increase of the bending moments reaches 50 % of the linear live load moments, see Fig. 6.

For the first iteration of the wind analysis, an uncracked section without non-linear effects has been investigated. The resulting forces of this study gave the governing moments for the design of the beam almost all along the bridge and lead to the dense reinforcement shown in Fig. 7. The four tendons with 9 x 0.5" strands per edge beam have been provided mainly for erection. Due to partial prestressing the ratio between reinforcement and post-tensioning could be optimized with regard to structural and construction requirements. The combined bar and duct arrangement provides easy access for concreting and vibrating, convenient and economical splices and a simple post-tensioning arrangement.

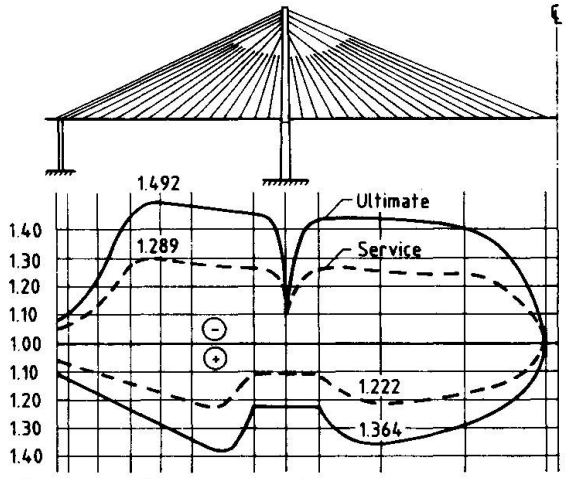

Fig. 6: Non-linear Beam Moments

The design for wind and live load was done in ULS, however the serviceablility had to be checked in SLS. The crack width is limited to 0.2 mm at the rebars and 0.1 mm at the tendons under dead plus 60 % live load. In the cracked section the steel stress is limited to 200 N/mm^2 for this load case. The post-tensioning is sufficient to avoid tension in longitudinal direction under permanent load conditions.

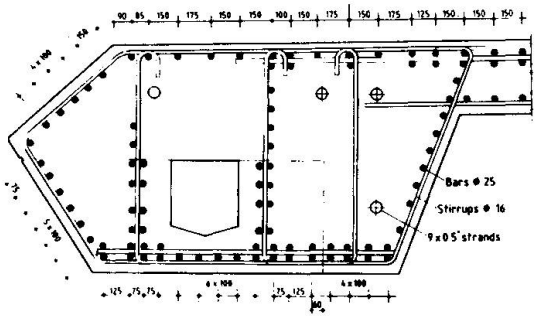

Fig. 7: Reinforcement in Edge Beam

3 AERODYNAMIC INVESTIGATION

The wind climate at the bridge site is very severe. The 50-year design wind speed (10 min. mean) at deck level is 50 m/s, with turbulence intensities horizontally of 10 m/s and vertically of 4 m/s. These rather large turbulences are due to the adjacent mountains.

An analytical time-history wind investigation was performed which is outlined in more detail in Ref. [2].

The non-linear force-deformation characteristics of the beam and the interaction between horizontal and vertical bending as well as torsion in the ultimate limit state were taken into account. For calculations in ULS action force versus deformation behaviour of the structure was followed up through a parametric analysis by a biaxial bending program, under consideration of the governing longitudinal force as well as of cracking of the tensile zone, see Fig. 8. These bending stiffnesses were essentially dependent on the actual reinforcement of the cross section.

A remaining tension stiffness of the concrete between the cracks of up to 1/3 was assumed. Calculations showed that nonlinear behaviour and bending interactions are satisfactorily described through the mathematical model shown in Fig. 9.

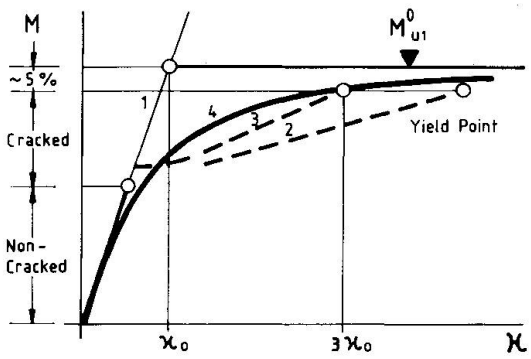

Fig. 8: Beam Stiffness Diagram

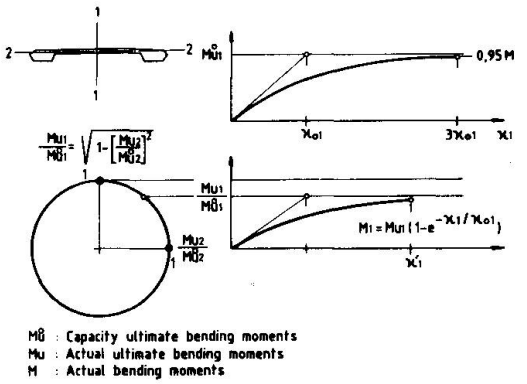

Fig. 9: Moment Interaction, ULS

The nonlinear behaviour in case of one-axial bending was estimated by

$$M_1 = M^0_{U1}\left(1 - e^{-\varkappa_1/\varkappa_{01}}\right)$$

with M_1 actual bending moment in the main plane 1
M_{U1} corresponding bending moment capacity
$\varkappa_1$ actual rotation
$\varkappa_{01}$ fictive roation by bending moment capacity, assuming full-elasticity

In view of a conservative supplementary checking of the ultimate load carrying capacity, the deformations were limited to the elastic limit of the reinforcement; this was found at about
A simultaneous moment in the ortogonal direction was found to be effective essentially through a reduction of the bending moment capacity M_{U1}. In dependence of the reduction factor,

$$\varepsilon = \sqrt{\left(\frac{M_1}{M^0_{U1}}\right)^2 + \left(\frac{M_2}{M^0_{U2}}\right)^2}$$

the reduced bending capacity becomes

$$M_{U1} = |M_1|/\varepsilon.$$

The stiffness receives the same reduction automatically, see definition in Fig. 9. The allowable roatation by achieving the elasticity limit of the reinforcement was found to be at about

$$\varkappa_1' = 3\varkappa_{01}\left(1 - \varkappa_2/3\varkappa_{02}\right).$$

The interaction effect on the torsional stiffness was set to

$$GJ_T = GJ_{T0}\left(1 - \frac{|M_1|}{M_{U1}^0}\right)\left(1 - \frac{|M_2|}{M_{U2}^0}\right).$$

The St. Venant torsional stiffness dropped in the ULS calculations occasionally to 10 - 30 % of the initial value.

The non-linear transverse moments at ULS at mid-span are reduced as a result of redistribution due to degressive stiffness, compared with the moments at service state multiplied by the safety factor of 1.6 as illustrated in Fig. 10.

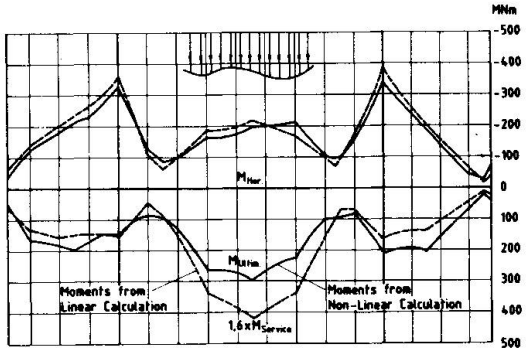

Fig. 10: Transverse Beam Moments, ULS

4. BEAM CONSTRUCTION

In order to facilitate the exact positioning of the stay cables and to provide an economical solution for the transmittal of the horizontal stay force component during casting, the concrete corbels and adjacent parts of the beam with the steel pipe are precast, see Fig. 11.

Governing stages in the erection phase were stressing the cables to final length for max. pos. moments and placing the precast elements and rebars into the catilevered formtraveller for max. neg. moments. The steel stress in the outermost bars was limited to 200 MPa, keeping the crack width at the exterior steel layers smaller 0,1 mm. The erection post-tensioing and the rebars had to be adjusted several times during the final design phase to take care of the changes in the equipment weight.

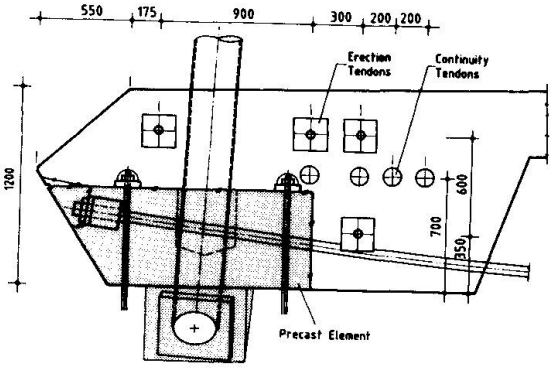

Fig. 11: Edge beam near cable anchorage

5. ACKNOWLEDGEMENT

The owner of the Helgeland Bridge is the Norwegian Road Administration, Nordland, with Mr Wilhelm B. Klaveness in charge. Main consultants are A. Aas Jakobsen, Oslo, Norway. Leonhardt, Andrä and Partners, Stuttgart, Germany, are special consultants for the cable-stayed bridge, including the aerodynamic investigation.

REFERENCES

[1] JORDET, E.A., SVENSSON, H.S.: Helgeland Bridge, a slender concrete cable-stayed bridge in location of severe winds. FIP 90, Vol.1, p. B95 to B99, Hamburg, 1990.

[2] KOVACS, I., SVENSSON, H.S., and JORDET, E.A.: Analytical investigation of the cable-stayed Helgeland Bridge in turbulent wind. To appear soon in the Journal of Structural Engineering, ASCE.